GEOCHEMICAL EVOLUTION AND ORIGIN OF EARLY ARCHEAN BASALTS FROM THE PILBARA BLOCK, WESTERN AUSTRALIA

by
Jinzhong Liu

Independent Study
Submitted in partial fulfillment
of the requirements for the degree of
Master of Science in Geochemistry

New Mexico Institute of Mining and Technology
Socorro, New Mexico
April 18, 1992

Abstract

The Warrawoona Group located in the Pilbara Black, is consists chiefly of 3.45-3.55 Ga volcanic and sedimentary successions and oval-shaped granitic batholiths, which formed one of the typical early Precambrian granite-greenstone belts of the world. Geochemical data of 51 basalts from the North Star Basalt, Mount Ada Basalt and Apex Basalt of the Warrawoona Group indicate that the alkali and alkaline-earth elements have been remobilized, but the other major elements and most incompatible elements are relatively stable during alteration. The basalts have SiO2 ranging from 45.17 to 54.73%, Al2O3 from 11.51 to 15.31%, TiO2 from 0.58-2.58%, FeO from 6.15-14.48%, MgO from 3.09-8.45%, CaO from 6.25-12.3%, Na2O from 0.85-5.15%, and K2O from 0.01 to 1.69%. The concentrations of the major elements show the basalts can be classfied into tholeiitic basalts. The incompatible elements Zr, Y, Nb, Hf, and Ta concentrations in Warrawoona tholeiites are 10X Primitive Mantle. Most tholeiitic basalts show a very slight enrichment in LREE relative to HREE, and the overall patterns show 10 to 20 times chondritic abundances. La_N/Yb_N ratios vary from 1.05 to 3.7, La_N/Sm_N from 0.71 to 2.9 and Gd_N/Yb_N from 0.96 to 1.56. Eu-anomalies are either slightly negative or positive (Eu/Eu^*=0.67-1.23), which compares to REE distribution in Archean low-K tholeiitic basalts. The basalts have compositions similar to Archean DAT (Condie, 1981), and the early Archean tholeiitic basalts from the greenstone belts in South Africa, South India, Canada, Greenland and North Minnesota.

Major and trace element concentrations of the basalts show that the concentrations have different change upward in the Talga Talga Subgroup and the Salgash Subgroup. (i). For the Talga Talga Subgroup, incompatible elements show a generally upward decrease, and a discontinuity in compositions between the North Star Basalt and Mount Ada Basalt which implies two cycles of the basalt eruption. (ii). For Salgash Subgroup, the basalts show opposite trends with upward increasing incompatible element concentrations, which indicate that incompatible elements increase with eruption of the basalts.

The Warrawoona Group have geochemical similarities to primitive mantle, but not to the mixture of the primitive mantle and continental composition. The Talga Talga Subgroup shows that the basalts were probably derived from the 5-20% partial melting of primitive mantle. The Salgash Subgroup shows that the basalts were probably formed by 5-30% residual melting of primitive mantle in the process of fractional crystallization. The Warrawoona Group basalts have geochemical similarities to the arc tholeiitic basalts or oceanic type basalts. It is possible that the Warrawoona Group basalts formed in the 3.55 Ga rift of a plate.

Acknowledgements

I wish to express sincere thanks to the many people who contributed their time, patience and expertise. Kent Condie, my advisor, created this project and guided me through it with a tremendous amount of support and understanding. Andrew Glikson sent all samples of the basalts, related information and unpublished major element data to me. Philip Kyle, Christopher Mckee and Mark Boryta gave freely of their time and knowledge concerning analytical procedures, data reduction, and other aspects of relevance to geochemistry, as well as providing a significant amount of entertainment.

Table of Contents

List of Figures

List of Figures (continued)

List of Tables

I. Introduction

The Pilbara Black is located in the northwestern part of the Western Australian Precambrian shield, which has an area extent of about 60,000 km^2. The Block is consists chiefly of Early Precambrian volcanic and sedimentary successions and oval-shaped granitic batholiths, which formed one of the typical early Precambrian granite-greenstone belts of the world. Many geological similarities with the Early Precambrian greenstone belts of India, Southern Africa, and other fragments of the former supercontinent Gondwanaland, appear in the Pilbara Block(Purvis, 1990). The 3.55-3.45 Ga Warrawoona Group of the Pilbara Block is one of the oldest greenstone sequences with lower grade metamorphism in the word(Hall and Hughes, 1990), which is important to study mantle and continental evolution.

Since the Pilbara Block was investigated by Greory in 1861, it has been studied for more than one century. In the late 1970's, the early Precambrian stratigraphy was established in the Pilbara. Lipple (1975) established stratigraphic subdivisions of greenstone belts in the Marble Bar area in the eastern Pilbara Block and, following earlier workers, grouped the layered sequence into the dominantly volcanic Warrawoona Group and, unconformably overlying it, the essentially sedimentary Gorge Creek Group. Fitton et al. (1975) independently mapped an area in the western Pilbara Block and established a stratigraphic sequence in which the Whim Creek Group unconformably overalls the Gorge Creek Group. The three groups form the Archean Pilbara Supergroup, which is overlain unconformably by the early Proterozoic Fortescue Group(2.6-2.2 Ga). The Fortescue Group is composed chiefly of sedimentary rocks and minor mafic volcanic rocks. Following the previous

research, Hickman (1983) published the stratigraphic subdivision of the greenstone sequences in the Pilbara Block listed in Table 1.

Table 1. Early Precambrian Stratigraphic Column of the Pilbara Block:

Supergroup	Group©	Age@
Early Proterozoic Mount Bruce Supergroup	Fortescue Group	2.6 to 2.2 Ga
	-------Regional Unconformity-------	
Archean Pilbara Supergroup	Whim Creek Group	2.95 to 2.60 Ga
	-------Regional Unconformity-------	
	Gorge Creek Group	3.30 to 2.95 Ga
	-------Regional Unconformity-------	
	Warrawoona Group	3.55 to 3.45 Ga

© after Hickman (1983), @ after Gruau (1987), Jahn (1981), Pidgeon (1984).

Isotopic ages from the Pilbara rocks rage from 3.45 to 3.55 Ga (Pidgeon, 1978, 1984, Gruau, 1987), based on results from the Sm-Nd, Rb-Sr and U-Pb methods on mafic to felsic volcanic rocks from the Warrawoona Group. The Warrawoona Group is the oldest volcanic and sedimentary sequence in Pilbara Block. For the largely sedimentary units of the Gorge Creek Group (overlying

the Warrawoona Group) there is no definitive geochronological evidence on the timing of sedimentation. It has been suggested that the Gorge Creek Group sediments are not much younger than 3.3 Ga (Hickman, 1983). Most ages dated in volcanic rocks from the Whim Creek Group are 2.6 to 2.95 Ga (Pidgeon, 1984, Jahn, 1981), which come from the upper part of the Archean volcanic and sedimentary sequences.

The Archean structural styles of the Pilbara Block are dominated by granitic domes and greenstone synclines. The domes and synclines commenced development at slightly different times in different areas (H. Jones, M. Minister, 1982). Hickman (1975) described four Archean episodes of deformation from the Marble Bar and Nullagine areas, as follows: (i) interfolding of greenstone and granitic material, granitic intrusion and migmatization; (ii) diapiric movement of granitic material and downward movement of the surrounding greenstones, with greenschist to amphibolite-facies metamorphism; and (iii) conjugate folding and faulting associated with regional east-west compression; and (iv) tight to open folding about subhorizontal axial planes.

The excellent outcrop, stratigraphic and structural definition, and the establishment of regional geological controls, render the eastern part of this terrain particularly suited to systematic geochemical investigations (Glikson, et al., 1981). But, previous geochemical investigations have been limited to study of REE and major elements of the felsic to mafic volcanic and related plutonic rocks from the upper Pilbara Supergroup(Jahn, 1981, Glikson et al, 1981, Bickle, et al., 1983, Barley, et al, 1984, Gruau, 1987).

In the present study, the approach was to restrict the analyses solely to samples of tholeiitic basalts in the Warrawoona Group. The main aims of this work are: (i) to study the geochemical stratigraphy of the basalts; (ii) to interpret the origin of the basalts; and (iii) to characterize the tectonic setting.

II. Regional Geology of Warrawoona Group

A. Stratigraphy of the Warrawoona Group

The Warrawoona Group, the oldest volcanic and sedimentary succession of Pilbara Supergroup, mainly occurs in the eastern Pilbara Block (Figure 2-1). It was subdivided by Lipple (1975), from base to top, into the Talga Talga Subgroup, the Duffer Formation and Salgash Subgroup (Hickman, 1983), as shown in table 2. The Talga Talga Subgroup and the Salgash Subgroup are assemblages of subaqueous mafic flows separated by thin sedimentary layers and tuffs. These interflow horizons have been preferentially intruded by felsic to ultramafic sills. The Duffer Formation is composed of intermediate to felsic, coarse to fine grained tuffs, sills, and flows, but mafic flows and tuffs also occur (Horwitz, 1990). The stratigraphic relationships between the three subgroups are locally unconformable (Horwitz, 1990).

1. The Talga Talga Subgroup

The Talga Talga Subgroup is well exposed over 50 km^2 south and east of Talga Talga mining centre. The type section follows the road between the Great Northern Highway and McPhee Reward Mine (Hickman, 1983). The thickness of the Talga Talga Subgroup is about 4000 to 4700 m, and is subdivided from base to top, into the North Star Basalt, McPhee Formation and Mount Ada Basalt. Both Basalt formations consist chiefly of the pillowed, massive tholeiitic basalts, high-Mg basalts and minor peridotitic komatiites, but the McPhee Formation is essentially composed of dacitic to andesitic volcanics, minor volcaniclastic sediments, and chert.

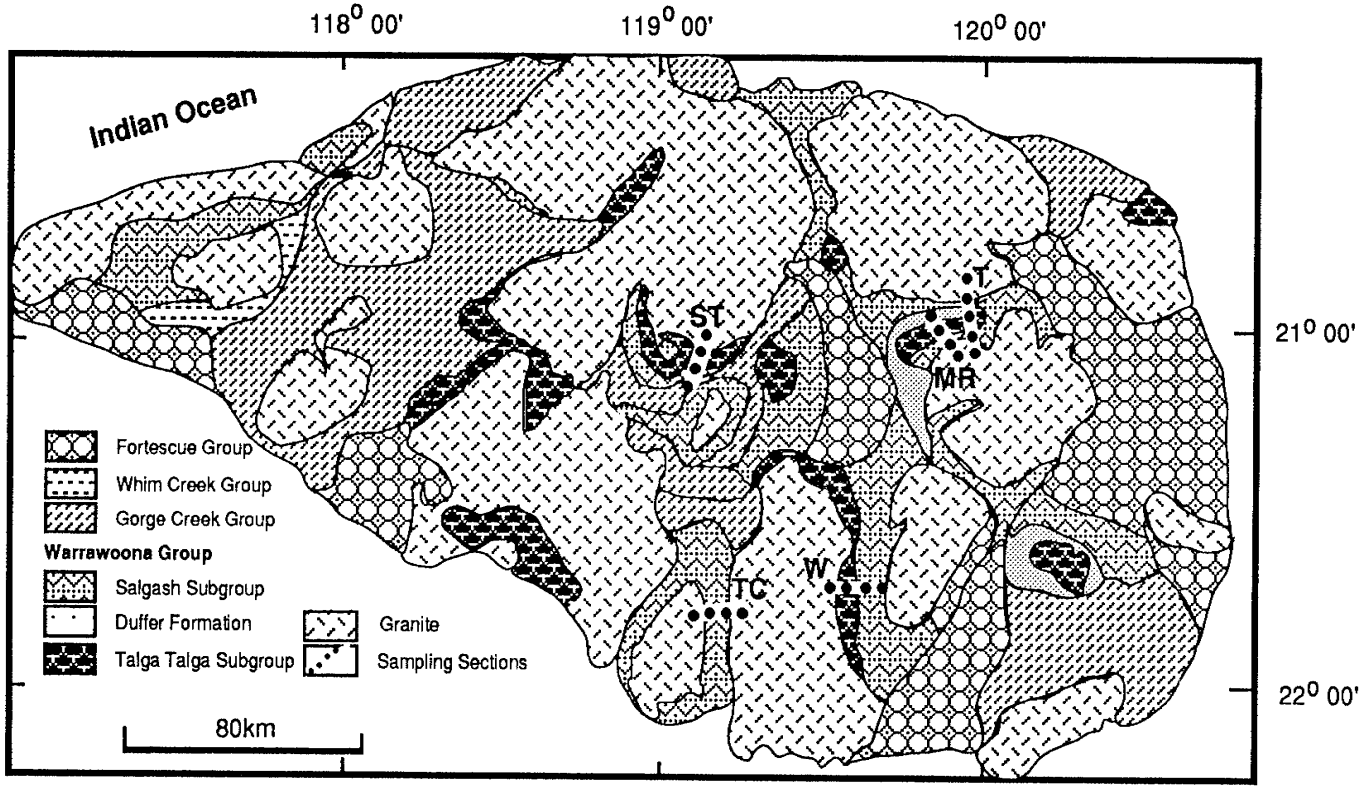

Figure 2-1. Geological map of the Pilbara Block, Western Australia, showing the localities of sampling sections through volcanic units of the Warrawoona Group: **MR** McPhee Reward section, **W** Withnell Creek section, **ST** Strelley Gorge section , **T** Talga River section, **TC** Talga Coongan section (after Glikson, 1983).

Table 2. Stratigraphic Column of the Warrawoona Group (after Hickman, 1983):

Subgroup	Formation	Lithology	General Thickness (m)	Age in Ga
	----- local unconformity----			
	Wyman Formation	Porphyritic columnar-jointed rhyolite. Local tuff, agglomerate and basalt	0 ~1000	
	-----local unconformity---			
Salgash Subgroup	Euro Basalt	Pillow basalt with minor chert and felsic volcanic unites. Local peridotitic komatiite near base.	2000	
	Panorama Formation	Dacitic lava, tuff and agglomerate, and chert. Local sandstone, conglomerate and ultramafic rocks.	0 ~1000	3.34(Richard, 1978)
	Apex Basalt	Pillow basalt and high-Mg basalt. Numerous chert units and minor dolerite and gabbro sills.	1.5 ~ 2000	
	Towers Formation	Three chert members separated by basalt, komatiite, felsic volcanics or sediments. Includes the Marble Bar Chert Member (100 m thick)	500	3.42 (Richard, 1978)
Duffer Formation	Duffer Formation	Dacitic tuff, agglomerate and lava. Minor chert, shale and basalt. Local porphyritic intrusions.	0 ~ 8000	3.45-3.50 (Pidgeon)
	---- local unconformity------			
Talga Talga Subgroup	Mount Ada Basalt	Pillow basalt, massive basalt, and minor chert, dolerite and gabbro. Local chert, black shale and felsic tuff.	2000 ~ 2500	
	McPhee Formation	Carbonate-chlorite quartz schist. Subordinate chert. BIF, pelite and tuff. May include carbonate sediments.	50 ~ 200	
	North Star Basalt	Massive basalt and pillow basalt with numerous sills of dolerite and gabbro. Minor chert, serpentinite and felsic lava.	2000	3.55-3.57 (B. Jahn, 1981)

The Talga Talga Subgroup is metamorphosed to greenschist and lower amphibolite facies. Metabasalt now consists of clumps of green amphibole set

in a finer grained mass of albite with lesser amounts of chlorite, epidote, clinozoisite, quartz, opaques,sphene and carbonate minerals.

North Star Basalt: The North Star Basalt, the oldest basalt, consists chiefly of massive basalts, pillow basalt and numerous sills of dolerite and gabbro. At McPhee Reward mine and Shark mining centre a thin felsic lava member at the top of the unit is overlain by clastic sediments, chert, and tuff of the McPhee Formation. Rare chert and serpentinite units are locally developed in the centre of the North Star Basalt, and the unit's general thickness is about 2000 meters. **McPhee Formation:** Carbonate-chlorite-quartz rocks comprise the bulk of the McPhee Formation. Schistosity, or layering, is a prominent feature of the rock both in the field and under the microscope. It is probably significant that this foliation is confined to the ultramafic unit, and is parallel to bedding in the adjacent chert and basalt units (Hickman, 1983). It's about 50 to 200 meters thick. **Mount Ada Basalt:** The Mount Ada Basalt is a 2000 to 2500 m thick succession of pillow and massive basalt flows, dolerite sills, and minor thin chert units. Basalt is estimated to comprise about 80% of the formation. Immediately beneath the Duffer Formation, chert, BIF and siltstone form the top of the Mount Ada Basalt, but these members wedge out southwestwards suggesting the existence of a low-angle unconformity at the top of the formation (Hickman, 1983). The Mount Ada section contains two central bands of pelite, ferruginous chert and felsic tuff, but sediments are not present at the top of the formation.

2. Duffer Formation:

The Duffer Formation occurs in eastern Pilbara Block, from Salgash mining center through Marble Bar to Coppin Gap, and in McPhee Creek,

Copper Hills, and Glen Herring. It is composed of dacitic lava, tuff and agglomerate, with subordinate rhyolite, basalt, chert and porphyritic intrusions. The thickness of the volcanic and sediment sequence range from 0 to 8000 meter. Thickness and facies variations are a pronounced feature of the Duffer Formation (Hicman, 1983). The formation becomes thinner from the Marble Bar and Coppin Gap towards north. The thickest section is composed chiefly of agglomerate, but thinner sections generally contain a greater proportion of lava and tuff, which imply a facies change in the Duffer Formation.

3. Salgash Subgroup

The Salgash Subgroup, the upper volcanic and sedimentary successions, mainly occurs chiefly between Reedy Creek on the east and Devil Creek on the west, a distance of 430 km. It was subdivided, from lower to upper, the Towers Formation, Apex Basalt, Panorama Formation, and Euro Basalt (Hickman, 1983), for total thickness of 4000 m to 6500 m.

Towers Formation: The Towers Formation is the main stratigraphic marker unit of the Warrawoona Group (Hickman, 1977), and consists of three chert members separated by two members of pillow basalt, felsic tuff or sedimentary rocks. **Apex Basalt:** The Apex Basalt is generally consists of tholeiitic pillow basalt, high-magnesium basalt (tremolite-chlorite rocks), peridotitic komatiite, several thin members of grey and white banded chert, and sills of dolerite, gabbro and rare altered ultramafic rocks. **Panorama Formation:** The Panorama Formation is 100 to 1000 m thick, consists of felsic lava, tuff, agglomerate, chert and metasediments in the east Pilbara, but in the West Pilbara it is composed chiefly of chert and tuff. **Euro Basal:** The Euro Basalt, the top of the Warrawonna Group, is unconformably overlain by the

Wyman Formation. It is consists generally of pillow basalt with minor chert and felsic volcanic units, and local peridotitic komatiite near the base. The Euro Basalt is lithologically indistinguishable from the Apex Basalt. Dolerite and gabbro sills are less common than in the Apex Basalt. Spinifex-textured basaltic rocks containing tremolite, chlorite, epidote and clinozoisite make up the bulk of the formation south of Camel Creek. Some of these rocks represent high-magnesium basalt, but in general the Euro Basalt of the east Pilbara appears to be less mafic than the Apex Basalt (Hickman, 1983, Horwitz, 1990). Lenticular structures in the amphibolite may represent flattened pillow structures, but no clear facing evidence has been observed (Hickman, 1983).

B. Structural Geology

In the Pilbara Block, the structural style is dominated by granitic domes and greenstone synclines, which are unlike folds formed in the post-Archean and appear to have originated through tectonic processes no longer in operation (Hickman, 1983). The domes are essentially diapiric structures whereas the greenstone synclines occupy areas in which the Pilbara Supergroup sank into the granitic substratum. This process is thought to have involved progressive gravity deformation over a long period of time (Hickman, 1983).

The regional unconformity on the Warrawoona Group is the earliest regional unconformity in the Pilbara Block, and indicates that significant earth movements and resulting erosion commenced only after deposition of the Euro Basalt (Hickman, 1983, Horwitz, 1990). The deformation of the Warrawoona Group is described in terms of four episodes by Hickman (1975). The four episodes are respectively: Stage 1. interfolding of greenstone and granitic material, granitic intrusion, and migmatization; Stage 2. diapiric movement of

granitic material and downward movement of the surrounding greenstones, with greenschist to amphibolite-facies metamorphism; Stage 3. conjugate folding and faulting associated with regional east-west compression; Stage 4. tight to open folding about subhorizontal axial planes.

C. Geochronology

Most isotopic ages, from the mafic to felsic volcanic rocks from Warrawoona Group and rage from 3.45 to 3.55 Ga (Pidgeon, 1978, 1984, Gruau, 1987). The dates from the three subgroups are different from each other, and most ages are from mafic rocks in the North Star Basalt, Duffer Formation, and Panorama Formation.

North Star Basalt and Mount Ada Basalt: Hamilton et al (1981) reported a data at 3560 ± 32 Ma on the basis of a linear array of five whole rock Sm-Nd data points. Jahn et al (1981) published a Sm-Nd Whole-rock isochron age of 3560 ± 54 Ma for three dacites and one andesite, and a Rb-Sr whole rock isochron age on the dacite samples of 3570 ± 18 Ma. But the oldest age at 3712 ± 98 Ma with εNd of +1.64 ± 0.4 on komatiites,high-Mg basalts and tholeiites, was reported by G. Gruau, B. M. Jahn, et al (1987), and support the existence of ancient LREE-depleted reservoirs in the early Archean mantle, and further suggest that source regions for the Pilbara volcanic rocks were isotopically heterogeneous, with εNd values ranging from at least 0 to +4.0.

Duffer Formation: One zircon U-Pb age of 3452+16 Ma was reported by Sangster and Brook (1977). Sm-Nd model ages of 3400 and 3430 Ma for two dacite samples was reported by Collerson & McCulloch (1983), which indicate a time interval of up to 100 Ma separates the Duffer Formation from the

underlying North Star Basalt. **Panorama Formation:** A zircon U-Pb age of 3307 ± 19 Ma from felsic volcanics was obtained by Pigeon (1984), which constrains the age of the top of the Warrawoona Group.

III. Sample Sites and Analytical Methods

A. Sample Sites

The major rock types include tholeiitic basalts (TB), and high Mg basalts (HMB) from the Warrawoona Group, Whim Group and Fortescue Group in the eastern Pilbara Block. Rocks were collected by A. Glikson and his collaborators. The sampled sections, from east to west, include Withnell Creek, McPhee Reward, Talga Coogan, Talga River, Cleavervilie and Strelley Gorge, are shown in Figure 2-1. Fifty four samples of tholeiitic basalt and 8 samples of

Table 3. Samples of the Warrawoona Group basalts from the Pilbara Block

Group	Formation	Sections	Number of TB	Number of HMB
Fortescue	Maddina		3	
	Nymerina		3	
	Kylena		6	
	Mount Roe		3	
Whim Creek	Negri	Mt Negri	3	
	Louden	Louden		3
	Warrambie	Warrambie Station	5	
Warrawoona	Apex	Withnell Creek	3	2
		Strelley Gorge	5	2
		Cleavervilie	5	
	Mount Ada	Talga Coogan	6	
		Talga River	7	
		McPhee Reward@	8	
	North Star	Talga Coogan	9	4
		Withnell Creek	7	
		Mcphee Reward@	4	

@ The sample positions in the stratigraphic column are shown in Figure 4-18.

high-Mg basalt come from the Warrawoona Group, and 23 samples of tholeiitic basalt and 3 samples of the high-Mg basalt from other Groups (table 3). In the McPhee Reward Section, 12 samples of tholeiites are given positions in the stratigraphic column (Fig. 4-18) in order to study the stratigraphic geochemistry.

B. Analytical Procedures

1. X-Ray Fluorescence

Trace elements Y, Zr, Nb, Rb, Sr, Ba were determined by X-Ray Fluorescence (XRF) analysis on pressed powder pellets, using an automated Rigaku 3064 XRF spectrometer coupled with a PDP-11 computer and associated software at the New Mexico Bureau of Mines and Mineral Resources X-ray Lab. The techniques are involved, following the methods of Norrish and Hutton (1969) and Norrish and Chappel (1977). Pressed powder pellets were made by adding one drop of polyvingl alchohol (a binder) per gram of sample powder to about 8 grams of powder; this mixture is pressed with a boric acid backing to 20 tons per square inch for about 2 minute.

A list of measured energies, detection limits and lower limits of determination are given in table A-1. Detection limits give the excited electron shells, minimum concentration of an element needed for qualitative analytical detection. The lower limit of determination describes the minimum concentration of an element needed for quantitative analytical determination. Precision and accuracy table for XRF is given by Boryta (1988) in Table A-2.

2. Instrumental Neutron Activation Analysis

Cs, Th, U, Sc, Cr, Co, Ni, Hf, Ta, La, Ce, Sm, Eu, Tb, Yb and Lu are determined by INAA using methods similar to those described by Jacobs et al.

(1977) and Gibson and Jagam (1980). Approximately 300 milligrams of powder are sealed in polethylene vials and irradiated in the Annular Core Research Reactor at Sandia National Laboratory in Albuquerque, New Mexico. The vials are subjected to a neutron flux estimated at 2.7×10^{13} for ten thousand seconds. The pertinent information for neutron activation is shown in table A-3 (from Hallett, 1990). An air hose attached to the container in the irradiation chamber assures an even flux on all samples. Gamma ray counts are conducted after about 7 and 40 days with a coaxial intrinsic Ge-crystal detector using a Nuclear Data 6600 mutichannel analyser coupled with an LSI-11 computer. Three vials containing approximately 200 mg of fly ash standard NBS-1633a are irradiated with the samples for use as reference standards using methods similar to those of Korotev (1987). Data are reduced by computer using TEABAGS (Trace Element Analysis By Automated Gamma-ray Spectrometry, Lindstrom and Korotev, 1982) software. Precision and accuracy tables for INAA are given in Appendix A-4.

The Fe measured from INAA was compared with the Fe collected from Glikson to further insure each sample saw the same flux gradient. The ratio $((Fe_{XRF}-Fe_{INNA})/Fe_{XRF})$ was used as a correction factor and multiplied by each trace-element abundance determined by INAA.

IV. Geochemistry of Basalts in the Warrawoona Group

A. Geochemical Features

The significance of geochemical data to magmatic processes may be obscured by interaction of water with the lava surface, burial metamorphism, thermal metamorphism, attendant metasomatism and/or dehydration (Glikson, 1981). The greenschist-facies metamorphosed basalts in the Pilbara Block have been exposed at the surface and have interacted with ground water for a long time. Previous studies indicate that the alkali and alkaline-earth elements have been remobilized, and the siderophile (Fe, Ti, Mn, V), magnesia-related (Ni, Cr, Co) elements, some LILE, and HFSE are relatively stable (Glikson, 1981). The alteration of the basalts in the Warrawoona Group is not very great. As a result, we can discuss the geochemical features in terms of the origin of basalts.

1. Major elements

Major element analyses for 51 tholeiitic basalts of the Warrawoona Group are presented in Appendix B. Most of the basalts have SiO_2 ranging from 45.17 to 54.73%, Al_2O_3 from 11.51 to 15.31%, TiO_2 from 0.58-2.58%, FeO from 6.15-14.48%, MgO from 3.09-8.45%, CaO from 6.25-12.3%, Na_2O from 0.85-5.15%, and K_2O from 0.01 to 1.69%. SiO_2 versus other major elements are shown in diagram 4-1, which indicates that the average concentration of major elements is similar to the 3.5-Ga tholeiitic basalt in the Onverwacht Group in South Africa (Jahn, 1982). The ratio of SiO_2/Al_2O_3 ranges from 3.01 to 4.26, FeO/MgO from 0.84 to 3.73, Al_2O_3/TiO_2 from 4.72 to 25.63, and K_2O/Na_2O from 0.01 to 0.92, are shown in Figure 4-2 and Figure4-3a. Figure 4-3b shows that the range of ratio of Al_2O_3 is much larger than K_2O/Na_2O. The diagrams of

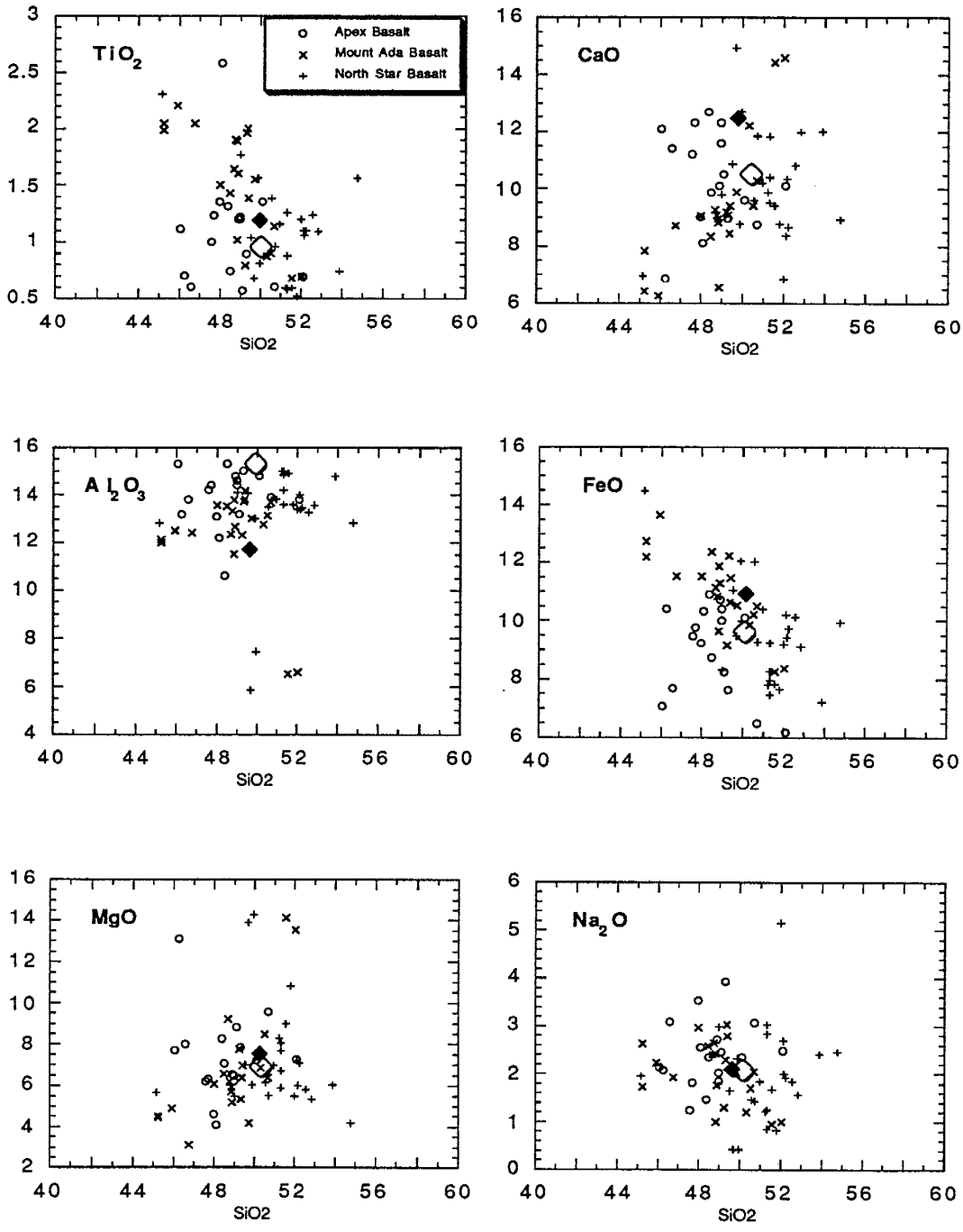

Figure 4-1. Diagrams of SiO2 vs. TiO2 (Al2O3, MgO, FeO, CaO and Na2O) of basalts from the Warrawoona Group. Solid diamond is average tholeiitic basalts from Onverwacht, South Africa (Jahn, 1982), diamond is DAT (Condie, 1981).

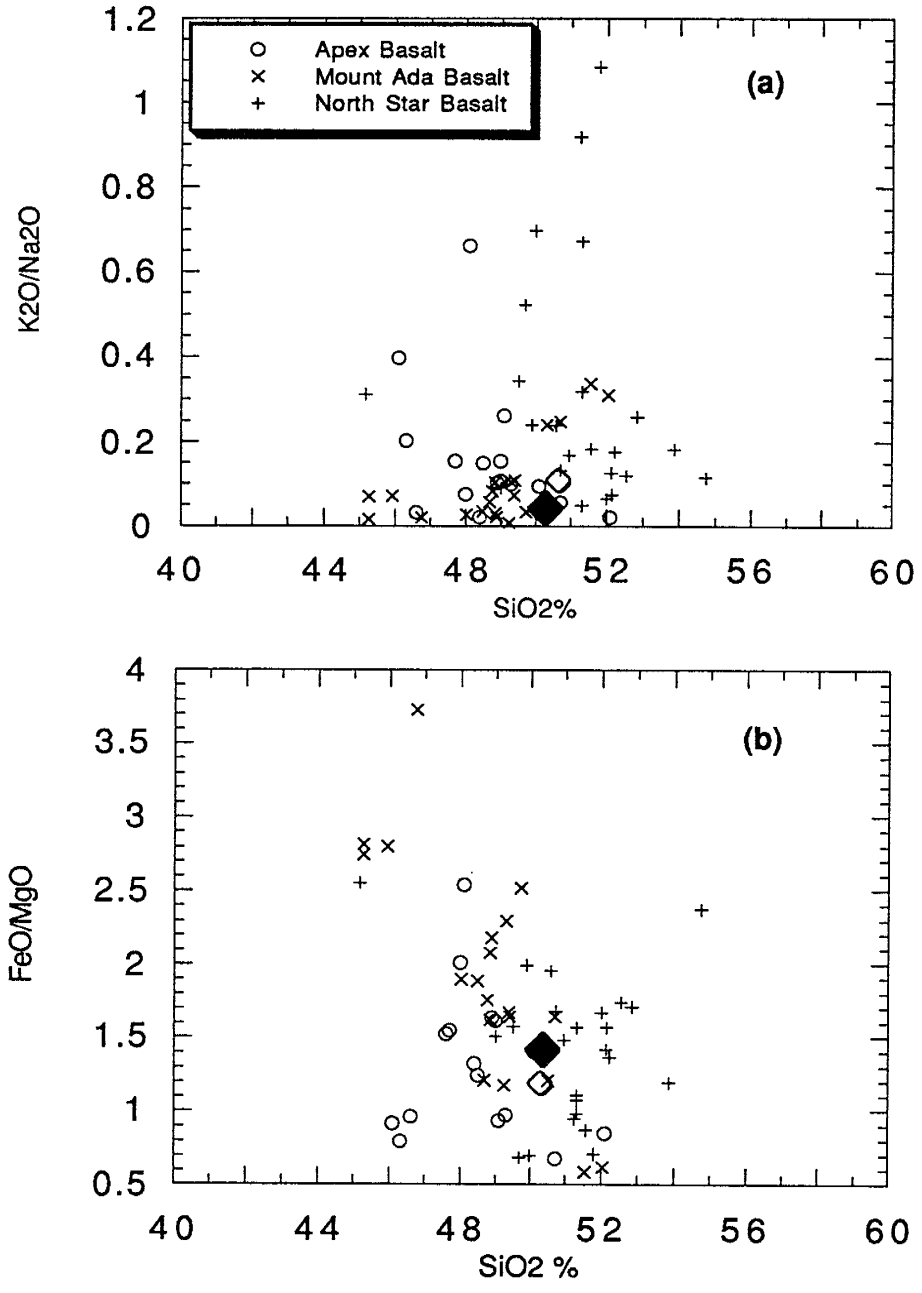

Fig. 4-2. Diagram of SiO2 vs K2O/Na2O and FeO/MgO of basalts from the Warrawoona Group. Solid diamond is average tholeiitic basalts from the Onverwacht Group, South Africa (Jahn, 1982), and diamond is DAT (Condie, 1981).

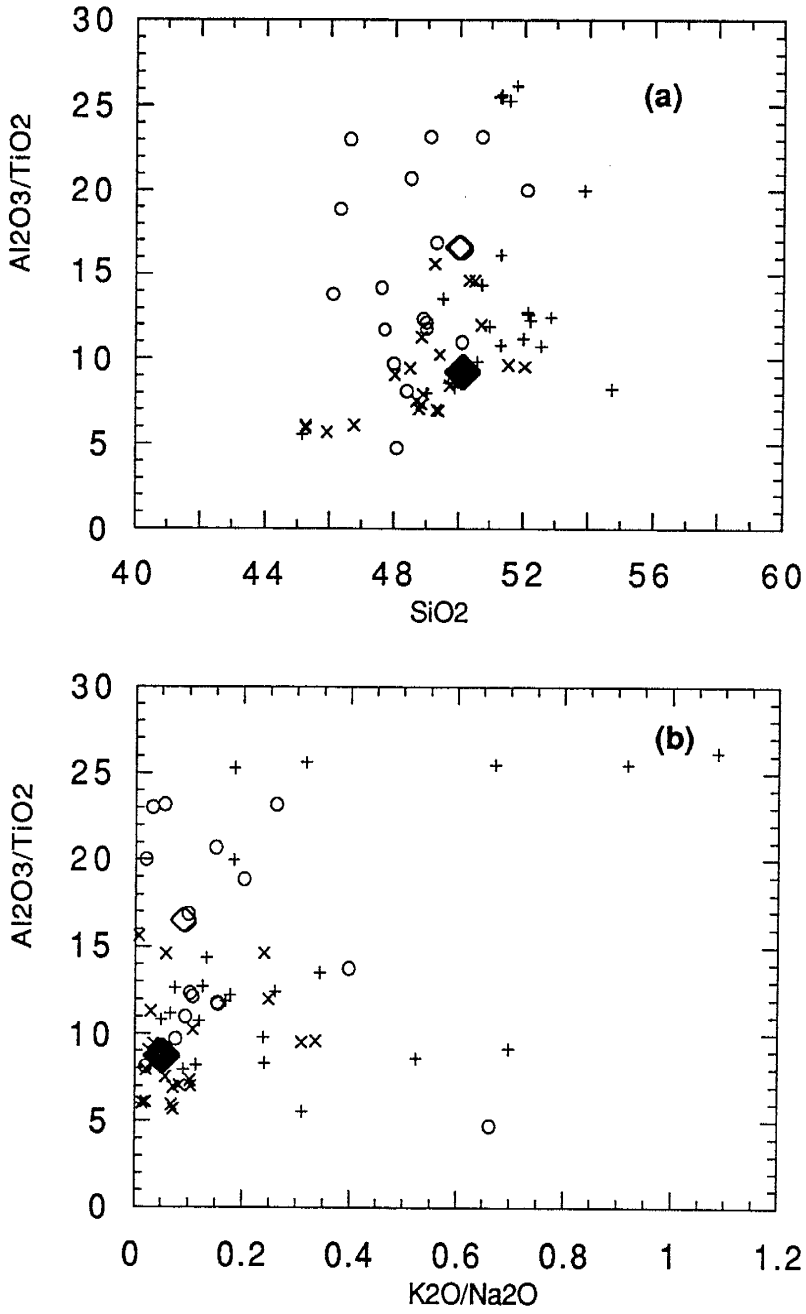

Fig. 4-3. Diagrams of Al2O3/TiO2 vs. SiO2 and K2O/Na2O of basalts from the Warrawoona Group. Solid diamond is average tholeiitic basalts from the Onverwacht Group, South Africa (Jahn, 1982), and diamond is DAT (Condie, 1981).

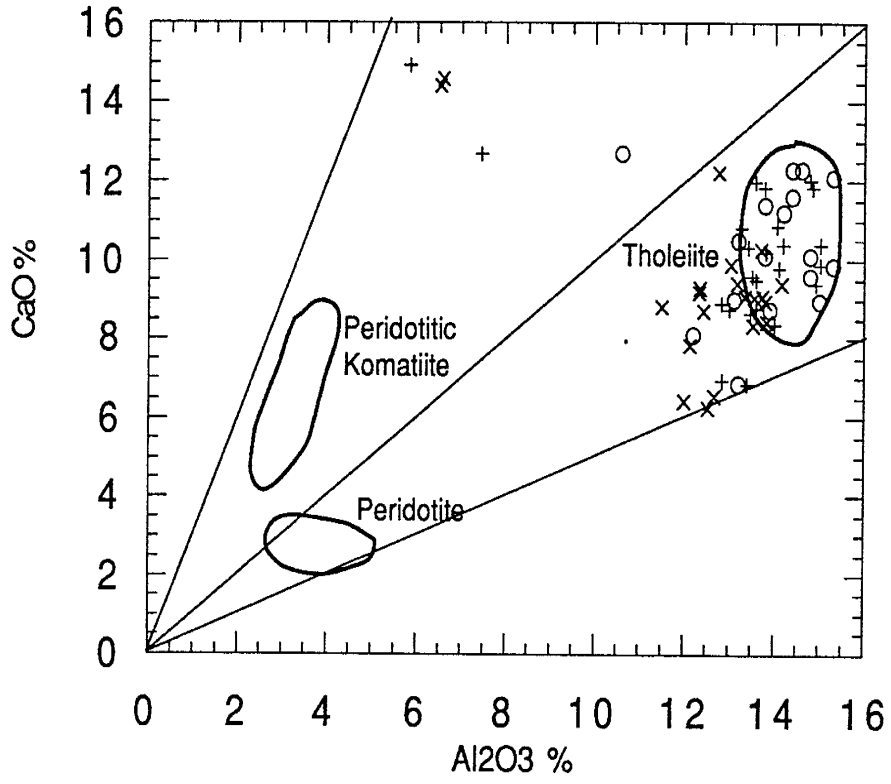

Fig. 4-4. Diagram of CaO vs. Al2O3 for basalts of the Warrawoona Group. Most samples of the Warrawoona basalts plot in the area of Tholeiite, few samples plot around the Tholeiite.

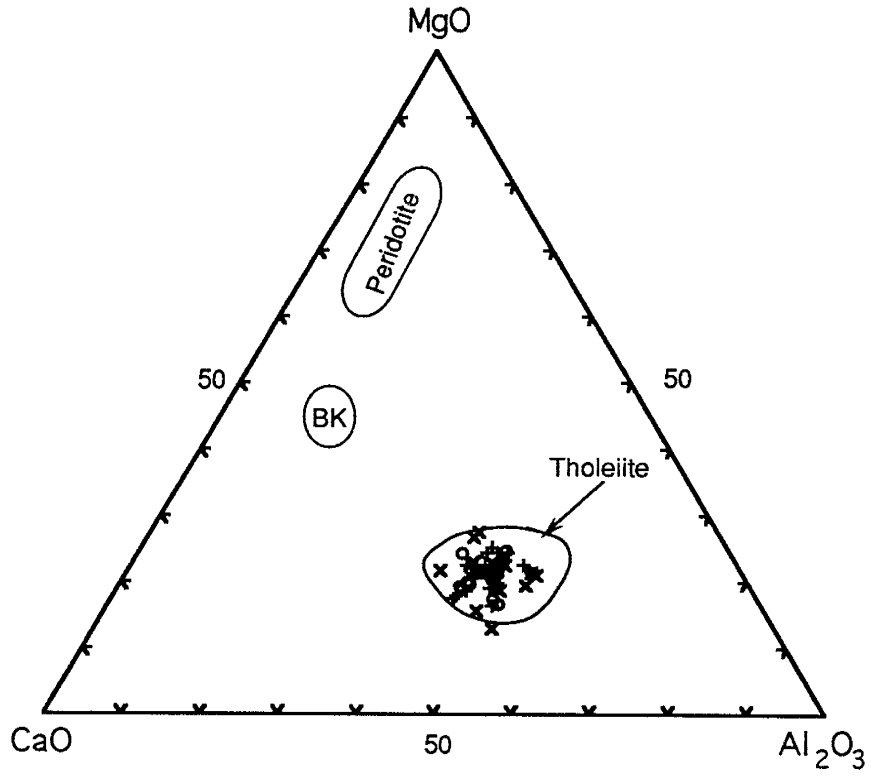

Fig. 4-5. MgO-CaO-Al2O3 diagram of basalt from the Warrawoona Group. Most samples of the Warrawoona basalts plot into the area of the Tholeiite (after Vijoen et. al., 1969)

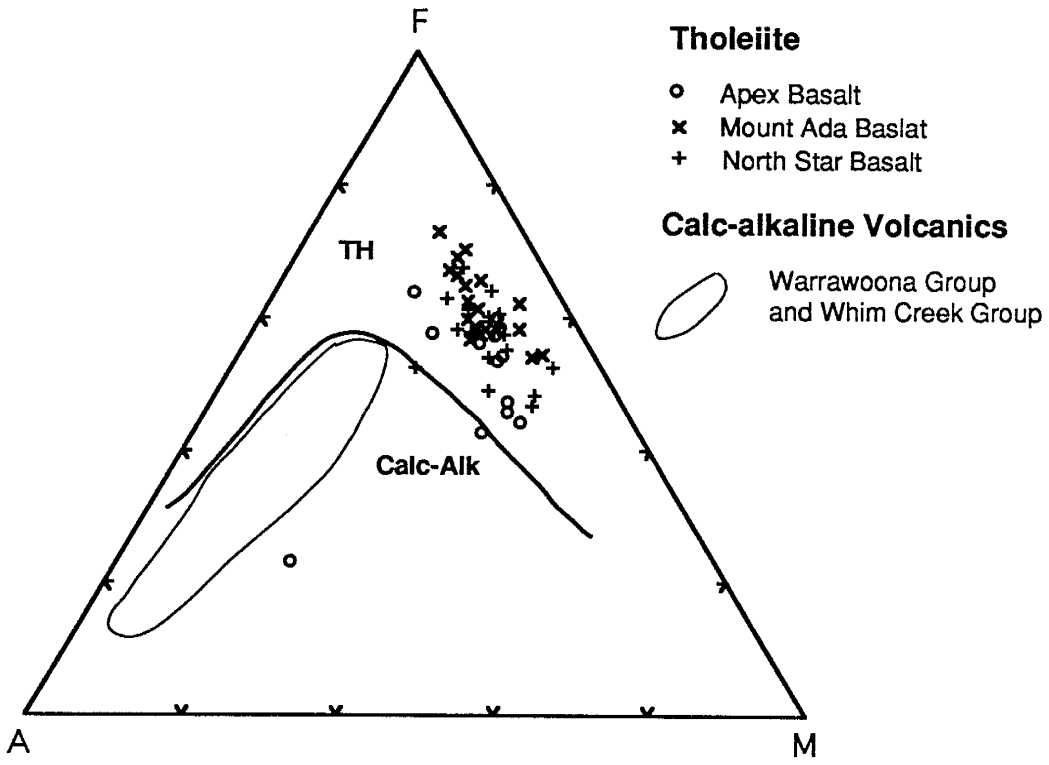

Fig. 4-6. AFM plots of basalts from the Warrawoona Group. Most basalts from the Warrawoona Group plot in the area of the Tholeiite, which are different from the calc-alkaline volcanics of the Warrawoona Group and Whim Creek Group (Bickle, 1983, 1984)

$CaO-Al_2O_3$ (Figure 4-4), and $MgO-CaO-Al_2O_3$(Figure 4-5, after Viljoen, 1969) show that most Warrawoona basalts plot into the areas of tholeiitic basalt. In Figure 4-6, most basalts of the Warrawoona Group plot in the area of tholeiitic basalt. The basalts are different from the calc-alkaline volcanics of the Warrawoona Group and Whim Creek Group (Bickle, et. al., 1983, 1984) in Diagram AFM (Fig. 4-7). Compared to the basalts in late Archean greenstone belts in Figure 4-1, 4-2 and 4-3, the basalts of the Warrawoona Group have similar to Archean DAT of the greenstone belts (Condie, 1981).

2. Trace elements

Trace element data of the 51 basalts of the Warrawoona Group are presented in Appendix C.

Large-Iron Lithophile Elements (LILE)

Sr, Th, Ba are the relatively stable elements, but Rb and K are relatively mobile elements in the alteration of the basalts of the Warrawoona Group. In Figure 4-7, most basalts have Rb/Sr ratio ranging from 0.01 to 0.1, and average is about 0.03 similar to the primitive mantle (Jahn, 1989). Compared to primitive mantle (PM), the Warrawoona Group has 10 times greater concentration of Sr, Ba, Th than the PM (Figure 4-8, 4-9, 4-10), and greatly variation in the concentration of Rb and K. For the North Star Basalt, Rb has concentrations of 20-40X PM, and K has 10X PM in the McPhee Reward section. Rb is 20-80X PM and K is 10-30X PM in Talga Coongan section. For the Mount Ada Basalt, Rb and K have concentrations of 1-4X PM in the McPhee Reward section, and Rb is 20X PM and K is 10X PM in Talga Coongan section. For the Apex Basalt, Rb has concentrations of 10X PM, and K has concentrations of 5-7X PM. The variability of concentrations of Rb and K in the stratigraphic column of the

Table 4. Average compostions of Zr, Ti, and Y of the Warrawoona Group basalts, compared the tholeiite basalts from other regions

	South India			Canada			SW Greenland			NE Minnesoda			Ar Greenstone Belts		Warrawoona Group		
	n	mean	δ	n	mean	δ	n	mean	δ	n	mean	δ	DAT	EAT	n	mean	δ
TiO2	43	0.93	0.23	31	1.06	0.39	9	1.14	0.67	10	1.05	0.32	0.94	1.49	51	1.30	0.49
Zr	43	64.04	23.49	31	81.55	48.22	9	61.89	33.85	10	64.30	24.21	53.00	135.00	51	102.76	38.30
Y	43	18.88	4.58	31	24.87	15.59	9	21.56	13.40	10	20.40	8.36	20.00	30.00	51	30.92	8.98
Ti/Y	43	304.97	87.96	31	299.80	133.33	9	331.19	60.22	10	326.75	79.94	286.20	297.00	51	249.90	40.23
Zr/Y	43	3.43	0.98	31	3.44	1.25	9	3.03	0.57	10	3.30	1.23	2.70	4.50	51	3.28	0.49
Ti/Zr	43	91.81	22.78	31	93.45	39.15	9	109.86	10.43	10	106.79	37.67	106.00	66.00	51	77.43	14.33

n: Number of the data for the basalts; δ: Standard Deviation

Reference: South India (Drury, 1982 and Rajamani, 1984), Canada (Fryer, 1978, and Lafieche, 1991), Archean DAT and EAT(Condie, 1981).

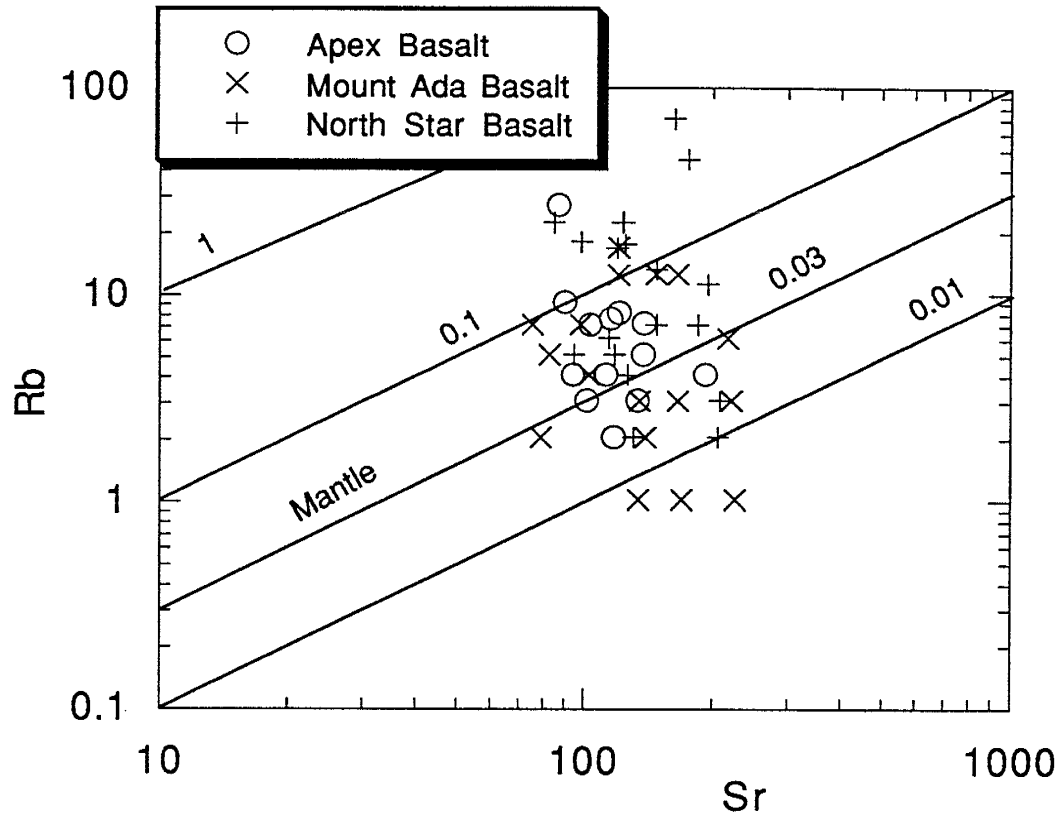

Fig. 4-7. Plot of Sr (ppm) vs. Rb (ppm) for the basalts from the Warrawoona Group. Most samples have Rb/Sr ratio of 0.1 to 0.01, of which average is similar to Mantle (Jahn, 1989).

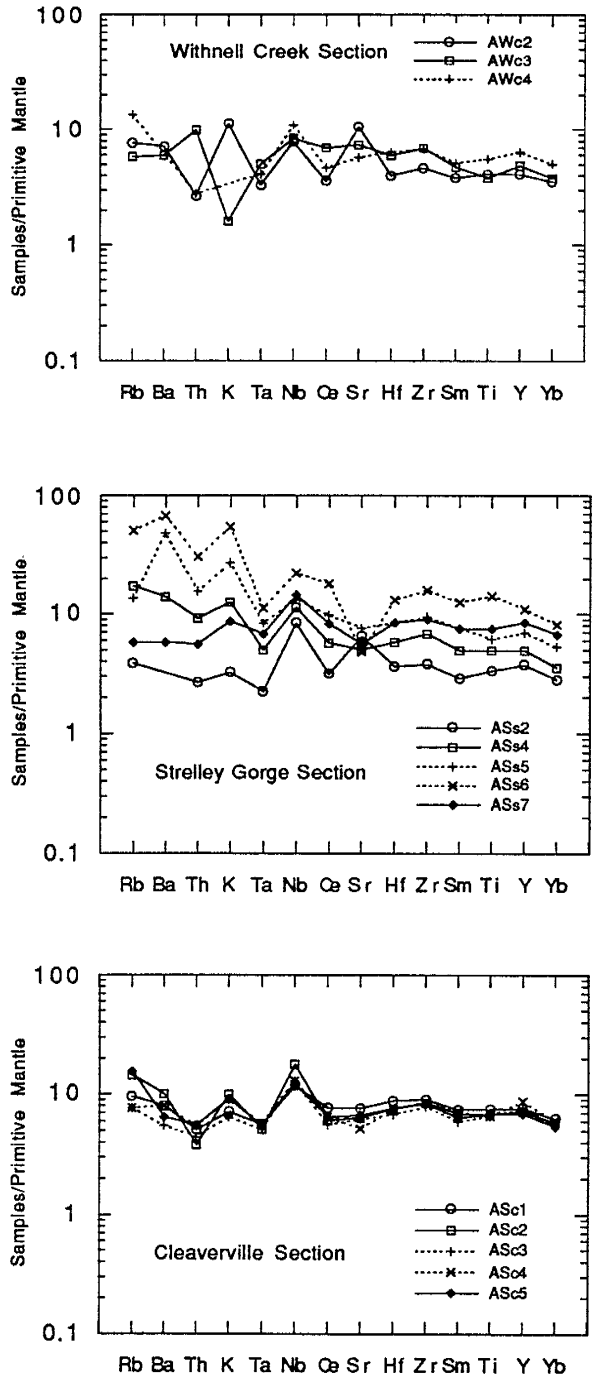

Fig. 4-8. Diagrams of incompatible elements distribution pattern to primitive mantle of basalts from the Apex Basalt.

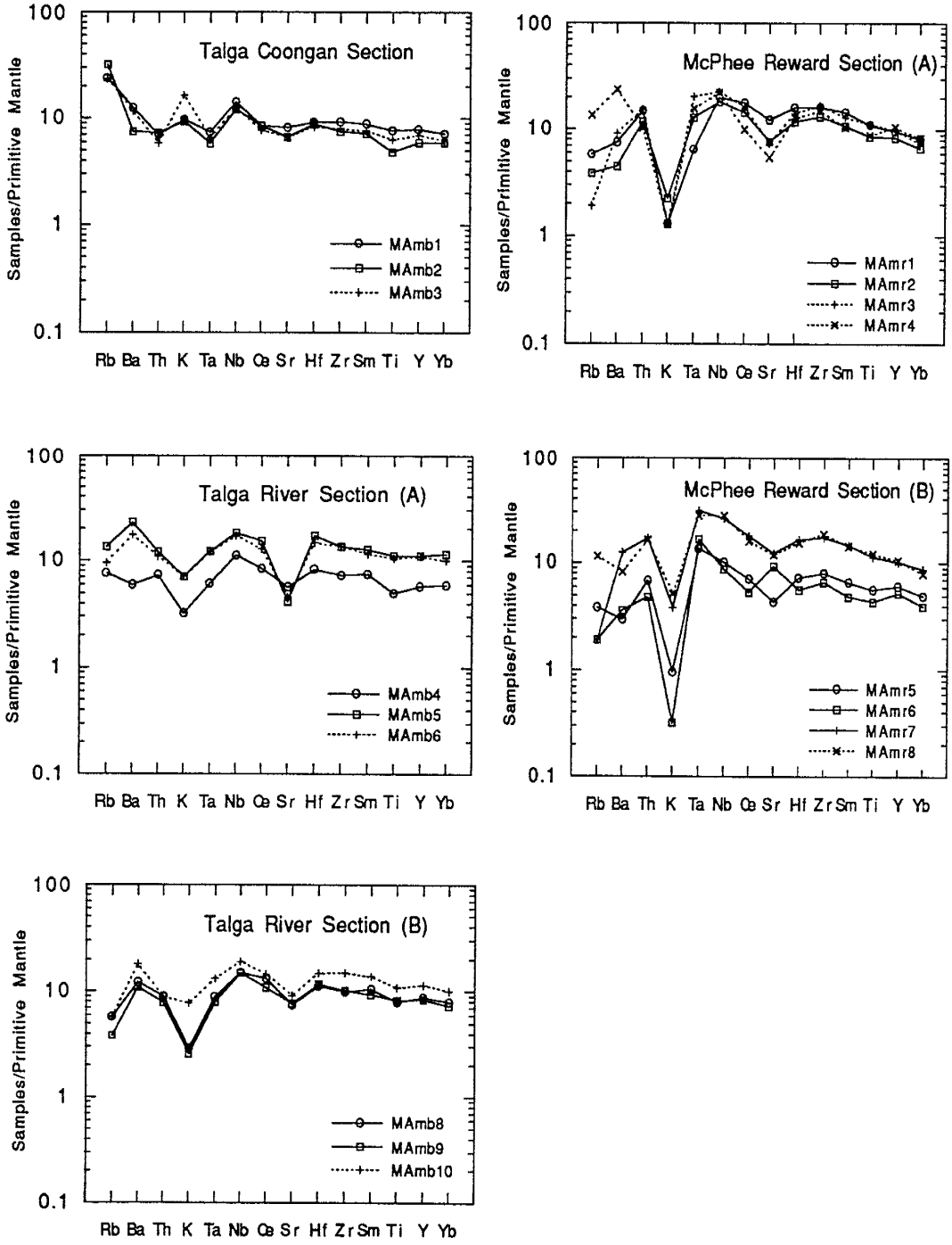

Fig. 4-9. Diagrams of incompatible elements distribution pattern to primitive mantle of basalts from the MOunt Ada Basalt

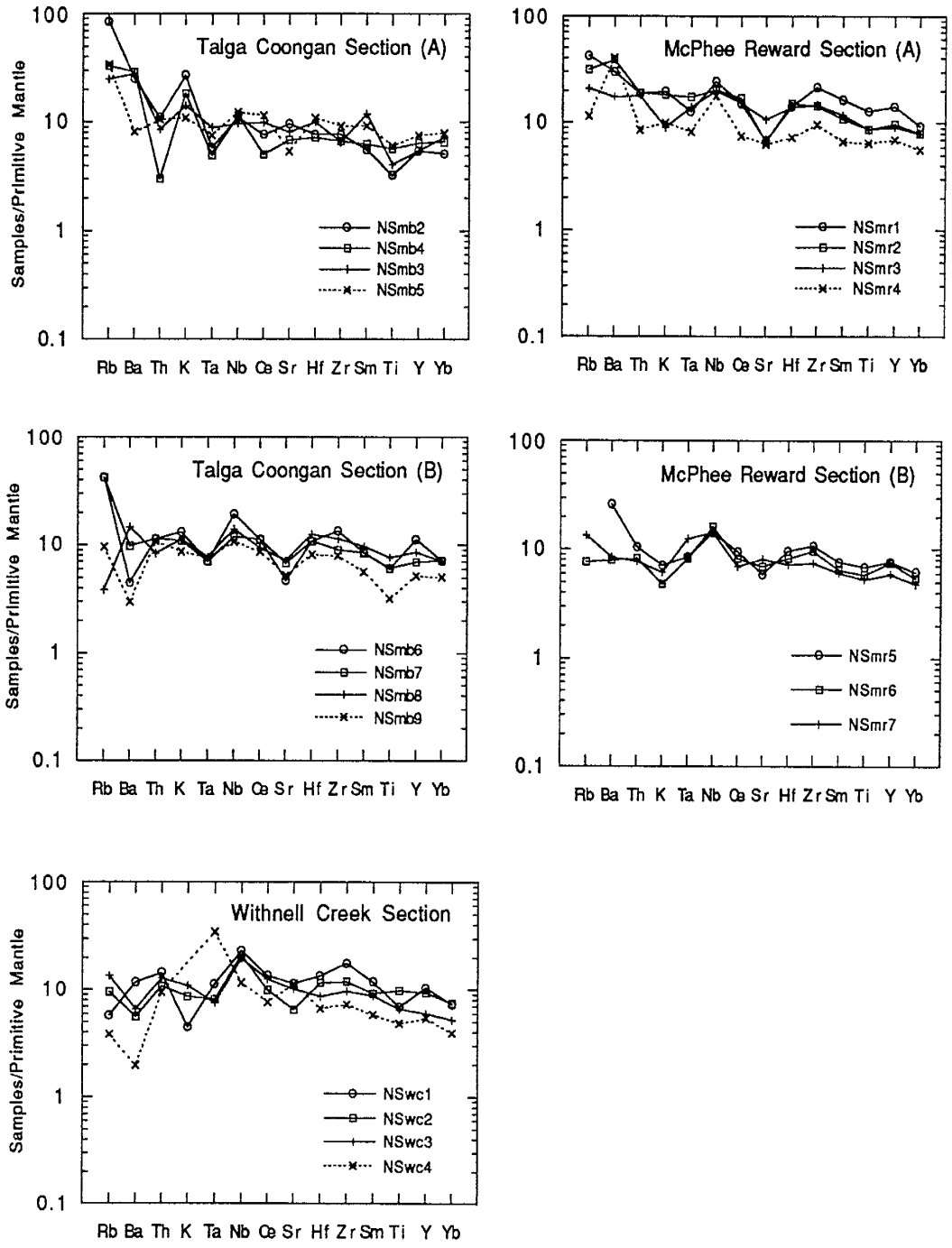

Fig. 4-10. Diagrams of basalts/Primitive Mantle patterns from the North Star Basalt.

Warrawoona Group may be affected by the alteration in the basalts. Compared to other Archean greenstone belts, the Warrawoona tholeiitic basalts have similar features of the both enrichment and depletion of K, Rb, Sr, and Ba(Jahn, 1977).

High Field Strength Elements (HFSE)

The incompatible elements Zr, Y, Nb, Hf, and Ta in Warrawoona tholeiites are compared to Primitive Mantle(PM) shown in Figure 4-8, 4-9 and 4-10. Zr, Hf and Ta are 10X PM, and Y is lower with 5X PM. Nb is slightly enriched with 20X PM, except for the Apex Basalt in the Strelley Gorge section and the North Star Basalt in the Talga Coongan section. The basalts of the Warrawoona Group show slightly greater concentrations of Nb than the Archean basalts described by Sun (1984), in which Nb is slightly depleted relative to Zr, Y, Hf, and Ta. Table 4 shows the average composition of Zr, Ti and Y for basalts from the Warrawoona Group, south India (Drury, 1982, Rajamani, 1984), Canada (Fryer, 1978, and Lafieche, 1991), northeastern Minnesota, and southwestern Greenland and two classes of Archean tholeiites (Condie, 1981). The average concentrations of TiO2 (1.3%), Zr (102.8 ppm), and Y (30.92 ppm) are slightly greater than tholeiites of other Archean greenstone belts, but the ratio of Zr/Y (3.28), Ti/Zr (77.43), and Ti/Y (249.9) are similar to other tholeiites. The average concentrations of Zr, Ti, Y, Nb, Hf, Ta of basalts of the Warrawoona Group are also similar to the 3.5 Ga tholeiitic basalts in the Onverwacht Group(Jahn, 1982). The Warrawoona Group basalts have ratio of Th/Yb, Ta?Yb similar to primitive mantle (shown in Fig. 4-11). The basalts have lower ratio of Hf/Th and Th/Yb than those of primitive mantle (Figure 4-12), but similar to those of PM. Compared to the modern basalts of ARCS, MORB, ALALI (Shervais, 1982), the Warrawoona Group basalts are similar to the basalts of ARCS and

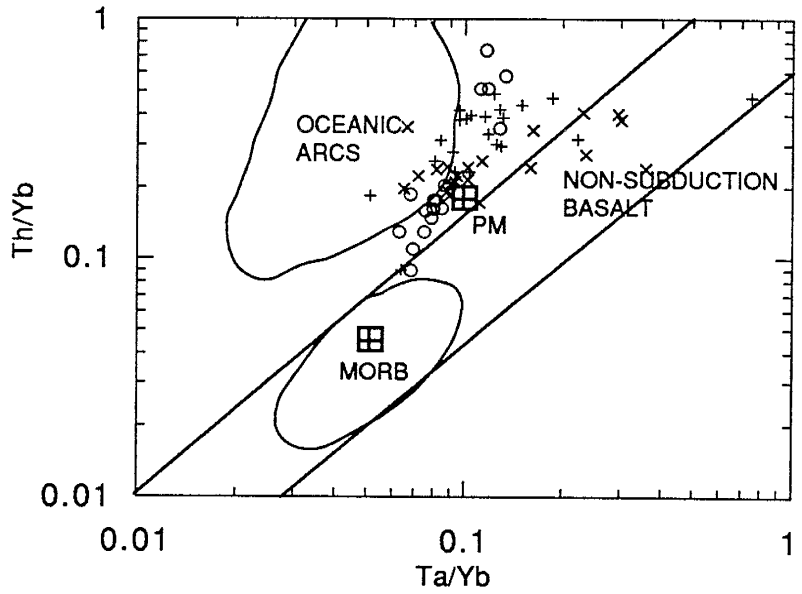

Fig. 4-11. Plot of Ta/Yb vs. Th/Yb for basalt of the Warrawoona Group compared to the fields of modern Oceanic ARC, MORB and NON-Subduction basalts (after Pearce1983).

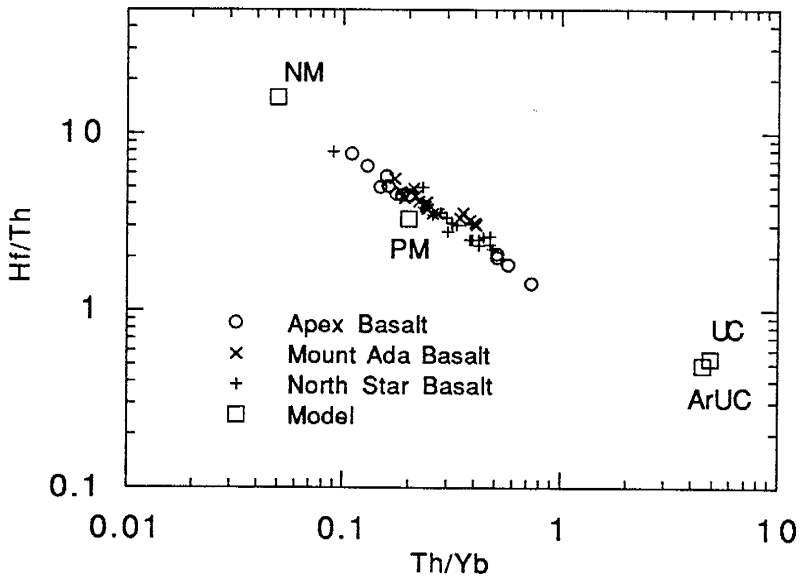

Fig. 4-12. Diagram of Hf/Th vs. Th/Yb for the basalts from the Warrawoona Group. PM: primitive mantle, NM: N-MORB, UC: upper continental crust, ArUC: Archean upper continental crust (from Condie, 1991).

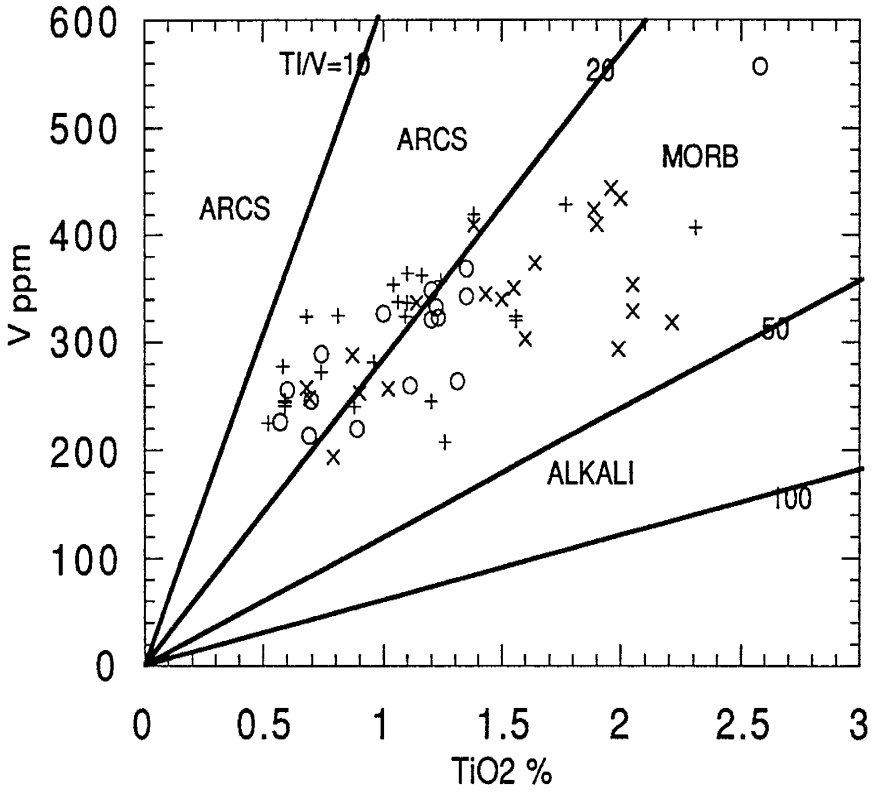

Fig.4-13. Diagram of TiO2 vs. V of basalts from the Warrawoona Group. Most samples plot into the area of ARCS and MORB, where the ARCS, MORB and ALKALI after Shervais (1982).

MORB in Figure 4-13. However, HFSE of Warrawoona tholeiitic basalts indicate that they have similar geochemical features to Archean DAT (especially earlier Archean tholeiites) in greenstone belts.

Rare Earth Element (REE)

Chondrite-normalized REE patterns of basalts from the Warrawoona Group are given in Fig. 4-14, 4-15, 4-16. Most tholeiitic basalts show very slight enrichment in LREE relative to HREE, and the overall patterns show 10 to 20 times chondritic abundances. Most basalts of the Warrawoona Group have the ratio of La_N/Yb_N ranging from 1.05 to 3.7, but the basalts of the Apex Basalt in the Cleavervill section have ratios of La_N/Yb_N from 0.75 to 1 showing slightly depleted LREE. The La_N/Sm_N ratios of the basalts vary from 0.71 to 2.9 and Gd_N/Yb_N from 0.96 to 1.56. Eu-anomalies are either slightly negative or positive (Eu/Eu^*=0.67-1.23), which compares to REE distribution in Archean low-K tholeiitic basalts.

Generally, the REE contents of Archean tholeiites are 6 to 15 times chondritic abundances (Jahn, 1977). Condie (1976, 1981) divided Archean tholeiites in the greenstones belts into: (1) DAT(depleted Archean tholeiites) is characterized by flat REE patterns (about 10x chondrites) with or without small Eu anomalies, and is comparable to MORB and island arc tholeiites; and (2) EAT(enriched Archean tholeiites) is characterized by enriched LREE and a sloping REE pattern, is comparable to ocean island or calc-alkaline tholeiites. He noted that DAT is the most common volcanic rock type in most greenstone belts composing 50-80% of a typical section, and that EAT becomes more abundant at higher stratigraphic levels in many belts although it appears to be absent in some (Condie, 1981). Fig. 4-17 shows the envelope and average

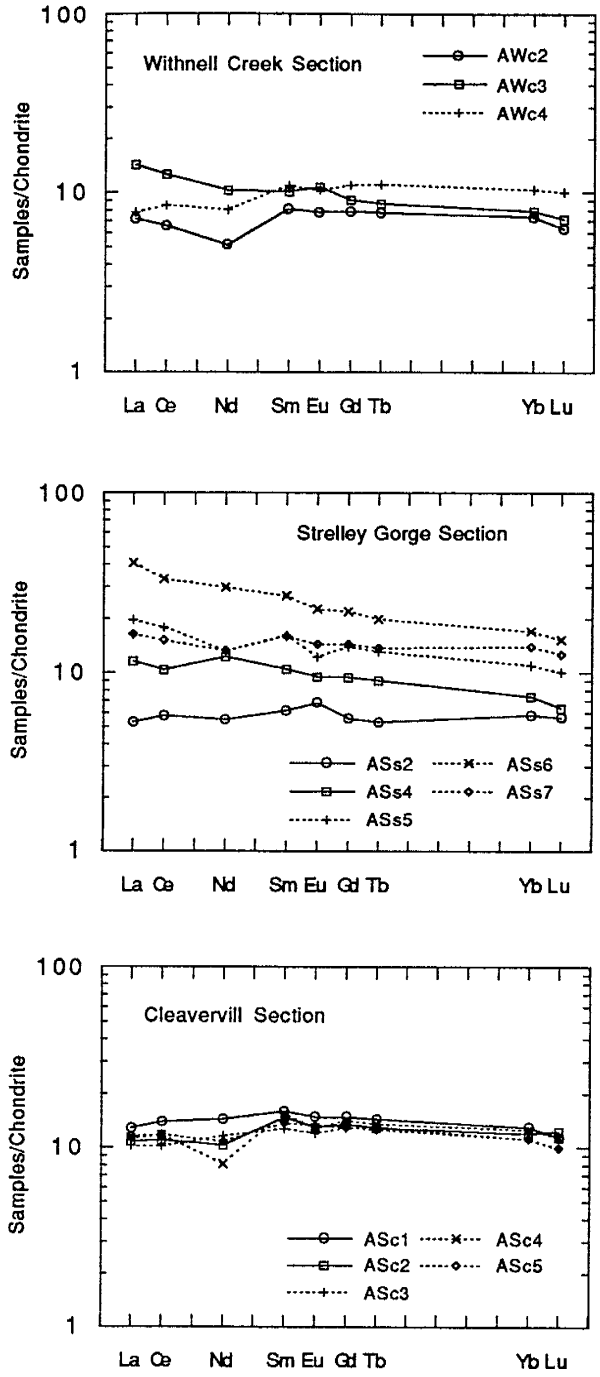

Fig.4-14 Rare-earth element (REE) distribution patterns of basalts from the Apex Basalt.

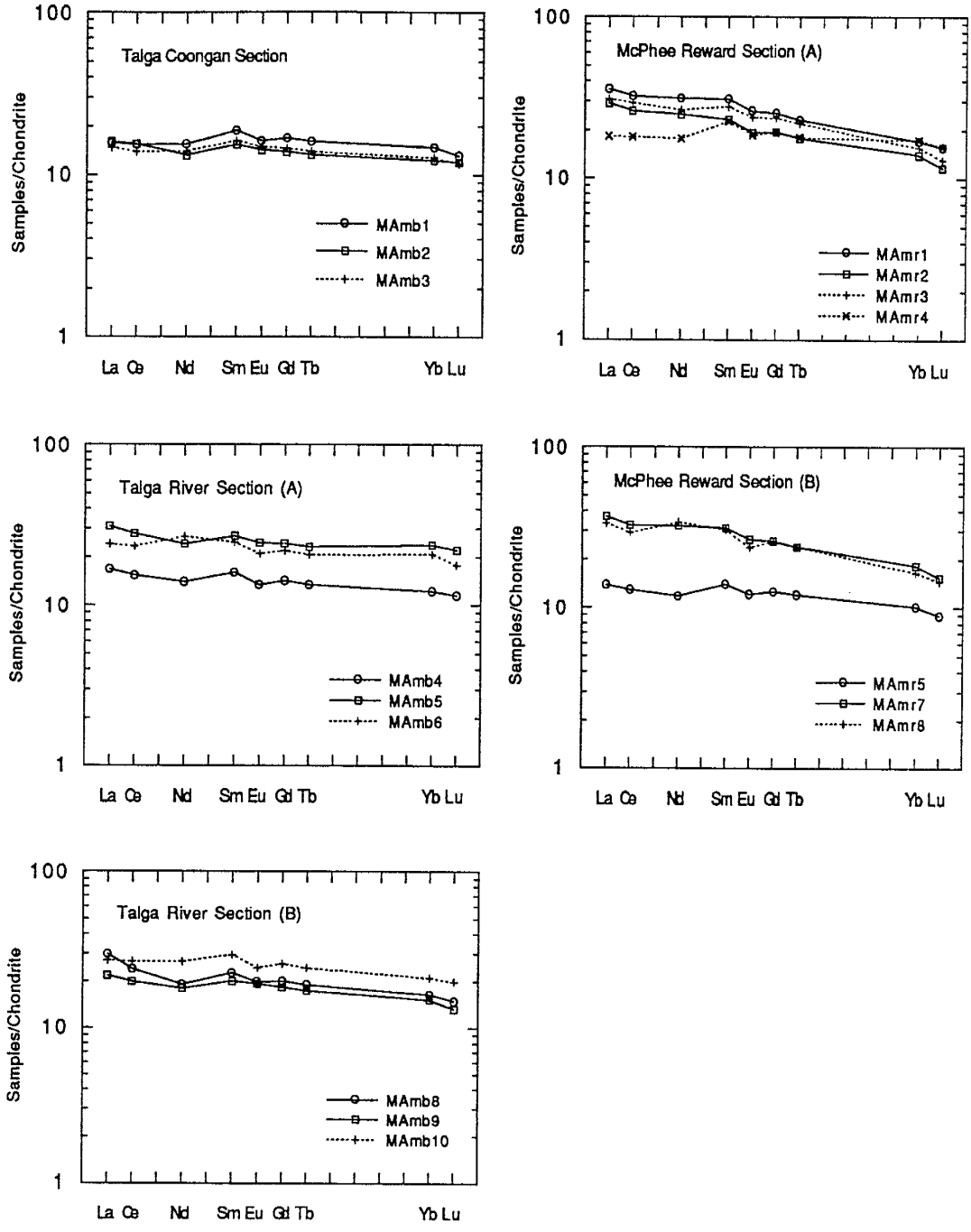

Fig.4-15 Rare-earth element (REE) distribution patterns of basalts from the Mount Ada Basalt.

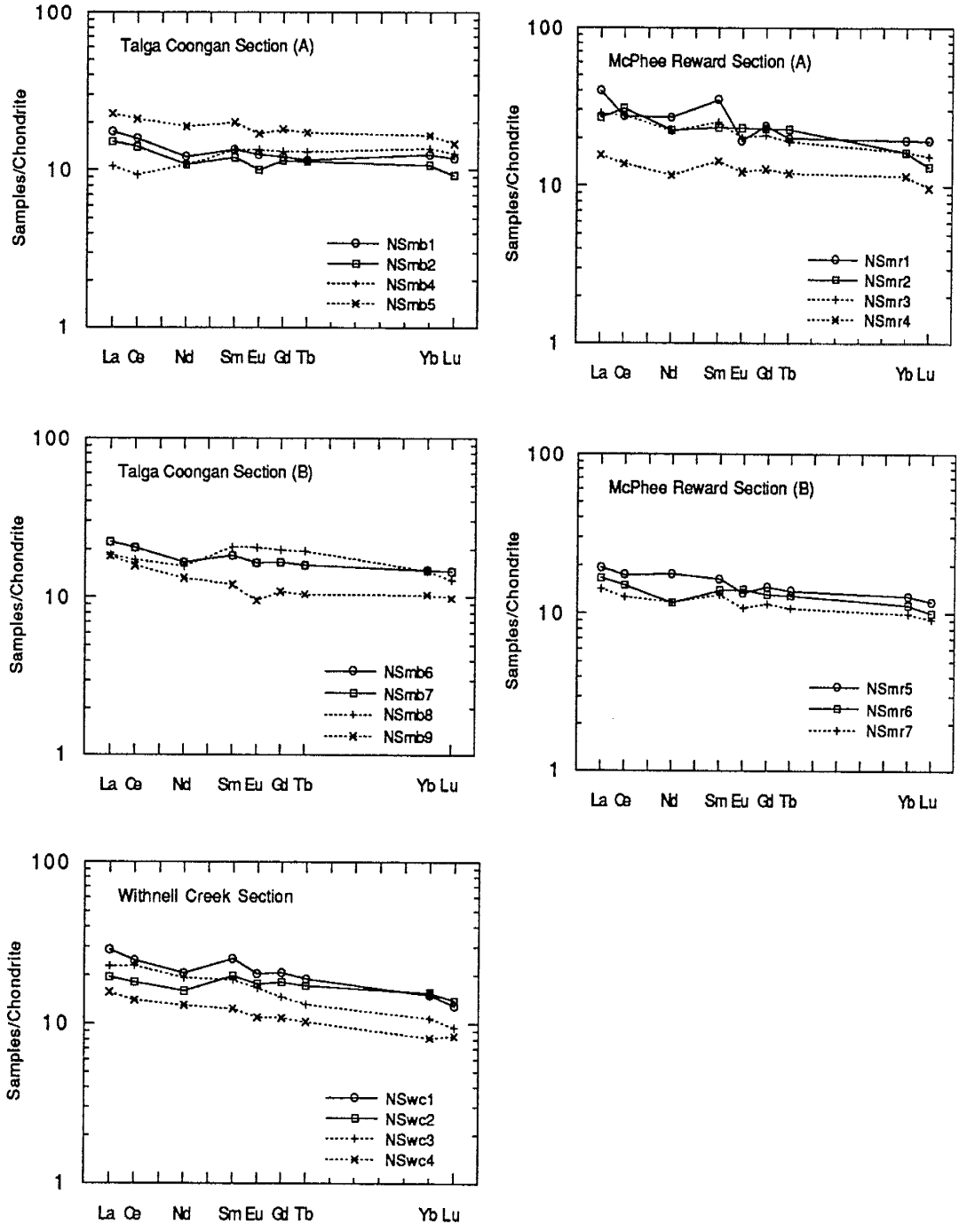

Fig.4-16 Rare-earth element (REE) distribution patterns of basalts from the North Star Basalt.

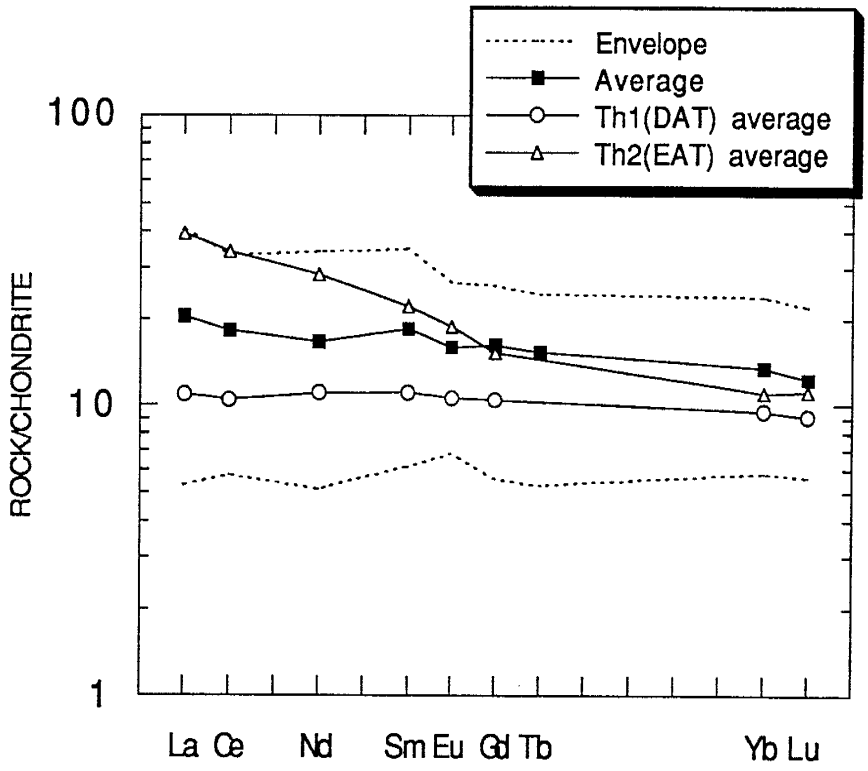

Fig. 4-17. Chondrite-normalized envelopes of variation (52 samples) of basalts in the Warrawoona Group, compared to the average of the Archean tholeiite group Th1 and Th2 (after Condie, 1981)

REE distribution pattern of Warrawoona basalts and averages of DAT and EAT described by Condie (1981). REE distribution patterns of the tholeiitic basalts of the Warrawoona Group parallel to the Archean DAT with a flat pattern, and different from EAT with LREE enrichment. The REE patterns of the Warrawoona Group are still similar to the 3.5 Ga tholeiites in the Onverwacht Group (Jahn, 1982).

B. Stratigraphic Geochemistry

1. Talga Talga Subgroup in the McPhee Reward Section

McPhee Reward section located in the eastern of Pilbara Block is well exposed, and is consists of the North Star Basalt, McPhee Formation, and Mount Ada Basalt, from the base upwards. Figure 4-18 shows the stratigraphic column of McPhee Reward section, in which the sample positions of the basalts are given. The total thickness of the three formations is about 4500 meters, including about 3000 meters of basalt, 700 meters of dolerite or gabbro, 500 meters of high-Mg basalts, 100 meters of peridotite, and 200 meters of altered ultramafic rock.

Major elements show a general upward decrease in TiO_2, FeO, CaO, Na_2O and K_2O, and increase in SiO_2, Al_2O_3, (shown in Figure 4-19, and in Table B-4 and B-6). Incompatible elements Th, Sr, V, Zr, Nb, Y, Hf, Ta, REE generally decrease upward, shown in Figure 4-20, 4-21 and 4-22. But some LIL elements (Rb, U, K) show upward increases in the North Star Basalt, and scatter in the Mount Ada Basalt. Rb, U, and K are mobile elements during alteration, so that they cannot explain the variation in composition of the basalts in the stratigraphic column. The lowest units in Mount Ada Basalt have higher Ti2O,

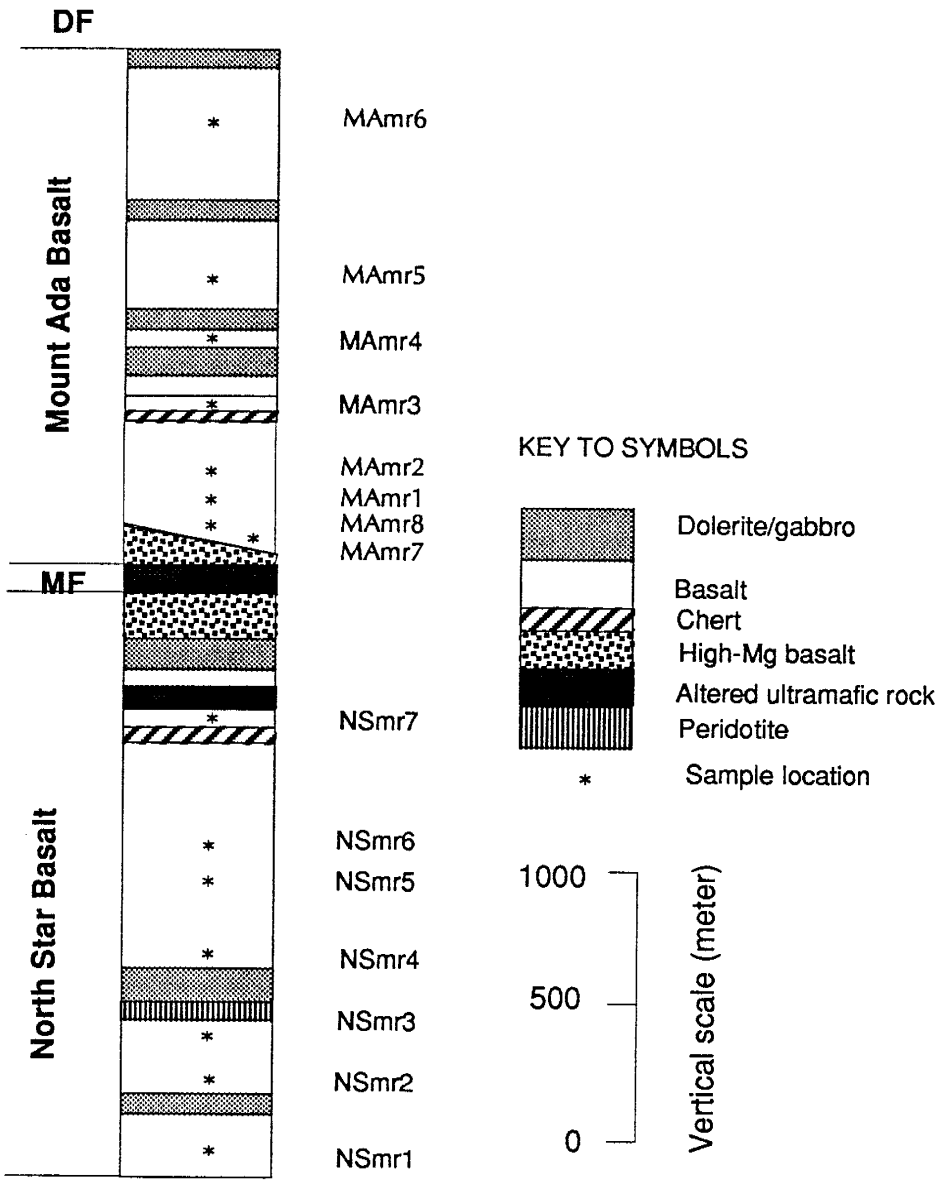

Fig. 18. Stratigraphic column of McPhee Reward section showing the different lithologies of the Talga Talga Subgroup and Duffer Formation as well as sampling localities. MF-McPhee Formation, DF-Duffer Formation.

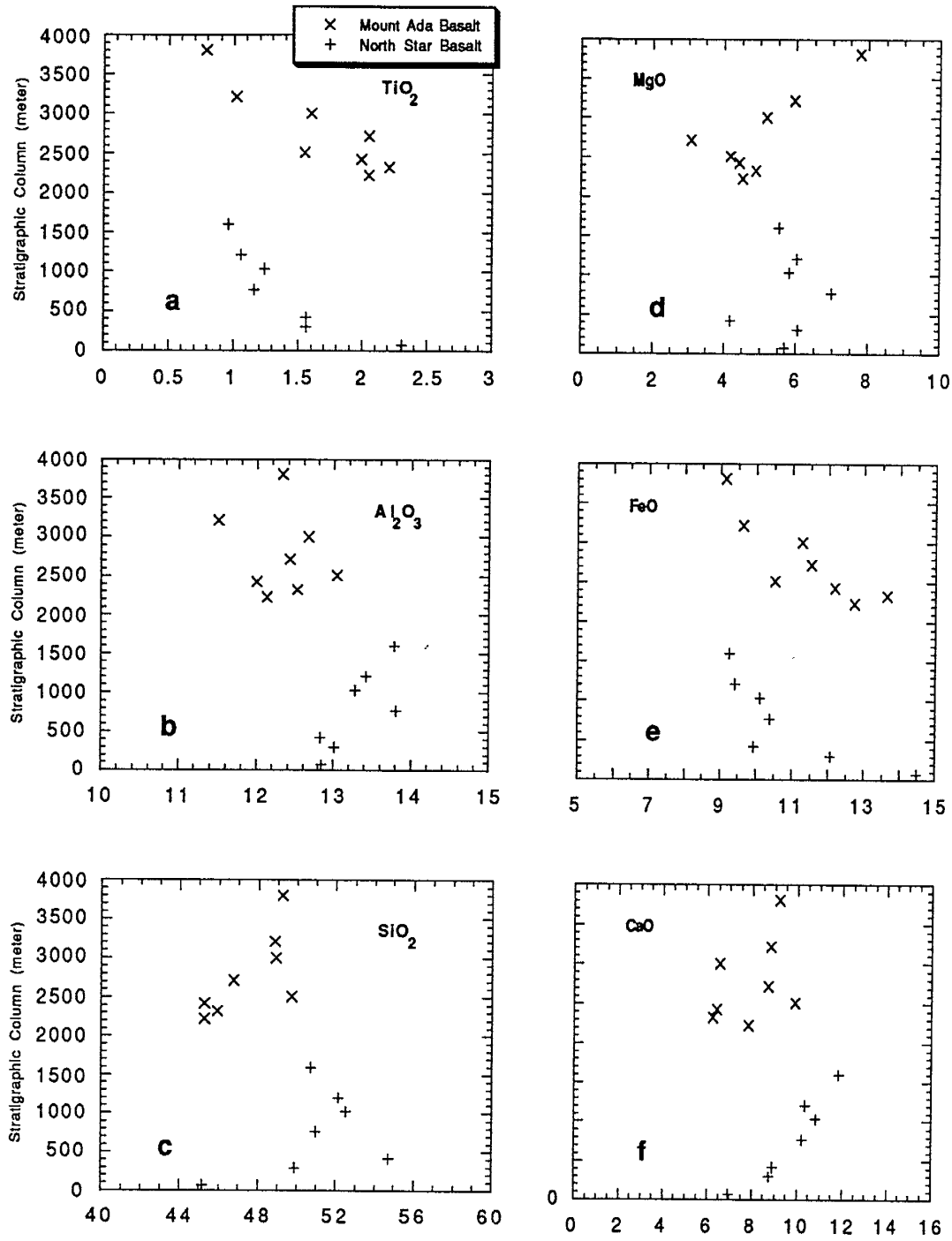

Fig. 4-19. Stratigraphic-geochemical columnar plots of the McPhee Reward section through the North Star Basalt and the Mount Ada Basalt. The vertical scale relates to stratigraphic level above the base of the North Star Basalt. The McPhee Formation is positioned between 2100 and 2200 metres.

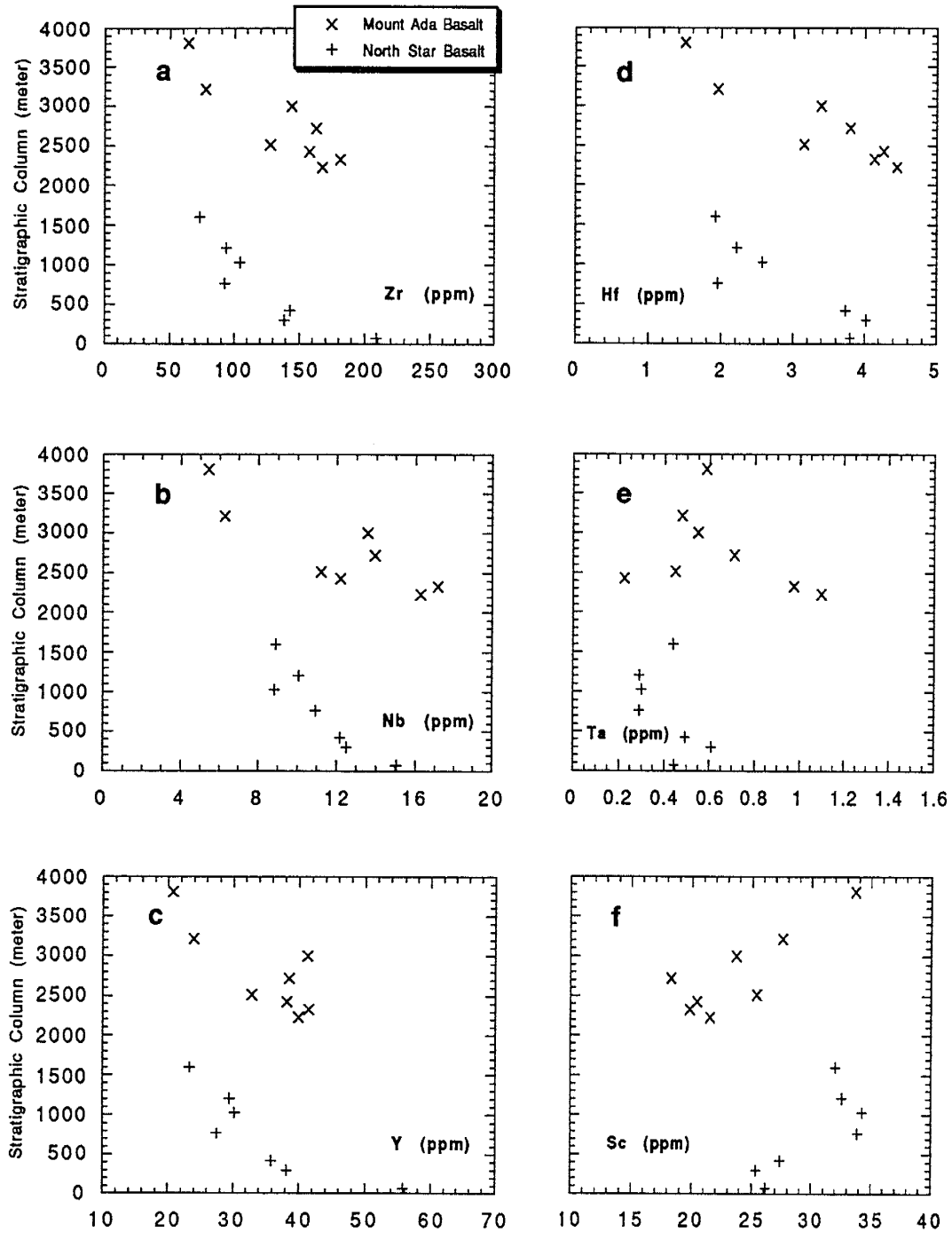

Fig. 4-20. Stratigraphic-geochemical columnar plots of the McPhee Reward section through the North Star Basalt and the Mount Ada Basalt. The vertical scale relates to stratigraphic level above the base of the North Star Basalt. The McPhee Formation is positioned between 2100 and 2200 metres.

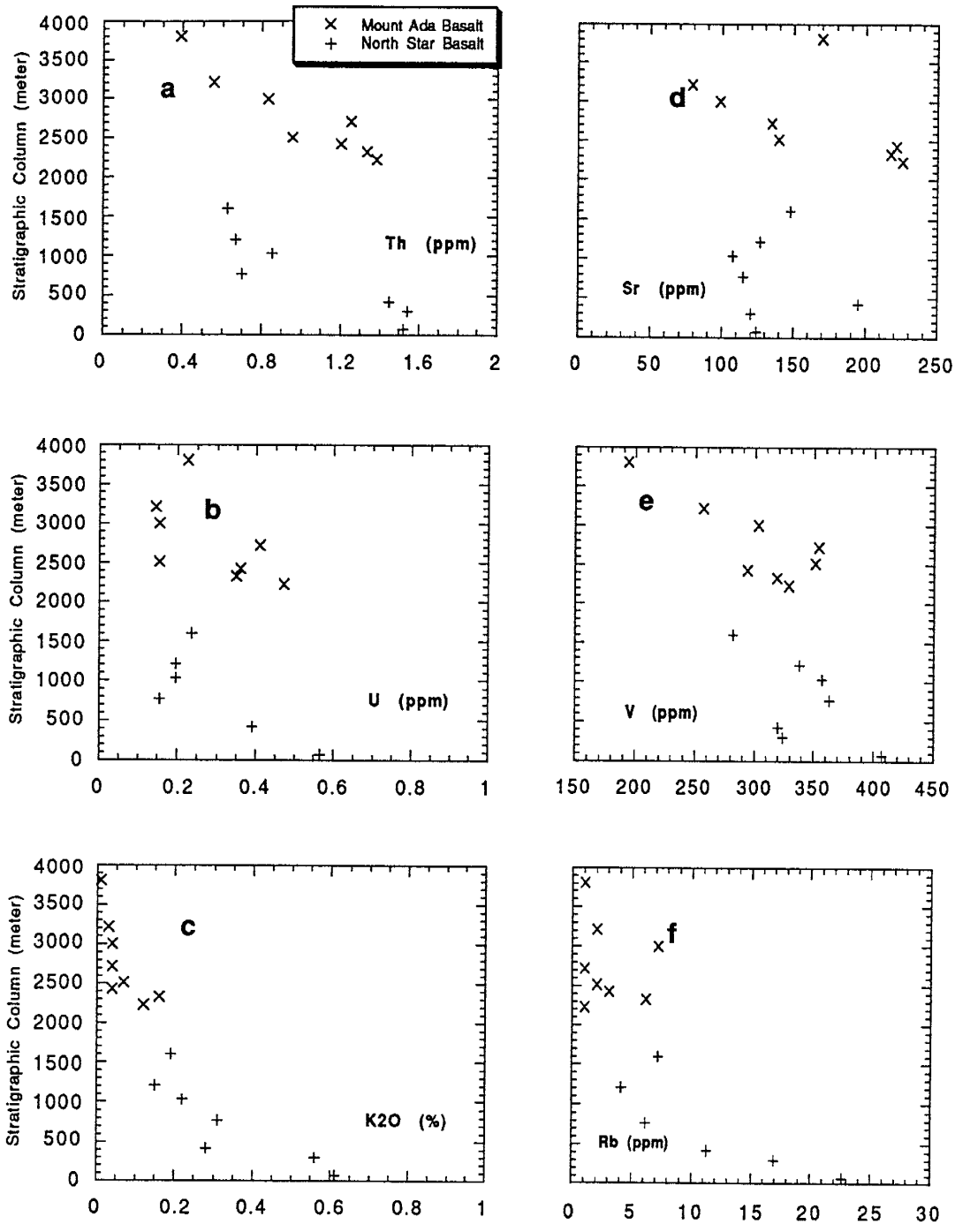

Fig. 4-21. Stratigraphic-geochemical columnar plots of the McPhee Reward section through the North Star Basalt and the Mount Ada Basalt. The vertical scale relates to stratigraphic level above the base of the North Star Basalt. The McPhee Formation is positioned between 2100 and 2200 metres.

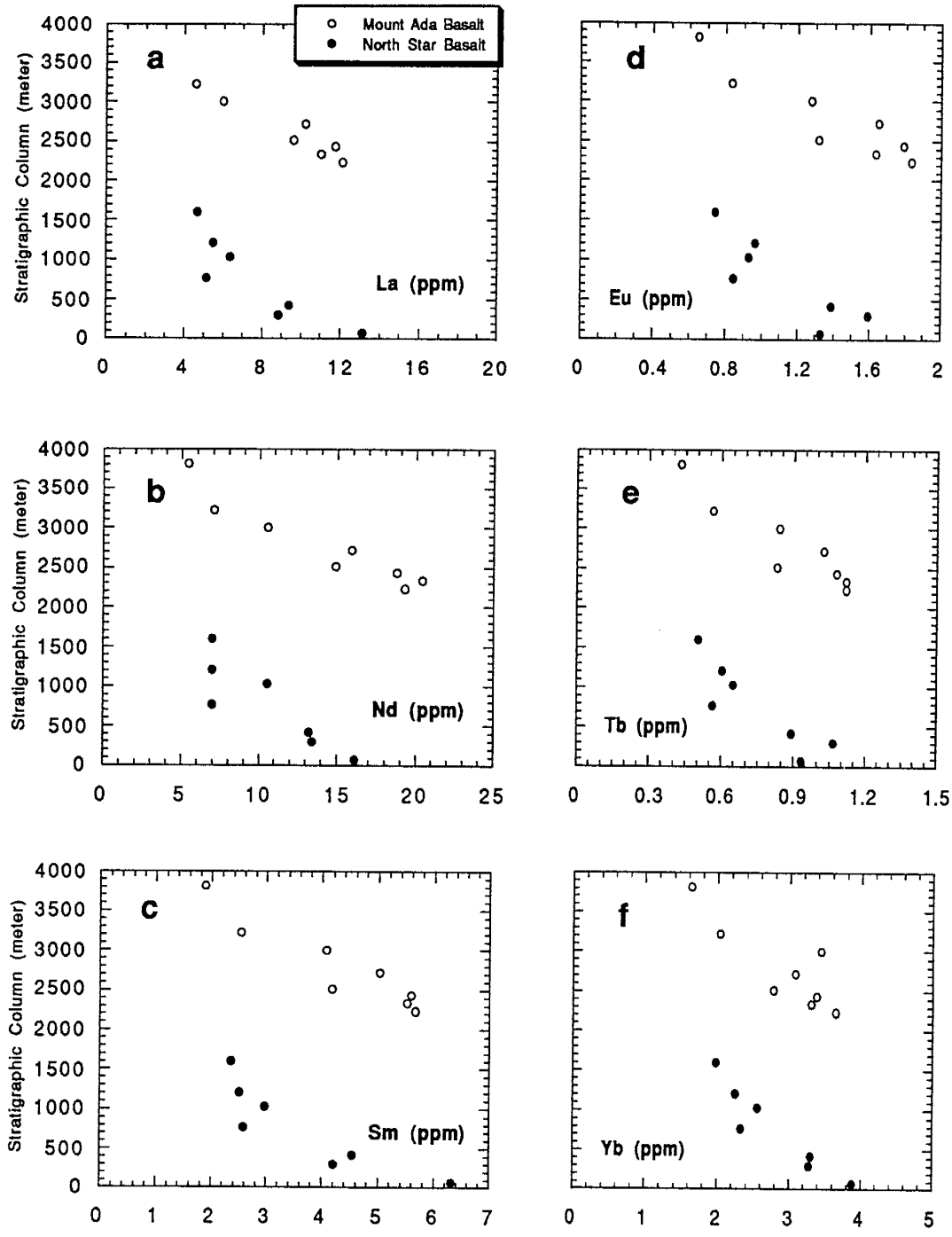

Fig. 4-22. Stratigraphic-geochemical columnar plots of the McPhee Reward section through the North Star Basalt and the Mount Ada Basalt. The vertical scale relates to stratigraphic level above the base of the North Star Basalt. The McPhee Formation is positioned between 2100 and 2200 metres.

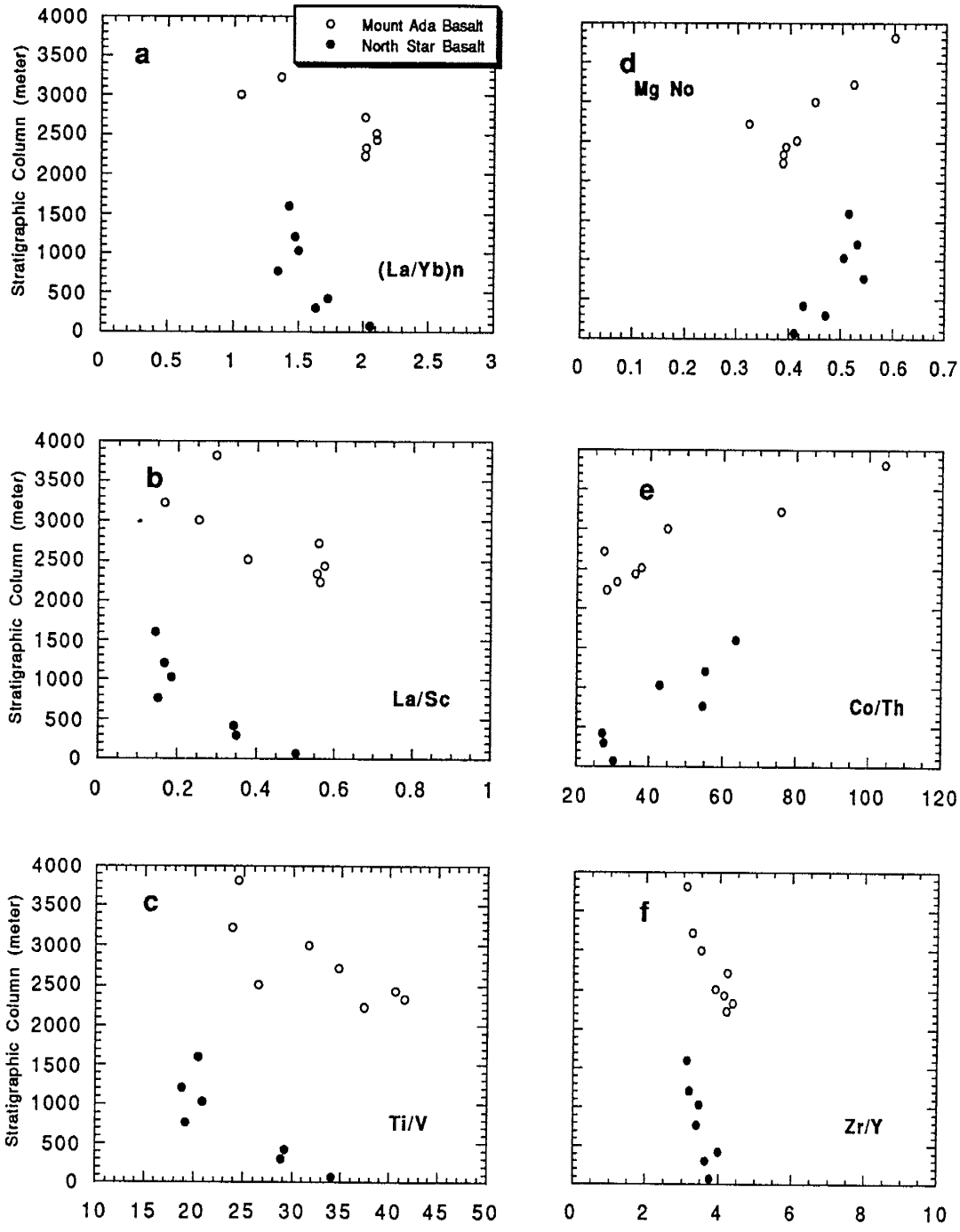

Fig. 4-23. Stratigraphic-geochemical columnar plots of the McPhee Reward section through the North Star Basalt and the Mount Ada Basalt. The vertical scale relates to stratigraphic level above the base of the North Star Basalt. The McPhee Formation is positioned between 2100 and 2200 metres.

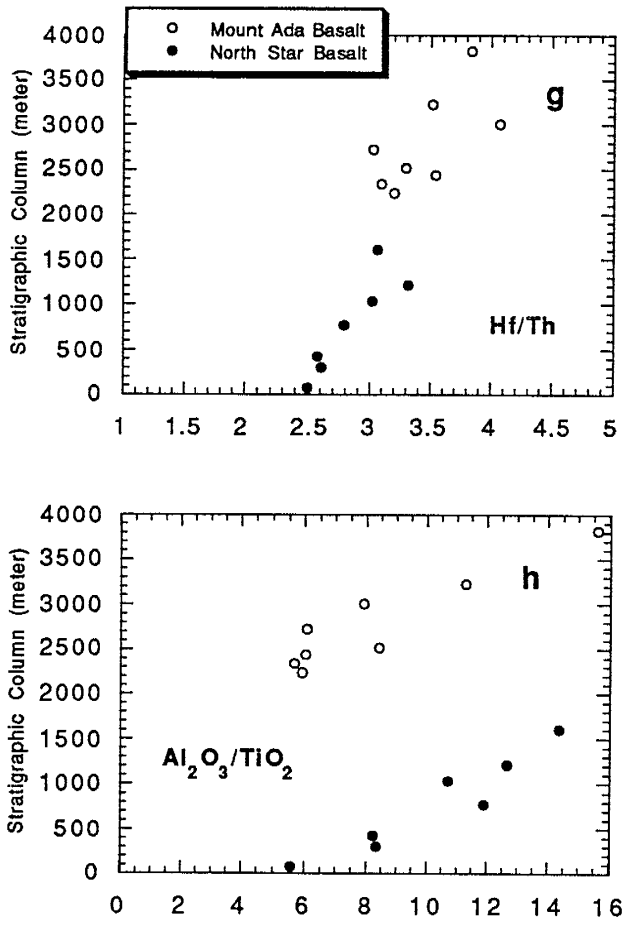

Fig. 4-23. Stratigraphic-geochemical columnar plots of the McPhee Reward section through the North Star Basalt and the Mount Ada Basalt. The vertical scale relates to stratigraphic level above the base of the North Star Basalt. The McPhee Formation is positioned between 2100 and 2200 metres.

FeO, Sr, Zr, Nb, Y, REE, V, and lower SiO2, K2O, Rb and Ba than the highest units of the North Star Basalt. The upward change in compositions show a discontinuity between the North Star Basalt and Mount Ada Basalt, which implies two cycles of the basalt eruption.

Ratios of $(La/Yb)_N$, La/Sc, Zr/Y, and Ti/V decrease upward, and ratios of Al_2O_3/TiO_2, Hf/Th, Co/Th, and Mg number increase upward (Figure 4-23). Both the increasing and decreasing trends show the geochemical discontinuity between the North Star Basalt and the Mount Ada Basalt.

The progressive depletion in Ti, Fe, Th, Zr, Y, Hf, REE in the North Star basalts and Mount Ada basalts, indicate that incompatible elements decrease with time, which implies the origin of basalt changed with time. The overall trend and repeated smaller-scale cycles are relative to the evolution of the mantle source. Glikson and Hickman (1981) described that the progressive depletion in Fe, Ti Zr and Y constituting both an overall trend and repeated smaller-scale cycles cannot be explained by magmatic fractionation, and reflect secular mantle depletion owing to repeated partial melting events and/or progressively deeper melting in a geochemically zoned low-velocity zone.

The progressive depletion of the Ti, Fe, Th, Zr, Y, Hf, and REE in the basalts in the Talga Talga Subgroup, constituting both an overall trend and repeated smaller-scale cycles in the McPhee Reward section also appear in the other sections including Talga Coongan section, Withnell Creek section and Talga River section (data shown in Table C-3 to C-7), which discussed by Glikson and Hickman (1981).

2. Salgash Subgroup in the Sandy Creek section

Apex Basalt of the Salgash Subgroup, especially in Camel Creek section and Sandy Creek section, shows opposite trends with increasing incompatible element concentrations (Glikson and Hickman, 1981). The difference in trends of incompatible elements between the Talga Talga Subgroup and Salgash Subgroup reflect different origin of the basalts in both subgroups. The progressive enrichment in Ti, Fe, Th, Zr, Y, Hf, REE in the Apex basalts and Euro basalts, indicate that incompatible elements increase with time (Glikson, 1981). The progressive enrichment in Fe, Ti Zr and Y and REE constituting both an overall trend and repeated smaller-scale cycles can be explained by magmatic fractionation.

V. Origin of Basalt in Warrawoona Group

A. Geochemical Models

Tholeiitic basalt can form by 10-30% melting of mantle peridotite, leaving a residue of olivine+orthopyroxene+clipyroxene (Wilson, 1989, and Hess, 1989, Green, 1971), or by fractional crystallization of picritic or komatiitic liquids (Arndt, 1977). The effects of contamination on the geochemical characteristics of magmas during the process of fractional crystallization were studied by McBirney (1979), DePaolo (1981), and Powell (1984). The formation of basalt has generally been conceptualized in terms of discrete and relatively simple stages in the generation and evolution of magma (DePaolo, 1981). The mode of the partial melting, fractional crustallization and assimilation and fractional crystallization will be discussed below.

1. The model of partial melting

Partial melting is classified into two models (Wilson, 1989): (a) Equilibrium or batch melting: the partial melt formed continually reacts and equilibrates with the crystalline residue until the moment of segregation. (b) Fractional or Rayleigh melting: the partial melt is continuously removed from the system as soon as it is formed, so that no reaction with the crystalline residue is possible.

Simple models have been developed to quantify the changes in trace element concentrations which occur during partial melting. The basic equations were given by Wood and Fraser (1976), which serve to illustrate the basic principles and the limiting effects of simple igneous processes. For the case of

batch melting, the concentration of a trace element in the liquid C_L is related to that in the original solid C_L^0 by the expression (Wilson, 1989):

$$\frac{C_L}{C_L^0} = \frac{1}{D(1-F)+F} \qquad (5\text{-}1)$$

Where $D=\sum_i X_i D_i$, and X_i is the weight fraction of phase i in the mineral assemblage and D_i is crystal-liquid partition coefficient. F is the weight fraction of melt formed, and D is the bulk distribution coefficient for the residual solids at the moment when melt is removed from the system. Obviously, in order to define D it is necessary to calculate the proportions of residual minerals, and so the above expression is often formulated in terms of the initial proportions and the relative melting rates of the different solid phases. Clearly, with increasing degrees of partial melting, different minerals may be progressively consumed, causing discontinuous changes in the value of D. This is particularly important in the partial melting of possible mantle materials since minor phases such as garnet, amphibole, biotite and clipyroxene, in general, complete their melting significantly earlier than olivine and orthopyroxene.

2. Fractional crystallization

The mathematical relations are used to model the quantity of trace elements in igneous systems is very similar to the partial melting model, but the processes of both fractional crystallization and partial melting are different. During batch melting or equilibrium fusion, equilibrium fusion requires that perfect equilibrium be obtained between the melt and the solid residue during the entire melting process, until the magma escapes from the zone of melting. The batch melting equation describes (Shaw, 1970):

$$\frac{C_L}{C_L^0} = \frac{1}{D(1-F)+F} \qquad (5\text{-}2)$$

where C_L^0 is the initial concentration of the element in the rock, C_L is the concentration of the element in the melt after some fractionation, F, of the rock is melted, and D is the bulk distribution coefficient of the solid residue. D is given as the sum

$$D=\sum_i X_i D_i$$

where X_i is the weight fraction of each mineral in the residue (that is, the mode of the residue) and D_i is the crystal/liquid distribution coefficient for each mineral. In effect, D is the distribution coefficient of a fictitious phase that has the same distribution coefficient as the weighted average of the mineral assemblage.

For the case of perfect fractional crystallization (Rayleigh fractionation):

$$\frac{C_L}{C_L^0} = F^{(D-1)} \qquad (5\text{-}3)$$

Where symbols of C_L, C_L^0, F and D have same meanings to equation 5-2.

3. Assimilation and fractional crystallization (AFC)

Crustal contamination occurred in the eruption of basalts, which can be used to explain some of the geochemical differences between oceanic tholeiites (MORB and OIB) and continental tholeiites. DePaolo (1981) and Powell (1984) have developed equations describing trace element behaviour

during concurrent assimilation and fractional crystallization. The mathematical equation on any trace element was given by DePaolo (1981):

$$C_L = C_L^0 f + \frac{r}{r-1+D} C_a (1-f) \qquad (5\text{-}4)$$

$$f = F^{-(r-1+D)/(r-1)} \qquad (5\text{-}5)$$

where C_L^0 is the concentration of the trace element in the original magma; C_L is the concentration of the trace element in the contaminated magma; C_a is the concentration of the trace element in contaminate; r is the ratio of the rate of assimilation to the rate of fractional crystallization; D is the bulk distribution coefficient for the fractional assemblage; and F is the fraction of magma remaining. Note that the derivation of this equation assumes that r and D are constants.

B. Implications for Basalt Origin in the Warrawoona Group

The incompatible elements indicate that the Talga Talga Subgroup is different from the Salgash Subgroup. Both overall trend and small cycles of basalts of the Talga Talga Subgroup show progressively decreasing incompatible elements, but those of the Salgash Subgroup show progressively increasing incompatible elements (Glikson, 1981). This difference is also shown by a local stratigraphic unconformity between the both subgroups.

1. Talga Talga Subgroup

Plot of Zr/Nb vs. Hf/Ta (Fig. 5-1) shows that basalts of the Talga Talga Subgroup plot near primitive mantle (Hofmann 1988), but are not related to depleted sources and enriched source of mantle (Condie, 1991). The

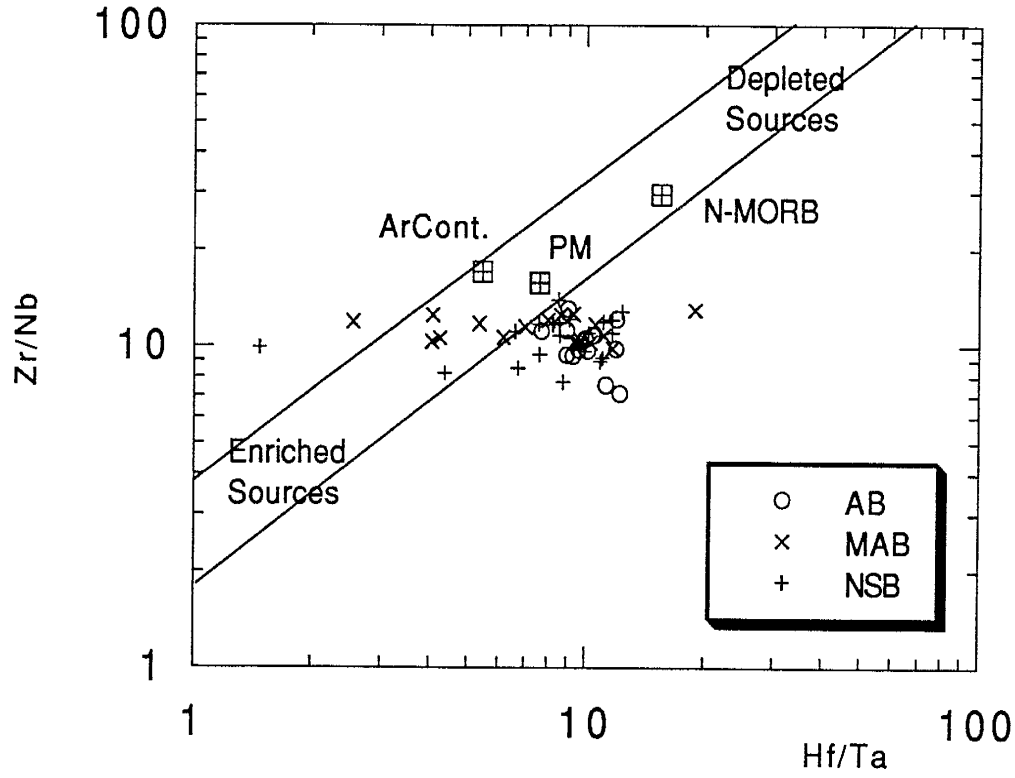

Fig. 5-1. Diagram of Zr/Nb vs. Hf/Ta of basalts from the Warrawoona Group: AB-Apex Basalt, MAB-Mount Ada Basalt, NSB-North Star Basalt. PM and N-MORB(Hofmann, 1988), ArCont-Archean continental crust. (Condie, 1991).

geochemical similarities of relations to primitive mantle are also given by the Th/Yb, Ta/Yb and Hf/Th ratios in Figure 4-11 and 4-12. These diagrams indicate that basalts of Talga Talga Subgroup are not mixtures of primitive mantle and early Archean continental crust. As a result, the source of the basalts was from the primitive mantle.

The upward decreasing trends of incompatible elements in McPhee Reward section (Figure 4-20, 4-21 and 4-22) imply that concentration of incompatible elements decreased during the eruption of the basalts. This process shows that the basalts were probably derived from the partial melting of primitive mantle (Jahn, 1982, 1984, Wilson, 1989, Condie, 1981).

Based on equation 5-1 of the batch melting model, we can get a series of REE patterns for degree of partial melting ranging from 0 to 50% (in Figure 5-2), assuming that the parent source and residual solids are the primitive mantle (Hofmann, 1988) and komatiites with olivine:orthopyroxene:clipyroxene =70:20:10 (Condie, 1991). Komatiites of the Talga Talga Subgroup in the eastern Pilbara Block discussed by Glikson (1981) probably are the residual solids separated from liquids composed of tholeiitic basalts derived from primitive mantle. In Figure 5-2, the envelope of REE patterns of basalts of the Talga Talga Subgroup plot between 5% and 20% and the average of the basalts is close to the 10% curve. In Figure 5-3a of $(La/Sm)_N$ vs. La_N, most basalts of the North Star Basalt and Mount Ada Basalt record 5-20% melting degree of PM source, and distributions of 38 samples of NSB and MAB are different from the Apex Basalt.

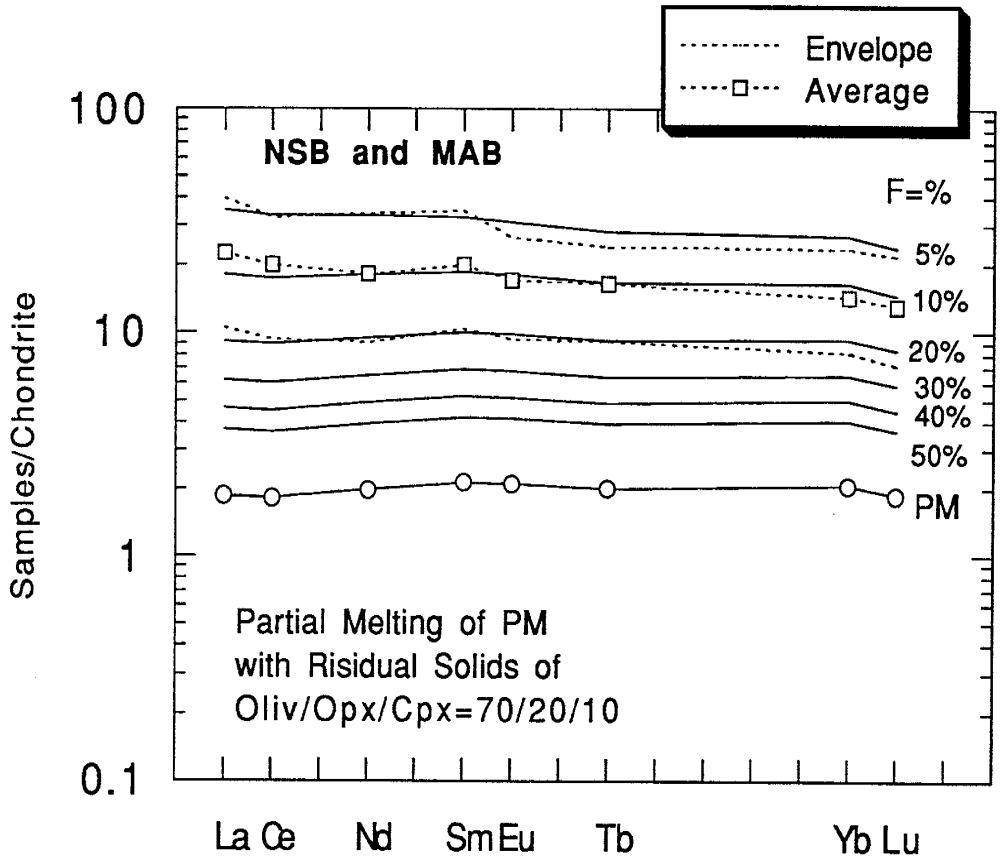

Fig. 5-2. Diagram of chondrite normalized REE patterns of average of 38 basalts from the Talga Talgal Subgroup and 0-50% melting curves of the primitive mantle (Hofmann, 1988), with residual solids of 70% olivine, 20% orthopyroxene and 10% clipyroxene.

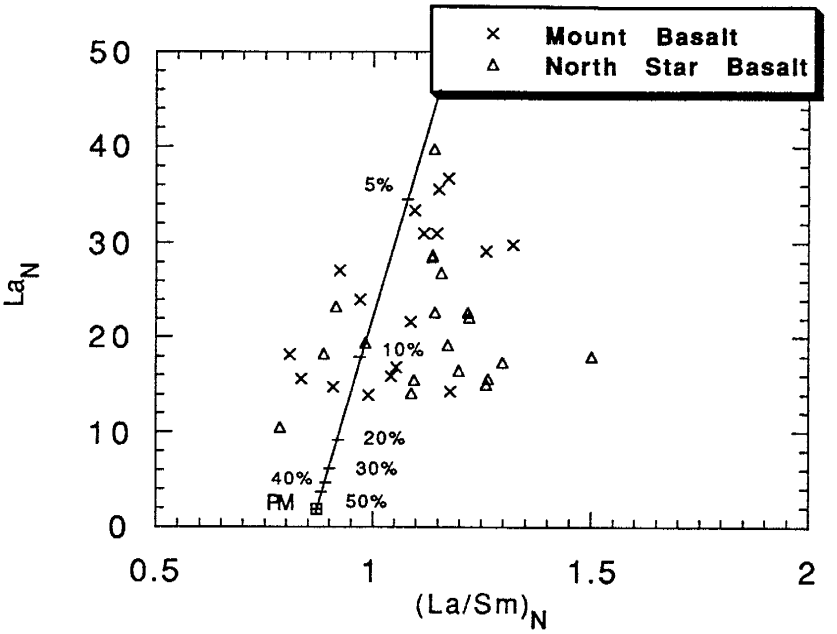

Fig. 5-3a. Diagram of (La/Sm)N vs. LaN of 38 balalts from the Talga Talga Subgroup. The solid line shows partial melting of primitive mantle (Hafomann, 1988), with 0-50% of melting degree assuming residual solids of 70% olivine, 20% orthopyroxene and 10% clipyroxene.

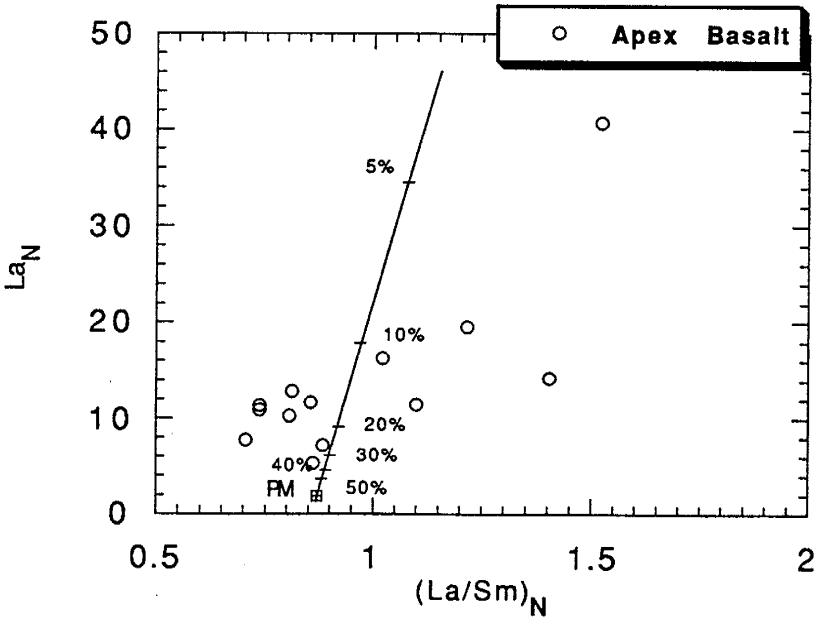

Fig. 5-3b. Diagram of (La/Sm)N vs. LaN of 38 balalts from the Salgash Subgroup. The solid line shows fractional crystallization of primitive mantle (Hafomann, 1988), with 0-50% of melting degree crystallization solids of 70% olivine, 20% orthopyroxene and 10% clipyroxene.

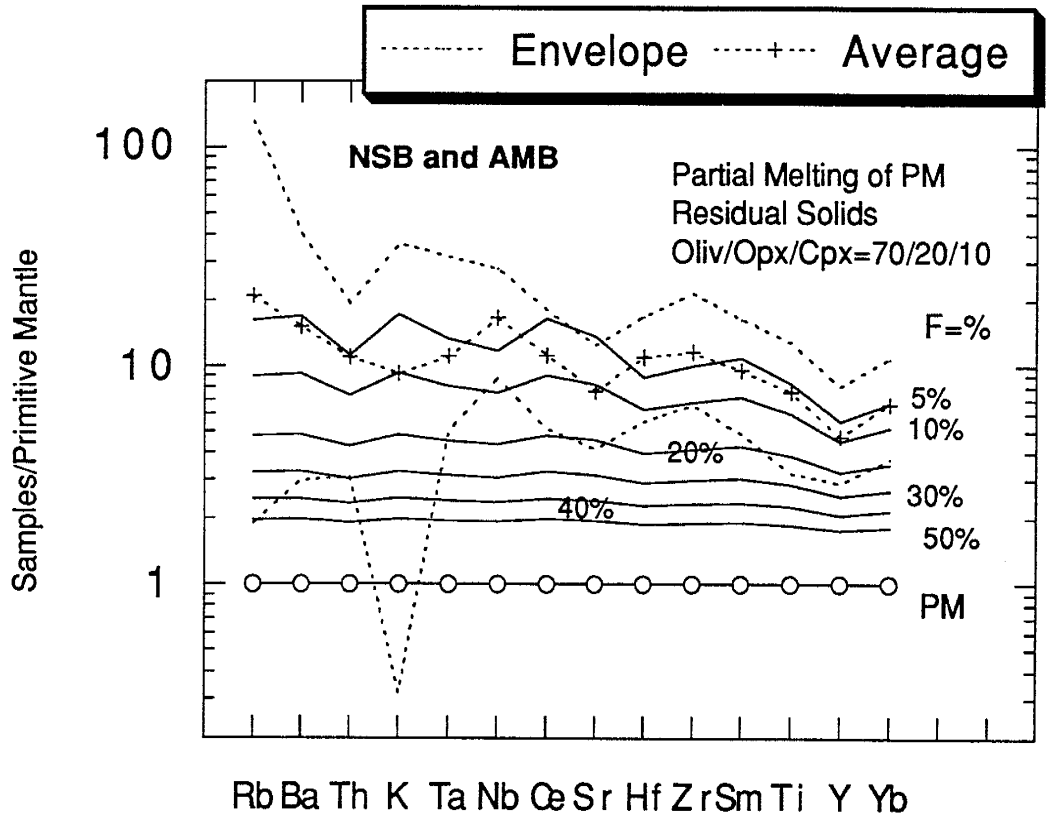

Fig. 5-4. Diagram of the primitive mantle normalized patterns of average incompatible element concentration of 38 balalts from the Talga Talgal Subgroup and 0-50% melting degree of the primitive mantle (Hofmann, 1988), with residual solids of 70% olivine, 20% orthopyroxene and 10% clipyroxene.

Figure 5-4 shows a series of 0-50% partial melting curves for 14 incompatible elements using Equation 5-1. We assume that parent solid and residual solids are, respectively, primitive mantle and komatiite with olivine:orthopyroxene:clipyroxene =70:20:10. The envelope of incompatible elements distribution patterns of Talga Talga Subgroup range from 2 to 30% melting. Compared to REE patterns in Figure 5-2, incompatible elements have larger ranges, especially mobile incompatible elements (K, Rb etc.).

As a result, the concentrations of incompatible elements in the North Star Basalt and Mount Ada Basalt indicate that basalts of Talga Talga Subgroup were derived from 5-20% partial melting of primitive mantle.

Figure 5-5 (after Wilson, 1989) shows the partial melting interval of a typical lherzolite. At the solidus the first trace of partial melt appears, while at the liquidus the system is completely molten. The interval between the solidus and liquidus can be contoured for the degree of melting, as shown in the diagram. Assume that mantle A is caught up in the ascending limb of a convection cell and rises adiabatically towards the surface. The pressure on this volume of lherzolite is reduced dramatically, but its temperature remains essentially constant, as shown by the ascent path A-A'. From A to A', partial melting progressively increases. At A', the ascending mantle diapir will consist of 20% partial melt and 80% residual crystals. A 20% partial melt should physically separate from its source and, at this depth, the magma could segregate from the residual crystals and ascend rapidly to the earth's surface.

Jaques and Green (1980) published their melting experiments (Figure 5-6a and 5-6b) for both depleted and enriched lherzolite source composition.

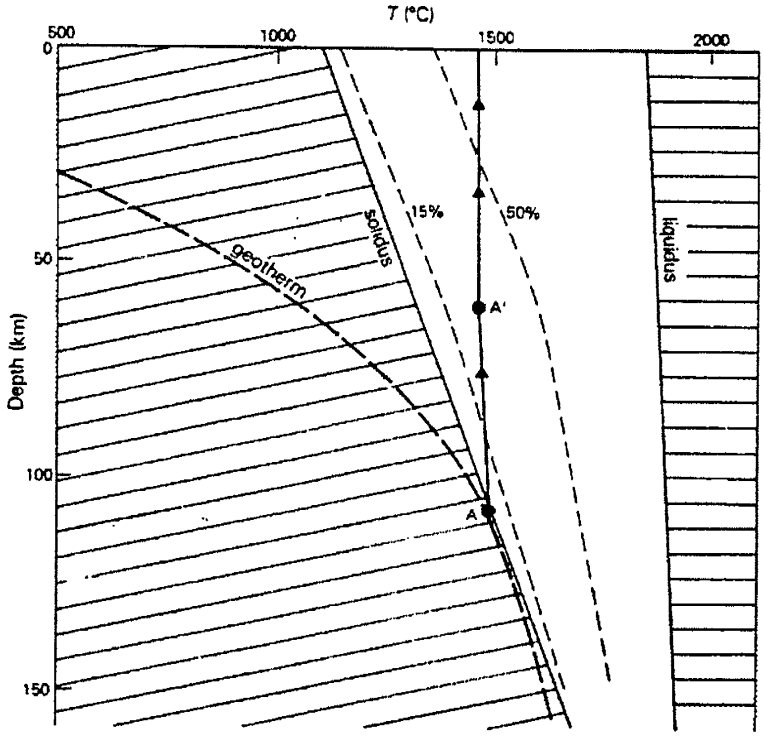

Figure 5-5. Partial melting of mantle lherzolite by adiabatic decompression. Magma segregates at A' (20% partial melt) and ascends rapidly towards the surface.Diagonal shading marks the subsolidus field and horizontal shading the completely molten field (which can never be achieved under present geothermal gradients). The interval between the solidus and the liquidus is contoured for the degree of melting (after wilson, 1989).

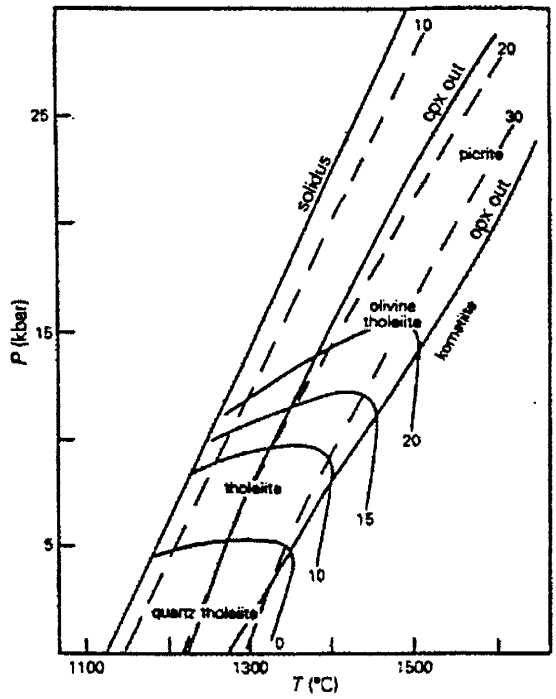

Fig. 5-6a. Experimentally determined partial melting characteristics of a depleted mantle lherzolite source. Dashed lines are partial melting contours for 10, 20 and 30% partial melting. Cpx-out and Opx-out lines mark the degree of melting at which cpx and opx respectively are completely consumed into the melt. The strongly curbed contours indicate the normative content of olivine in the melt (after Wilson, 1989).

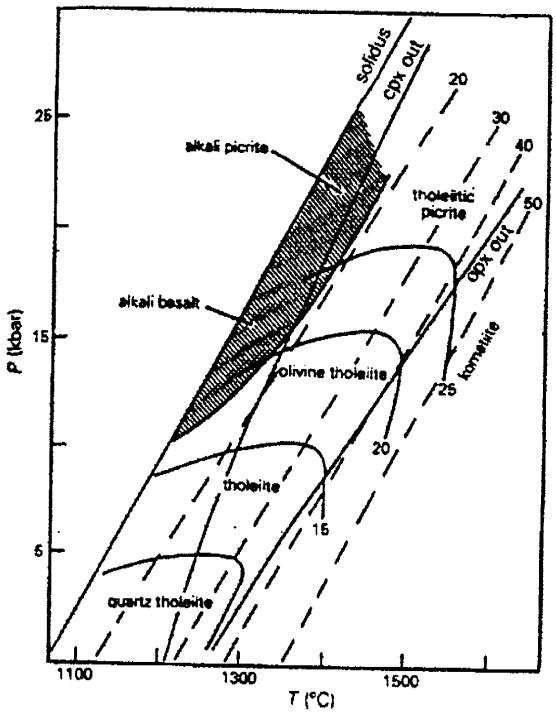

Fig. 5-6 b. Experimentally determined partial melting characteristics of an enriched lherzolite source. Dashed lines are partial melting contours for 20, 30, 40 and 50% partial melting. The shaded area represents the conditions necessary for the generation of alkalic basaltic magmas. Other symbols as Figure 5-6a (after Wilson, 1989).

Their experiments show that tholeiitic basalt magmas can be produced by moderate degrees of partial melting (20-30%) of either source at pressures below 15-20 kbar. At higher pressures picritic liquids are generated at the same degrees of partial melting. Alkali basaltic magmas appear to be generated by smaller degrees of partial melting (<20%) of enriched sources at pressures greater than 10 kbar, while liquids akin to perdotitic komatiites can be produced by 40-50% partial melting of fertile lherzolite, or 30-40% partial melting of a depleted lherzolite.

Geothermal gradients of Archean the crust and mantle was greater than present (Kroner, 1981, Goodwin, 1981, and Condie, 1981), and pressure and depth for partial melting of primitive mantle could be less than those of the present mantle discussed by Jaques and Green (1980). Tectonic process of partial melting for the Talga Talga basalts will be discussed in next part.

2. Salgash Subgroup

Basalts of the Apex Basalt also are related to primitive mantle, as shown by Zr/Nb vs. Hf/Ta in Figure 5-1 (Hofmann, 1988), Th/Yb vs. Ta/Yb (Figure 4-11) and Th/Yb vs. Hf/Th relations (Figure 4-12). These diagrams also show that basalts of the Apex Basalt are not mixture of primitive mantle and early Archean continental crust. As a result, the source of the basalts is related to primitive mantle. The upward increasing trends of incompatible elements in the Apex basalts implies that concentration of incompatible elements increased during the eruption of the basalts. This process shows that basalts were probably derived from the fractional crystallization of a primitive mantle source (Hess, 1989, Wilson, 1989).

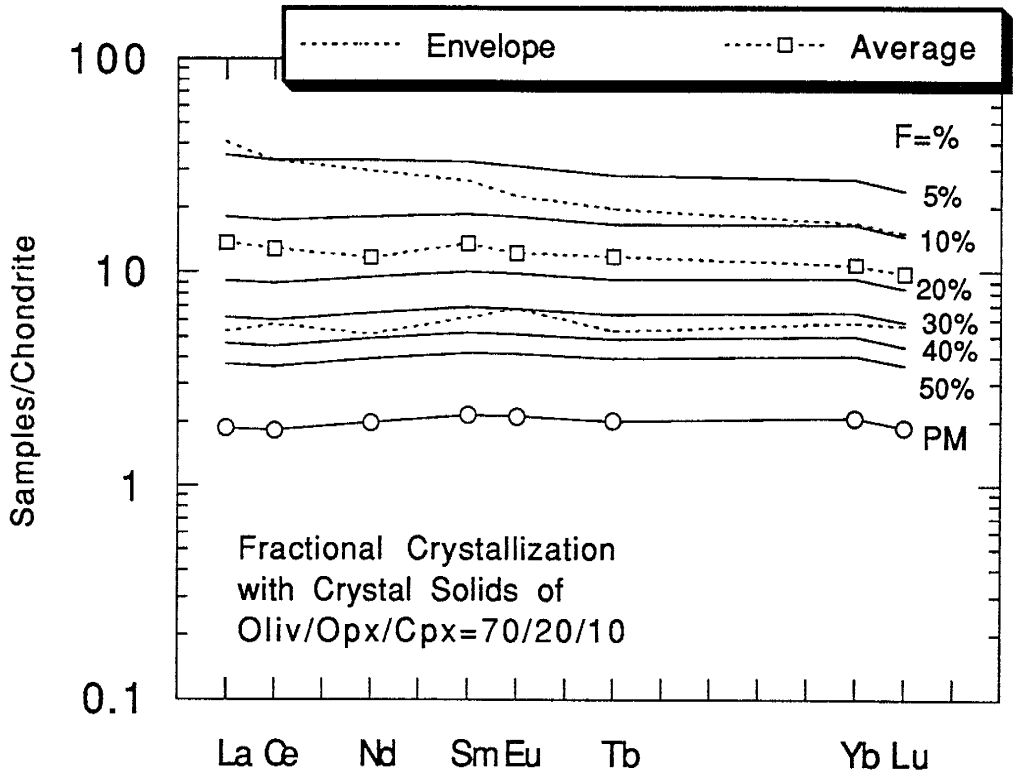

Fig. 5-7. Diagram of chondrite normalized REE patterns of average of 13 balalts from the Salgash Subgroup and 0-50% residual melting of the primitive mantle (Hofmann, 1988), during fractinal crystallization with crystallization solids of 70% olivine, 20% orthopyroxene and 10% clipyroxene.

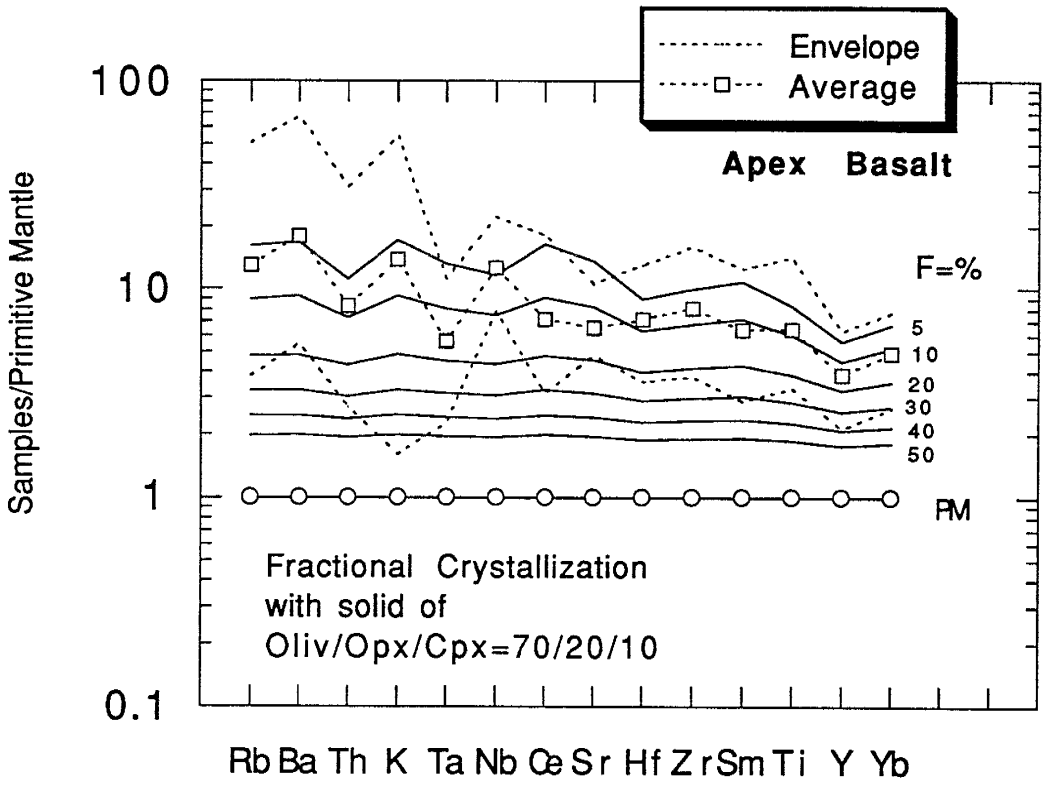

Fig. 5-8. Diagram of the primitive mantle normalized patterns of average incompatible element concentration of 13 balalts from the Salgash Subgroup and 0-50% residual melting of the primitive mantle (Hofmann, 1988), during fractinal crystallization with crystallization solids of 70% olivine, 20% orthopyroxene and 10% clipyroxene.

Based on equation 5-2 in the batch melting model, we can get a series of REE patterns for degree of melting ranging from 0 to 50% (in Figure 5-7), assuming that the parent source and crystal solids are, respectively, the primitive mantle (Hofmann, 1988) and komatiites with olivine:orthopyroxene:clipyroxene =70:20:10 (Condie, 1991). Komatiites of the Salgash Subgroup are greater in abundance than the Talga Talga Subgroup as discussed by Glikson (1981). These komatiites probably are the earlier crystal solids separated from the parent source from primitive mantle. In Figure 5-7, the envelope of REE patterns of 13 basalts of the Apex Basalt plot between the 5% and 35% curves and the average of the basalts is close to 17% curve. In Figure 5-3b of $(La/Sm)_N$ vs. La_N, 13 basalts of the Apex Basalt plot between 10 and 30% residual melt of PM source, and the $(La/Sm)_N$ and La_N values are less than Talga Talga Subgroup.

We also got a series of 0-50% partial melting curves for 14 incompatible elements(Figure 5-8) using Equation 5-2. In Figure 5-8, We assume parent source and crystal solids are, respectively, primitive mantle and komatiite with olivine:orthopyroxene:clipyroxene =70:20:10. The envelope of incompatible elements distribution patterns of the Apex Basalt plot the field ranging from 2 to 30% melting. Compared to REE patterns in Figure 5-7, incompatible elements have more variable range, especial for mobile incompatible elements (K, Rb et. al.).

The Euro Basalt of Salgash Subgroup has similar stratigraphic geochemistry to the Apex Basalt (Glikson, 1981). Its evolution is related to the Apex Basalt. As a result, basalts of the Salgash Subgroup were derived from 5-30% melting of primitive mantle, from which earlier komatiites crystallized.

VI. Tectonic Stetting of Pilbara Basalt

A. Models of tectonic Setting on the Precambrian Basalts

Much of the geological work on greenstone belts has been geared towards the understanding of their tectonic development and evolution. However, it is clear from the work carried out on the Archean greenstone belts that very few are sufficiently well understood to enable realistic tectonic models to be developed for these complex terrains. Nevertheless, many tectonic models have been proposed for their origin. It is difficult to explain the tectonic setting and evolution of greenstone belts because of uncertainties in such factors as the earth's thermal history, growth of continental crust, and the generation of igneous rocks of calc-alkaline affinity.

Many previous researchers described the tectonic evolution of greenstone belts by using the plate tectonics (Windley, 1977, Condie, 1976, 1981, Kroner, 1981, Goodwin, 1981, etc.). Kroner (1981) indicated that the granite-greenstone phase was characterized by vigorous sublithospheric convection, which induced varying degrees of crustal stretching, rifting and limited ocean opening. Under favourable conditions sag-subduction, partial melting and crust-mantle mixing processes added new crust to the early nuclei and culminated in a series of continental accretion-differentiation events. Goodwin (1981) stated that Archean greenstone belt diversity demands equally flexible tectonic development. Greenstone belt development is generally attributed to an Archean plate-tectonic process that involved limited movement of numerous small plates operating under a high geothermal gradient and thereby lacking conventional subduction zones. He indicated that the Archean

plate-tectonic process differed in significant respects from modern plate tectonics, yet produced similar volcanic and plutonic products.

Condie (1981) discussed the two classifications of tectonic evolutionary models of greenstone belts related to plate tectonics, as follows: **Continental rift models:** Such models, of course, presume the existence of older sialic crust (Condie, 1981). Condie and Hunter (1976) proposed a continental rift model for the development of the Barberton greenstone belt in South Africa, of which the major stages are as follows: (i). The sialic crust is formed 3.5 Ga, and a mantle plume ascends to the base of the lithosphere at 3.5 Ga and as it spreads laterally a continental rift develops; (ii). The rift system is partially filled with mafic-ultramafic lavas, and a steep geothermal gradient exists beneath the rift decreasing on the flanks; (iii). As the plume subsides, erosion of the flanks of the rift gives rise to sediments; (iv). Continued sinking of the Barberton succession and renewed plume activity at 3.1-3.2 Ga result in renewed partial melting of the amphibolite (again under wet conditions) giving rise to granitic rocks; (v). Plume subsidence between 2.8 and 2.9 Ga results in crustal downwarping and partial melting of the gneisses and granulites in the lower crust. Goodwin (1977) proposes multiple rifting of sialic crust to explain the superbelt pattern in the western Superior Province.This model begins with a primitive, thin sialic crust overlying a basaltic layer. Downwarps and/or rifts develop on this thin crust and are filled with greenstone volcanics.

Convergent plate boundary models: This model includes arc and back-arc basins. Condie and Harrison (1976) propose a model for the Midlands greenstone succession in Rhodesia involving a back-arc basin. The tectonic evolution was described as follows: (i). Older sialic crust to the east provides only minor detrital input into the back-arc basin; (ii). Finally, an activation-type

orogeny occurs and the arc system and back-arc basin are compressed and welded to the Rhodesian craton; (iii). During the late stages of deformation, quartz porphyries are emplaced and fragments of the upper mantle are tectonically emplaced as serpentinites.

B. Tectonic setting of the Early Precambrian Pilbara Block

Basalts of the Warrawoona Group in the east Pilbara Block are tholeiitic basalts, which are different from calk-alkaline volcanics. Horwitz (1990) discussed the palaeogeographic and tectonic evolution of the Warrawoona Group, and implied that the Warrawoona Group is a protocontinent along the southeastern margin of the Pilbara Block, overlapped by the Gorge Creek Group.

Glikson and Hickman (1981) indicated that comparisons between basalts of the Pilbara Supergroup and modern basalts provide no conclusive evidence on Archaean environments. Determination of Archean tectonic environments by geochemical comparison with modern volcanics is impeded by unknown factors such as possible changes in mantle composition since the Archean, changes in tectonic environments, secondary chemical changes such as migration of alkalis, and also the uncertainty as to what degree existing data on modern volcanics are representative (Glikson and Hickman, 1981).

Plot of TiO2 vs. MgO/(MgO+FeO) in Figure 6-1 show that most basalts of the Warrawoona Group plot in the field of the MORB. Few samples of the North Star Basalt and Mount Ada Basalt and about half the samples of the Apex Basalt fall also in the Margin Basin Tholeiite field, but no samples fall in the IAC Tholeiite (from Gill, 1979). Plot of Ce/Y vs. Sr/Y (Figure 6-2) indicates that

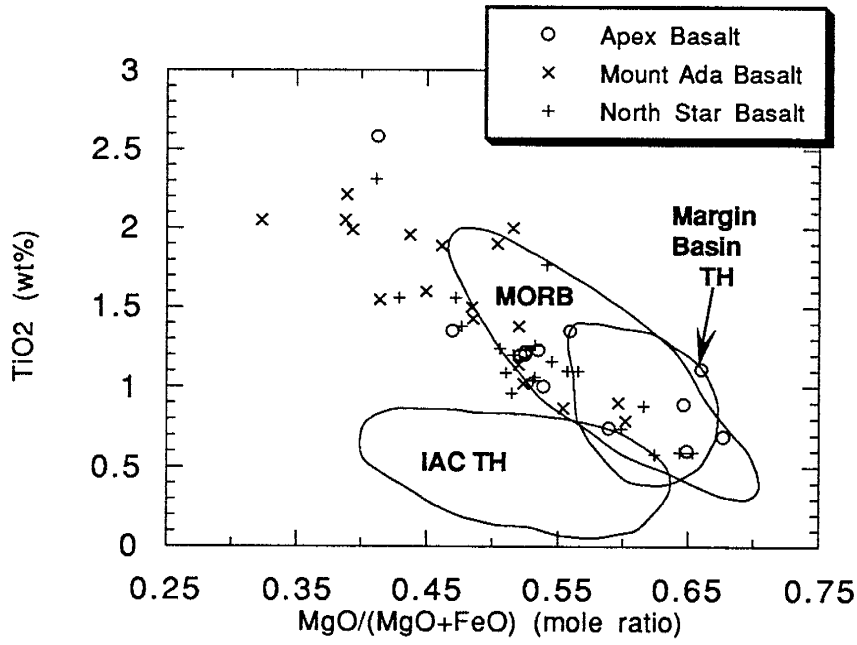

Figure 6-1. Diagram TiO2 (wt%) vs. MgO/(MgO+FeO) (mole ratio) of basalts from the Warrawoona Group, IAC TH, MORB and Margin Basin TH from Gill (1979).

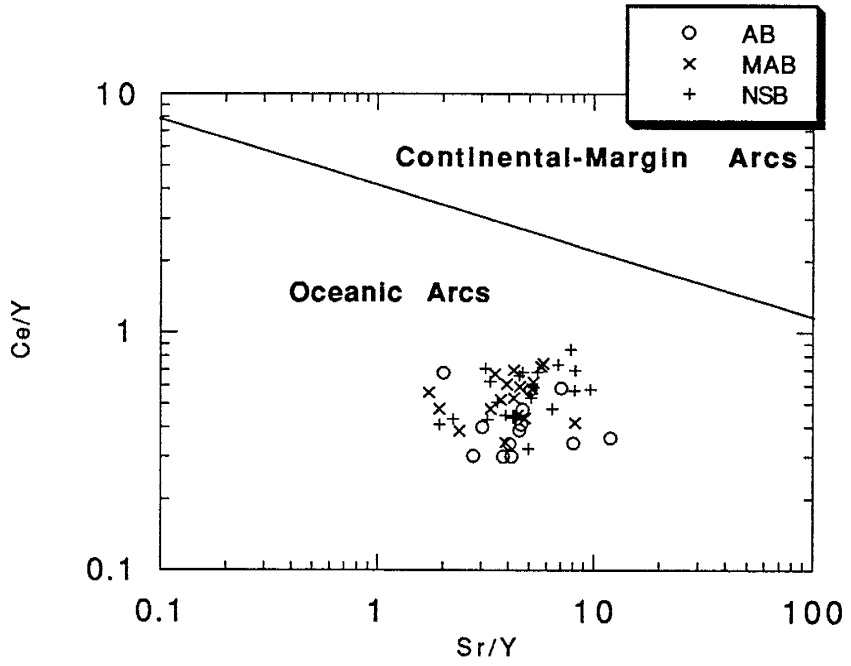

Figure 6-2. Diagram of Ce/Y vs. Sr/Y of basalts from the Warrawoona Group, and the fields of the oceanic arcs and continental-margin Arcs (after Morris, 1988).

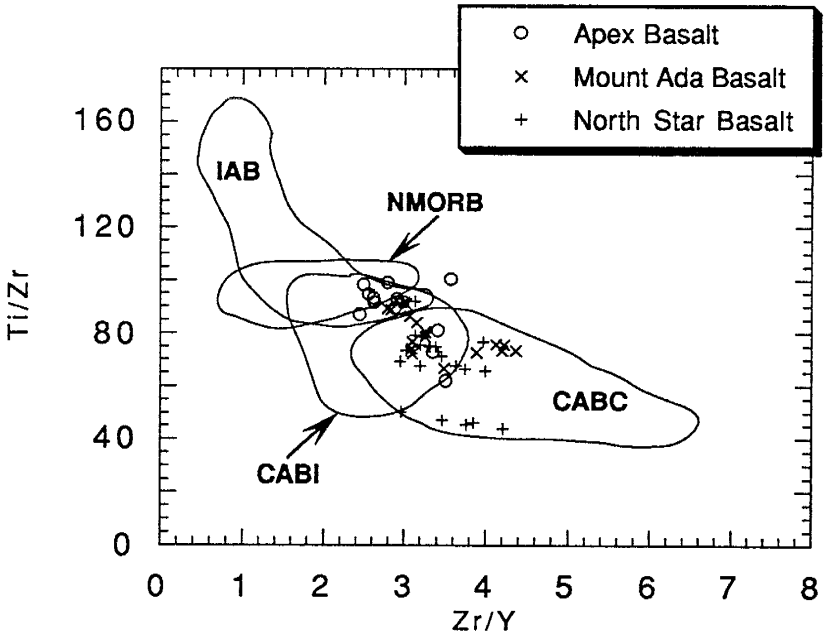

Fig. 6-3 Plot of Ti/Zr vs. Zr/Y for basalts from the Warrawoona Group compared to the fields of modern IAB, MORB and calc-alkaline basalts (after Condie 1989)..

basalts from the Warrawoona Group are similar to the Oceanic Arcs, but no samples are similar to the Continental-Margin Arcs (Morris, 1988).

Diagram of Ti/Zr vs. Zr/Y (Figure 6-3) shows that most samples of the Mount Ada Basalt and North Star Basalt plot in the ISL ARC Basalt field and some samples plot in the Continental Margin field, and that all samples of the Apex Basalt plot in the ISL ARC Basalt field. Figure 6-3 also shows some samples in the overlap of the ARC Tholeiite, NMORB, ISL ARC and Continental Margin Basalt, which implies that the relation between Ti/Zr and Zr/Y of the Warrawoona Group basalts has a great range. The relations of Ta/Yb and Th/Yb ratios in Figure 4-11 show that most basalts of the Warrawoona Group plot near oceanic arcs.

Plot of Nb*2-Zr/4-Y (Figure 6-4) indicates that most samples of the Warrawoona Group fall near the triple point of P-Type MORB, N-Type MORB and VAB (Meshede, 1986), but no samples fall in the WPA. The Hf/3-Th-Ta diagram (Figure 6-5) shows that concentrations of most basalts of the North Star Basalt and Mount Ada Basalt plot in IA and CPB fields, and that half the samples of the Apex Basalt plot in IA and CPB respectively. Figure 6-5 also shows a range of the Warrawoona Group along CPB+IA, but no samples plot in NMORB, E-Type MORB and WPB fields (Wood, et. al., 1979). The Ti/100-Zr-3Y plot (Figure 6-6) reveals most basalts of the North Star Basalt and Mount Ada Basalt fall in the Ocean Floor Basalt field, and few samples fall in the Within Plate Basalt field. Figure 6-6 also shows all samples of the Apex Basalt in Ocean Floor Basalt field.

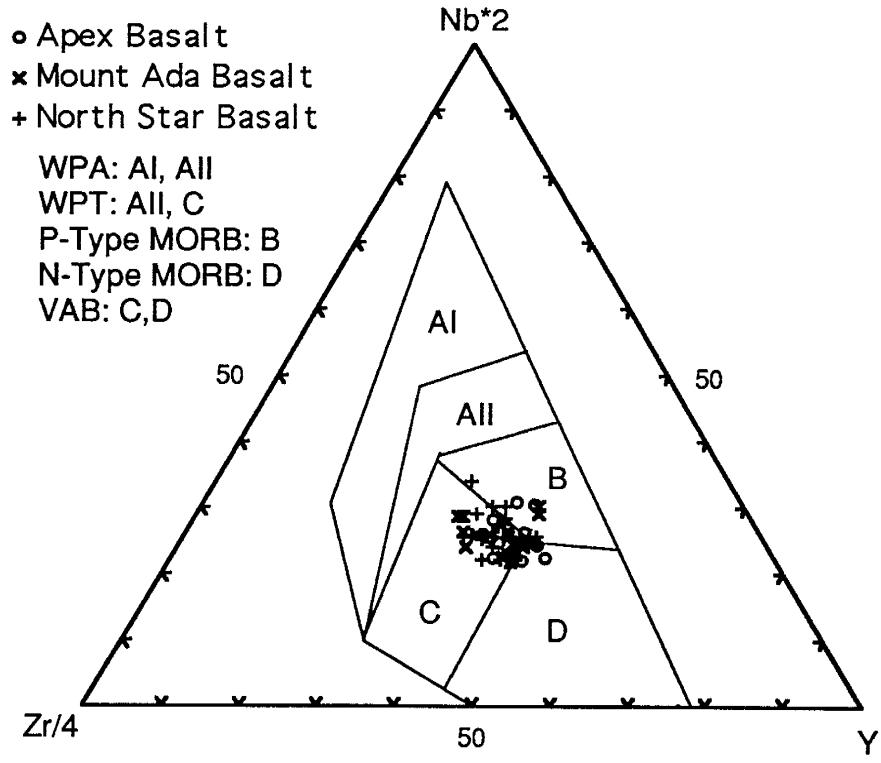

Fig.6-4. Nb*2-Zr/4-Y diagram for basalts of the Warrawoona Group. Compositional fields of WPA, WPT, P-Type MORB, N-Type MORB and VAB (from Meshede,1986).

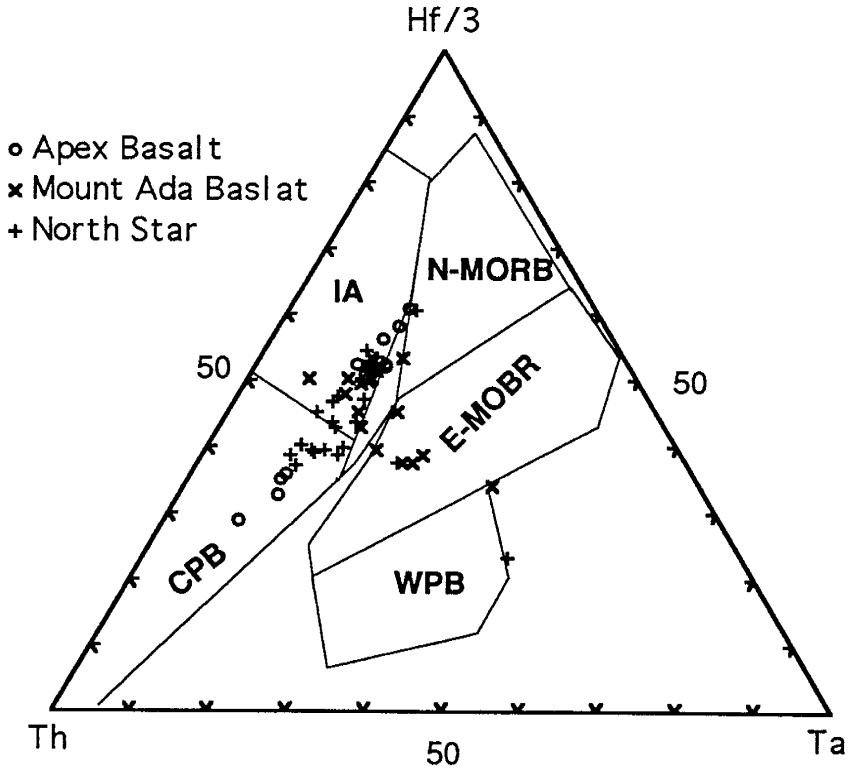

Fig. 6-5. Hf/3-Th-Ta diagram for basalts from the Warrawoona Group. Compositional fields of IA, N-MORB, E-MORB, WPB and CPB (from Wood, et. al., 1979).

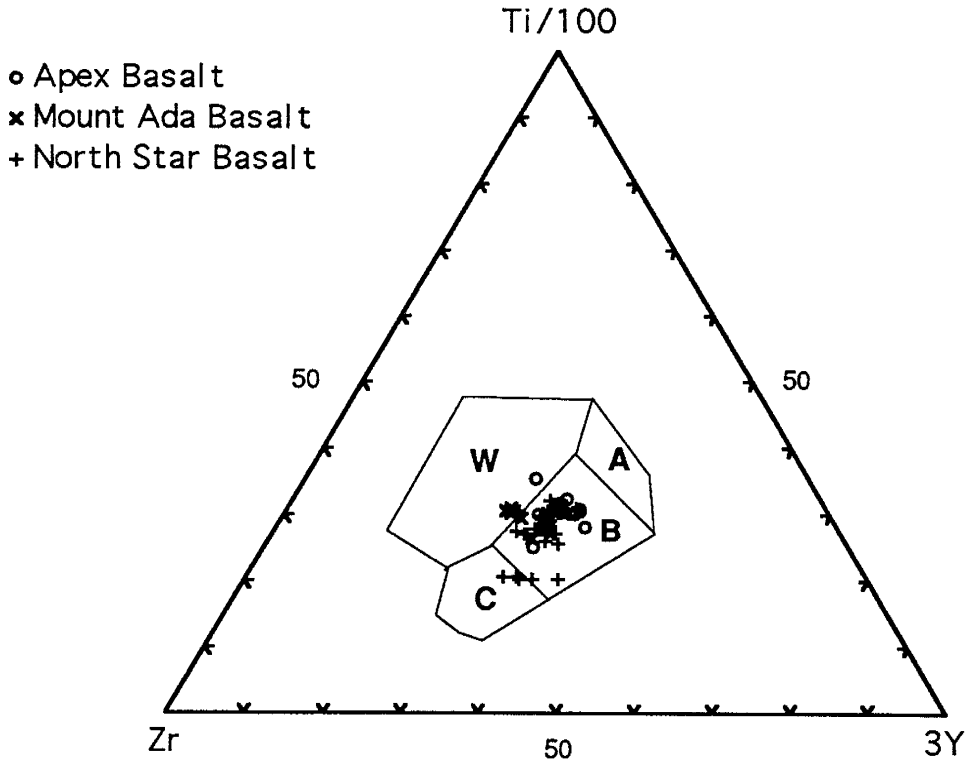

Fig. 6-6. Ti/100-Zr-3Y diagram for basalts from the Warrawoona Group. Compositional fields (from Wood et al., 1979) are: A+B: LK Tholeiites, B: Ocean Floor Basalt, C+B: Calc-Alk Basalt, W: Within Plate Basalt

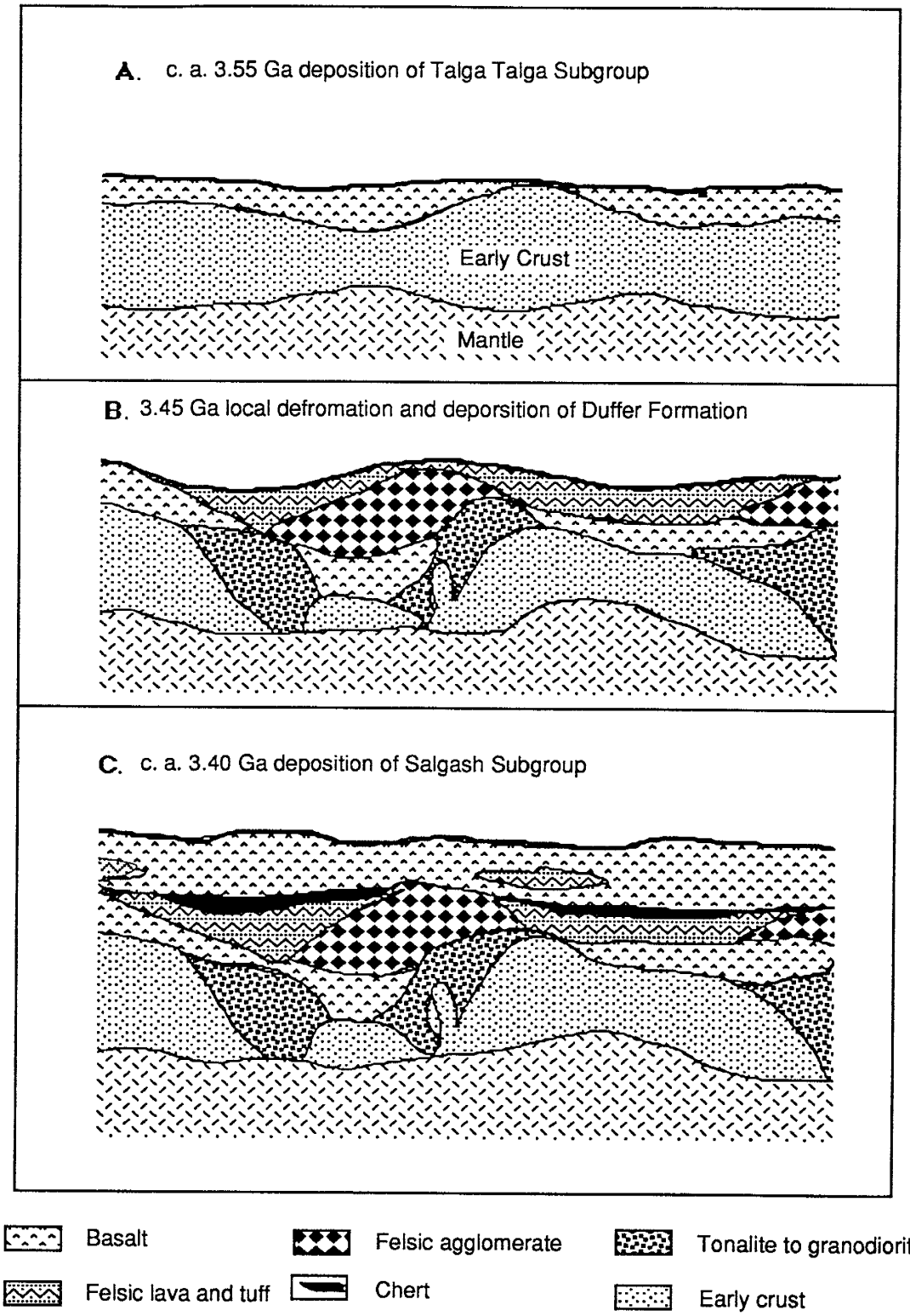

Fig. 6-7. Tectonic evolution of the Warrawoona Group (from 3.55 Ga to 3.40 Ga) in the Pilbara Block, in three stages (A, B, C), after Hickman (1983).

In conclusion, these plots generally indicate similarities between the arc tholeiitic basalts of margin basin of continental, or oceanic type basalts and the Warrawoona Group basalts. It is possible that the Warrawoona Group basalts formed in the rift or back-arc basin of the margin of plate at 3.55 Ga. Based on geochemical data, Hickman (1983) described basalts of the Warrawoona Group as marginal basin type, that they were derived by partial melting of the mantle, and extruded onto a relatively thin sialic crust.

Based on the stratigraphic features, structural deformation and geochemical data, the tectonic development of the Warrawoona Group may be described as three stages, shown in Figure 6-6 (after Hickman, 1983): (A) Before 3.55 Ga, tholeiitic basaltic rocks (Talga Talga Subgroup) were extruded (partly subaqueous) over a large part of the area of the Pilbara Block. Thin sedimentary and rhyolitic units could have been derived by erosion and partial melting of the granitic crust; (B) From 3.55 to 3.45 Ga, local deformation was followed by the development of calk-alkaline volcanic centres (Duffer Formation). Contemporaneous intrusion of granodiorite into the underlying sialic crust and the Talga Talga Subgroup probably occurred at this time; (C) Post 3.45 Ga, Stable conditions prevailed during which time a 4 km thick tabular succession of pillow tholeiite, komatiite and chert units (Salgash Subgroup) was deposited over the Pilbara Block.

VII. Discussion and Conclusion

A. Geochemical Stratigraphy of the Warrawoona Group basalts:

Geochemical data of 51 basalts from the Warrawoona Group in the Pilbara Block indicate that the alkali and alkaline-earth elements have been remobilized, but the other major elements and most incompatible elements are relatively stable during alteration. The basalts are tholeiitic basalts and have compositions similar to Archean DAT (Condie, 1981), and the early Archean tholeiitic basalts from the greenstone belts in South Africa, South India, Canada, Greenland and North Minnesota (Jahn, 1977, 1982, Drury, 1982, Fryer, 1978, Lafieche, 1991, Condie, 1981). Major and trace element concentrations of the basalts show that the concentrations have different changes upward in the Talga Talga Subgroup and the Salgash Subgroup. (1). For the Talga Talga Subgroup, incompatible elements show a generally upward decrease. The lowest units in Mount Ada Basalt have higher Ti2O, FeO, Sr, Zr, Nb, Y, REE, V, and lower SiO2, K2O, Rb and Ba than the highest units of the North Star Basalt. A discontinuity in compositions between the North Star Basalt and Mount Ada Basalt implies two cycles of the basalt eruption. (2). For the Salgash Subgroup, the basalts show opposite trends with upward increasing incompatible element concentrations, which indicate that incompatible elements increase with time.

B. Origin of the basalts

Geochemical data from the basalts of the Warrawoona Group have similarities to primitive mantle, but not to a mixture of the primitive mantle and continental composition. As a result, the source of the basalts was from the primitive mantle. The opposite upward changes in geochemical stratigraphy

between the Talga Talga Subgroup and Salgash Subgroup indicate different sources of the basalts. The process of upward decreasing incompatible elements in the Talga Talga Subgroup shows that the basalts were probably derived from the partial melting of primitive mantle. Using the partial melt model of primitive mantle, assuming residual solids are komatiites composed of 70% olivine, 20% orthopyroxene and 10% clipyroxene, we estimate that basalts of the Talga Talga Subgroup were probably derived from 5-20% partial melting of primitive mantle. The process of upward increasing incompatible elements in the Salgash Subgroup shows that the basalts were probably formed by fractional crystallization of basalts derived from primitive mantle. Based on the batch melting model, assuming that the parent source and crystal solids are, respectively, the primitive mantle (Hofmann, 1988) and komatiites with olivine:orthopyroxene:clipyroxene =70:20:10 (Condie, 1991), the basalts were derived from 5-30% melting of primitive mantle.

C. Evolution of Tectonic Setting

Geochemical data generally indicate that the Warrawoona Group basalts have similarities to the arc tholeiitic basalts or oceanic type basalts. It is possible that the Warrawoona Group basalts formed in a rift or back-arc basin at the margin of a plate. Based on geochemical data, stratigraphy and structural geological features, tectonic evolution of the Warrawoona Group may be described as follows: (i). Before 3.55 Ga, tholeiitic basalts of the Talga Talga Subgroup, which derived from partial melting of primitive mantle, were extruded over all, or a large part of the area of the Pilbara Block. Thin sedimentary and rhyolitic units could have been derived by erosion and partial melting of the granitic crust; (ii) From 3.55 to 3.45 Ga, the Duffer formation developed and local deformation was followed by the development of calk-

alkaline volcanic centres. Contemporaneous intrusion of granodiorite into the underlying sialic crust and the Talga Talga Subgroup probably occurred at this time; (iii) At 3.45 Ga, thick tabular succession of pillow tholeiite derived from fractional crystallization of primitive mantle, komatiite and chert units of the Salgash Subgroup were deposited over the Pilbara Block.

Appendix A: Precision and accuracy data tables for XRF and INAA

Table A-1. Pertinent information for X-ray fluorescence analyses (after Hallett, 1990)

Element	Electron Shell	Kev © Measured	Lower Limit Detection (ppm)	Lower Limit Determination (ppm)
Rb	Ka 1,2	13.373	1.02	3.0
Sr	Ka 1,2	14.140	0.94	3.0
Y	Ka 1,2	14.931	1.08	3.2
Zr	Ka 1,2	15.744	0.78	2.5
Nb	Ka 1,2	16.581	2.00	3.0

© from white and Johnson (1970).

Table A-2. XRF Data for BCR-1 (from Boryta, 1988)

Element	Accepted Values	n	X ± s	C. V.	∂X	% Accuracy
Y	39	14	37.90±1.8	4.88	0.49	95.26
Zr	191	13	190.1±5.0	2.61	1.38	97.40
Nb	14	14	13.40±1.7	12.87	0.46	87.69
Rb	47	14	51.30±0.8	1.58	0.22	98.27
Sr	330	14	334.0±4.0	1.31	1.17	98.67
Ba	680	11	686.0± 16	2.31	4.78	97.67
Pb	13.6	14	17.30±2.2	13.0	0.60	83.51
V	420	6	430.0±6.0	1.41	2.47	98.56
Ni	10	6	11.30±2.7	24.26	1.12	72.58

$$X=\frac{\sum_{n}^{n} Xi}{n}; \quad C.V.=\frac{s}{X} * 100; \quad \% \text{ Accuracy}=100-\frac{X\text{-Actual}}{\text{Actual}} * 100$$

X-the mean value, s-standard deviation, C. V.-coefficient of variation, ∂X-standard error of the mean.

Table A-3. Pertinent information for neutron activation

Parent Nuclide	Daughter Nuclide	* Kev Measured	Lower Limit Detection (ppm)	Lower Limit Determination (ppm)
Ba-130	Ba-131	373	2.0	25
Ce-140	Ce-141	145	0.12	1.5
Co-59	Co-60	1173	0.05	1.0
Cr-50	Cr-51	320	0.3	1.0
Cs-133	Cs-134	605	0.04	0.5
Eu-151	Eu-152	245	0.02	0.15
Hf-180	Hf-181	482	0.02	0.1
La-139	La-140	329	-	0.9
Lu-176	Lu-177	208	-	0.04
Nd-146	Nd-147	91	-	2.5
Sc-45	Sc-46	889	0.2	0.5
Sm-152	Sm-153	103	-	0.5
Ta-181	Ta-182	1189	0.002	0.04
Tb-159	Tb-160	299	0.01	0.05
Th-232	Pa-232	312	0.04	0.1
U-238	Np-239	228	0.017	0.02
Yb-174	Yb-175	177	0.017	0.02

(from R. Bruce Hallett, 1990)

Table A-4. INAA Data for BCR-1 (from Boryta, 1988)

Element	Accepted Values	n	X ± s	C. V.	∂X	% Accuracy
Cs	0.96	10	0.95±0.06	6.21	0.02	93.84
Th	6.04	10	5.80±0.30	5.51	0.10	94.75
U	1.72	10	1.70±0.10	8.24	0.04	92.09
Sc	33	10	31.6±1.90	5.97	0.60	94.28
Cr	15.5	10	13.8±1.00	7.40	0.32	93.41
Co	37	10	36.8±2.00	5.42	0.63	94.62
Hf	5	8	5.00±0.30	5.34	0.10	94.62
Ta	0.83	8	0.78±0.02	3.12	0.01	97.05
La	24	10	24.5±1.70	7.01	0.54	92.83
Ce	53.45	10	53.2±3.10	5.85	0.98	94.17
Sm	6.6	10	6.80±0.31	4.52	0.10	95.34
Eu	1.96	10	1.89±0.11	5.95	0.04	94.27
Tb	1.0	10	1.07±0.08	7.66	0.03	91.79
Yb	3.38	10	3.36±0.19	5.68	0.06	94.36
Lu	0.51	10	0.52±0.03	5.91	0.01	94.04

Appendix B: Major Elements of the Warrawoona Group Basalts

Table B-1 Major Elements of basalts from the Apex Basalt, Pilbara Block

Element	Apex Basalt							
	Withnell Creek Section			Strelley Gorge Section				
	AWc2	AWc3	AWc4	ASs2	ASs4	ASs5	ASs6	ASs7
SiO2	48.50	52.10	47.60	46.60	49.30	46.10	48.10	48.00
TiO2	0.74	0.69	1.00	0.60	0.89	1.11	2.58	1.35
Al2O3	15.30	13.80	14.20	13.80	15.00	15.30	12.20	13.10
Fe2O3	2.78	1.81	3.20	1.95	1.62	2.85	4.90	2.55
FeO	8.75	6.15	9.45	7.69	7.63	7.06	10.30	9.22
MgO	7.05	7.25	6.20	8.00	7.85	7.70	4.06	4.59
CaO	9.85	10.10	11.20	11.40	8.95	12.10	8.10	9.00
Na2O	2.34	2.48	1.24	3.08	3.92	2.14	2.55	3.53
K2O	0.35	0.05		0.10	0.39	0.85	1.69	0.27
MnO	0.18	0.13	0.19	0.19	0.16	0.18	0.19	0.17
P2O5	0.07	0.07	0.08	0.04	0.09	0.13	0.30	0.13
LOI	3.63	5.31	5.56	6.77	4.41	4.66	4.57	7.61
Total	99.54	99.94	99.92	100.22	100.21	100.18	99.54	99.52
SiO2/Al2O3	3.17	3.78	3.35	3.38	3.29	3.01	3.94	3.66
FeO/MgO	1.24	0.85	1.52	0.96	0.97	0.92	2.54	2.01
K2O/Na2O	0.15	0.02		0.03	0.10	0.40	0.66	0.08
Al2O3/TiO2	20.68	20.00	14.20	23.00	16.85	13.78	4.73	9.70

Table B-2 Major Elements of basalts from the Apex Basalt and Mount Ada Basalt

Element	Apex Basalt					Mount Ada Basalt		
	Cleaverville Section					Talga Coongan Section		
	ASc1	ASc2	ASc3	ASc4	ASc5	MAmb1	MAmb2	MAmb3
SiO2	50.10	49.00	49.00	48.90	47.70	49.40	50.31	50.69
TiO2	1.35	1.22	1.20	1.20	1.23	1.38	0.87	1.14
Al2O3	14.80	14.40	14.60	14.80	14.40	14.16	12.76	13.71
Fe2O3	1.67	1.64	2.59	1.81	2.26	2.30	1.97	2.10
FeO	10.10	10.40	10.00	10.70	9.75	11.48	9.85	10.49
MgO	7.20	6.45	6.20	6.55	6.30	6.98	6.87	6.38
CaO	9.60	11.60	12.30	10.10	12.30	9.39	12.21	10.28
Na2O	2.34	2.02	1.85	2.72	1.81	2.78	1.21	2.06
K2O	0.22	0.31	0.20	0.28	0.28	0.30	0.29	0.51
MnO	0.21	0.26	0.21	0.22	0.21	0.19	0.20	0.22
P2O5	0.11	0.12	0.10	0.12	0.10	0.10	0.08	0.08
LOI	2.43	2.20	1.81	2.33	3.00	0.58	1.34	0.60
Total	100.13	99.62	100.06	99.73	99.34	99.04	97.96	98.26
SiO2/Al2O3	3.39	3.40	3.36	3.30	3.31	3.49	3.94	3.70
FeO/MgO	1.40	1.61	1.61	1.63	1.55	1.64	1.43	1.64
K2O/Na2O	0.09	0.15	0.11	0.10	0.15	0.11	0.24	0.25
Al2O3/TiO2	10.96	11.80	12.17	12.33	11.71	10.26	14.67	12.03

Table B-3 Major Elements of basalts from the Mount Ada Basalt, Pilbara Block

Element	Mount Ada Basalt						
	Talga River Section						
	MAmb4	MAmb5	MAmb6	MAmb7	MAmb8	MAmb9	MAmb10
SiO2	50.50	49.38	48.76	48.85	48.49	48.02	49.30
TiO2	0.90	2.00	1.90	1.89	1.43	1.50	1.96
Al2O3	13.17	13.83	13.35	13.80	13.53	13.56	13.73
Fe2O3	2.04	2.13	2.17	2.37	2.47	2.30	2.45
FeO	10.19	10.63	10.84	11.87	12.37	11.52	12.23
MgO	8.45	6.36	6.18	5.71	6.55	6.08	5.34
CaO	9.41	8.44	9.08	8.95	8.34	9.06	9.07
Na2O	1.71	3.02	2.65	2.42	2.58	2.97	2.30
K2O	0.10	0.22	0.22	0.25	0.09	0.08	0.24
MnO	0.21	0.20	0.20	0.23	0.24	0.23	0.23
P2O5	0.07	0.17	0.16	0.15	0.11	0.11	0.16
LOI	2.39	2.91	3.73	2.21	2.85	2.88	2.06
Total	99.14	99.29	99.24	98.70	99.06	98.31	99.07
SiO2/Al2O3	3.83	3.57	3.65	3.54	3.58	3.54	3.59
FeO/MgO	1.21	1.67	1.75	2.08	1.89	1.89	2.29
K2O/Na2O	0.06	0.07	0.08	0.10	0.03	0.03	0.10
Al2O3/TiO2	14.63	6.91	7.03	7.30	9.46	9.04	7.01

Table B-4 Major Elements of basalts from the Mount Ada Basalt, Pilbara Block

Element	Mount Ada Basalt							
	McPhee Reward Section							
	MAmr1	MAmr2	MAmr3	MAmr4	MAmr5	MAmr6	MAmr7	MAmr8
SiO2	45.27	49.71	46.76	48.89	48.85	49.25	45.26	45.92
TiO2	1.99	1.55	2.05	1.60	1.02	0.79	2.05	2.21
Al2O3	12.00	13.04	12.43	12.67	11.51	12.33	12.13	12.52
Fe2O3	2.44	2.11	2.31	2.26	1.93	1.83	2.55	2.73
FeO	12.18	10.53	11.53	11.28	9.63	9.15	12.74	13.65
MgO	4.44	4.18	3.09	5.17	5.95	7.77	4.53	4.88
CaO	6.43	9.89	8.72	6.56	8.81	9.19	7.84	6.25
Na2O	2.63	2.08	1.92	1.77	1.00	1.30	1.73	2.23
K2O	0.04	0.07	0.04	0.04	0.03	0.01	0.12	0.16
MnO	0.22	0.22	0.26	0.17	0.17	0.18	0.23	0.27
P2O5	0.20	0.15	0.21	0.18	0.01	0.06	0.22	0.22
LOI	9.91	4.74	8.40	6.62	8.97	6.39	8.32	6.98
Total	97.75	98.26	97.71	97.21	97.88	98.25	97.72	98.02
SiO2/Al2O3	3.77	3.81	3.76	3.86	4.24	3.99	3.73	3.67
FeO/MgO	2.74	2.52	3.73	2.18	1.62	1.18	2.81	2.80
K2O/Na2O	0.02	0.03	0.02	0.02	0.03	0.00	0.07	0.07
Al2O3/TiO2	6.03	8.41	6.06	7.92	11.28	15.61	5.92	5.67

Table B-5 Major Elements of basalts from the North Star Basalt, Pilbara Block

Element	North Star Basalt								
	Talga Coongan Section								
	NSmb1	NSmb2	NSmb4	NSmb3	NSmb5	NSmb6	NSmb7	NSmb8	NSmb9
SiO2	51.25	51.32	49.51	53.86	52.23	52.84	52.12	50.57	51.32
TiO2	0.59	0.59	1.04	0.74	1.10	1.09	1.10	1.38	0.58
Al2O3	15.02	15.02	14.07	14.79	13.46	13.57	14.00	13.52	14.85
Fe2O3	1.56	1.59	2.21	1.44	1.94	1.82	2.04	2.41	1.65
FeO	7.80	7.96	11.05	7.22	9.71	9.11	10.19	12.04	8.25
MgO	8.26	8.07	7.02	6.05	7.10	5.33	7.19	6.15	7.69
CaO	9.89	10.39	10.87	12.02	8.65	11.98	8.36	9.58	11.83
Na2O	1.22	1.25	1.66	2.41	1.93	1.58	2.70	1.47	0.85
K2O	1.12	0.84	0.57	0.44	0.34	0.41	0.34	0.35	0.27
MnO	0.21	0.21	0.23	0.24	0.19	0.23	0.22	0.25	0.32
P2O5	0.04	0.04	0.07	0.05	0.10	0.10	0.10	0.13	0.03
LOI	1.57	1.47	0.80	0.29	1.16	0.35	0.92	1.12	1.27
Total	98.53	98.75	99.10	99.55	97.91	98.41	99.28	98.96	98.90
SiO2/Al2O3	3.41	3.42	3.52	3.64	3.88	3.89	3.72	3.74	3.46
FeO/MgO	0.94	0.99	1.57	1.19	1.37	1.71	1.42	1.96	1.07
K2O/Na2O	0.92	0.67	0.34	0.18	0.18	0.26	0.13	0.24	0.32
Al2O3/TiO2	25.46	25.46	13.53	19.99	12.24	12.45	12.73	9.80	25.60

Table B-6 Major Elements of basalts from the North Star Basalt, Pilbara Block

Element	North Star Basalt						
	McPhee Reward Section						
	NSmr1	NSmr2	NSmr3	NSmr4	NSmr5	NSmr6	NSmr7
SiO2	45.17	49.87	54.73	50.96	52.54	52.14	50.71
TiO2	2.31	1.56	1.56	1.16	1.24	1.06	0.96
Al2O3	12.84	13.01	12.83	13.81	13.28	13.42	13.79
Fe2O3	2.90	2.41	1.99	2.07	2.02	1.89	1.85
FeO	14.49	12.06	9.94	10.37	10.11	9.43	9.27
MgO	5.68	6.05	4.19	6.98	5.81	6.02	5.52
CaO	6.95	8.76	8.91	10.21	10.82	10.34	11.84
Na2O	1.96	2.33	2.45	1.85	1.84	2.01	1.43
K2O	0.61	0.56	0.28	0.31	0.22	0.15	0.19
MnO	0.26	0.22	0.17	0.22	0.24	0.20	0.21
P2O5	0.23	0.16	0.18	0.08	0.13	0.10	0.08
LOI	1.80	1.68	1.11	0.85	1.25	1.53	3.32
Total	95.19	98.67	98.34	98.88	99.51	98.28	99.17
SiO2/Al2O3	3.52	3.83	4.27	3.69	3.96	3.89	3.68
FeO/MgO	2.55	1.99	2.37	1.49	1.74	1.57	1.68
K2O/Na2O	0.31	0.24	0.11	0.17	0.12	0.07	0.13
Al2O3/TiO2	5.56	8.34	8.22	11.91	10.71	12.66	14.36

Table B-7 Major Elements of the North Star basalts

Element	North Star Basalt			
	Withnell Creek Section			
	NSwc1	NSwc2	NSwc3	NSwc4
SiO2	51.30	49.00	52.00	51.30
TiO2	1.26	1.77	1.20	0.88
Al2O3	13.60	14.10	13.40	14.20
Fe2O3	3.32	4.38	3.18	3.22
FeO	9.25	8.30	9.20	7.45
MgO	5.90	5.50	5.50	6.70
CaO	9.50	9.79	6.85	10.40
Na2O	2.84	2.98	5.15	3.02
K2O	0.14	0.27	0.34	
MnO	0.20	0.17	0.13	0.16
P2O5	0.25	0.18	0.09	0.07
LOI	2.56	3.31	3.13	2.81
Total	100.12	99.75	100.17	100.21
SiO2/Al2O3	3.77	3.48	3.88	3.61
FeO/MgO	1.57	1.51	1.67	1.11
K2O/Na2O	0.05	0.09	0.07	
Al2O3/TiO2	10.79	7.97	11.17	16.14

Appendix C: Trace Elements of the Warrawoona Group Basalts

Table C-1. Trace Elements of basalts from Apex Baslat, Pilbara Block

Element	Apex Basalt							
	Withnell Creek Section			Strelley Gorge Section				
	AWc2	AWc3	AWc4	ASs2	ASs4	ASs5	ASs6	ASs7
Rb	4.11	3.08	7.19	2.05	9.24	7.29	27.22	3.08
Ba	43.00	36.00			85.00	291.00	409.00	35.00
Sr	192.72	134.09	103.83	118.01	90.16	138.59	87.16	101.66
Th	0.22	0.80	0.23	0.22	0.75	1.26	2.49	0.45
U	0.07	0.24		0.04	0.21	0.26	0.69	0.25
Sc	36.05	31.22	33.59	34.92	23.61	24.23	31.02	30.61
V	289.00	213.00	327.00	256.00	220.00	260.00	557.00	369.00
Cr	113.39	337.91	181.79	533.05	305.04	266.01	60.19	239.31
Co	44.88	34.92	46.12	46.42	42.83	38.82	45.71	42.93
Ni	118.11	106.82	140.71	157.14	175.63	161.25	43.14	93.46
Y	16.07	19.05	24.94	14.70	19.32	27.32	43.23	33.26
Zr	44.91	66.97	65.63	36.68	66.03	91.59	154.41	87.13
Nb	4.84	5.14	6.74	5.18	7.05	8.25	13.80	9.00
Hf	1.07	1.58	1.72	0.97	1.55	2.27	3.52	2.26
Ta	0.12	0.18	0.14	0.08	0.17	0.29	0.39	0.24
La	2.36	4.68	2.56	1.75	3.79	6.45	13.42	5.36
Ce	5.75	11.09	7.50	5.03	9.14	15.61	29.17	13.25
Nd	3.08	6.16	4.83	3.29	7.29	7.91	17.87	7.91
Sm	1.47	1.83	1.98	1.11	1.89	2.91	4.84	2.88
Eu	0.54	0.74	0.71	0.47	0.66	0.84	1.55	0.99
Gd	1.95	2.26	2.74	1.38	2.35	3.47	5.43	3.57
Tb	0.36	0.41	0.52	0.25	0.42	0.61	0.93	0.64
Yb	1.46	1.57	2.06	1.16	1.47	2.20	3.38	2.78
Lu	0.21	0.24	0.34	0.19	0.21	0.34	0.52	0.43
Ti/Y	276.29	217.32	240.58	244.90	276.40	243.78	358.08	243.54
Zr/Nb	9.28	13.03	9.74	7.08	9.37	11.10	11.19	9.68
Zr/Y	2.79	3.52	2.63	2.50	3.42	3.35	3.57	2.62
Th/U	3.00	3.39		5.25	3.65	4.92	3.61	1.83
La/Th	10.95	5.85	11.32	8.10	5.05	5.11	5.40	11.86
Zr/Hf	42.04	42.34	38.26	37.99	42.58	40.35	43.83	38.56
Nb/Ta	42.07	29.27	46.87	65.50	40.62	28.09	35.08	38.10
(La/Yb)N	0.98	1.81	0.75	0.91	1.56	1.78	2.41	1.17
Eu/Eu*	0.97	1.11	0.94	1.16	0.96	0.82	0.93	0.95

Table C-2. Trace Elements of the Apex baslats & Mount Ada basalts

Element	Apex Basalt					Mount Ada Basalt		
	Cleaverville Section					Talga Coongan Section		
	ASc1	ASc2	ASc3	ASc4	ASc5	MAmb1	MAmb2	MAmb3
Rb	5.14	7.70	4.11	4.11	8.22	12.63	17.05	12.53
Ba	48.00	61.00	33.00	48.00	39.00	76.00	45.00	70.00
Sr	138.09	116.08	113.06	94.39	121.37	147.98	120.92	120.93
Th	0.41	0.31	0.36	0.44	0.45	0.56	0.59	0.47
U	0.15	0.04	0.05	0.08	0.02	0.12	0.11	0.01
Sc	33.28	36.26	33.89	34.00	30.46	41.60	48.27	39.54
V	343.00	333.00	321.00	349.00	323.00	409.00	288.00	337.00
Cr	169.37	244.44	255.74	172.04	280.39	158.89	372.83	143.59
Co	43.03	47.76	45.71	44.68	41.29	50.74	57.00	49.40
Ni	134.55	129.41	142.76	121.20	163.31	95.52	108.87	98.60
Y	29.97	28.47	29.85	33.95	26.94	30.94	23.38	27.23
Zr	87.26	81.98	76.24	83.05	80.54	89.73	72.45	77.21
Nb	7.21	10.88	7.90	7.92	7.49	8.74	7.41	7.64
Hf	2.35	2.01	1.81	2.00	2.01	2.42	2.35	2.22
Ta	0.20	0.18	0.18	0.20	0.19	0.26	0.20	0.23
La	4.23	3.57	3.38	3.73	3.84	5.17	5.25	4.87
Ce	12.22	9.65	8.94	10.27	10.37	13.45	13.56	12.22
Nd	8.63	6.16	6.98	4.87	6.47	9.24	7.91	8.42
Sm	2.86	2.66	2.30	2.77	2.46	3.40	2.76	2.94
Eu	1.02	0.89	0.83	0.89	0.92	1.12	0.98	1.03
Gd	3.68	3.33	3.19	3.50	3.21	4.20	3.47	3.65
Tb	0.67	0.60	0.61	0.64	0.59	0.75	0.63	0.66
Yb	2.59	2.38	2.23	2.51	2.23	2.94	2.46	2.57
Lu	0.39	0.42	0.34	0.39	0.34	0.45	0.41	0.40
Ti/Y	270.27	257.11	241.21	212.08	273.94	267.61	223.27	251.19
Zr/Nb	12.10	7.53	9.65	10.49	10.75	10.27	9.78	10.11
Zr/Y	2.91	2.88	2.55	2.45	2.99	2.90	3.10	2.84
Th/U	2.67	7.50	7.00	5.37	22.00	4.58	5.18	46.00
La/Th	10.30	11.60	9.40	8.44	8.50	9.15	8.96	10.30
Zr/Hf	37.10	40.72	42.18	41.47	40.01	37.02	30.80	34.80
Nb/Ta	36.75	60.88	44.21	39.54	38.79	33.63	36.81	33.21
(La/Yb)N	0.99	0.91	0.92	0.90	1.04	1.07	1.29	1.15
Eu/Eu*	0.97	0.92	0.94	0.88	1.00	0.91	0.98	0.97

Table C-3. Trace Elements of the Mount Ada basalts

Element	Mount Ada Basalt						
	Talga River Section						
	MAmb4	MAmb5	MAmb6	MAmb7	MAmb8	MAmb9	MAmb10
Rb	4.11	7.19	5.14	12.63	3.08	2.05	3.08
Ba	36.00	139.00	105.00	130.00	74.00	66.00	109.00
Sr	102.98	75.47	82.93	166.35	135.68	139.86	166.58
Th	0.60	0.98	0.89	0.70	0.73	0.64	0.72
U	0.04	0.09		0.18	0.05	0.15	0.16
Sc	48.48	53.00	39.65	38.41	36.56	36.36	34.61
V	253.00	434.00	410.00	424.00	345.00	340.00	444.00
Cr	356.40	238.28	183.13	182.20	198.33	188.57	1140.06
Co	58.95	48.79	40.57	45.81	51.87	49.20	45.60
Ni	85.25	66.76	59.57	100.65	94.49	80.11	79.09
Y	22.72	43.67	42.98	42.91	34.48	32.82	44.95
Zr	70.54	130.96	132.09	135.36	96.25	99.03	146.52
Nb	6.90	11.23	10.52	11.31	9.25	9.22	11.80
Hf	2.22	4.53	3.94	2.45	3.01	3.11	4.00
Ta	0.22	0.43	0.42	0.31	0.31	0.28	0.46
La	5.55	10.23	7.91	4.72	9.83	7.15	8.94
Ce	13.45	24.44	20.54	14.79	20.95	17.36	23.31
Nd	8.42	14.48	16.02	6.78	11.40	10.78	15.92
Sm	2.89	4.89	4.47	2.20	4.08	3.61	5.31
Eu	0.93	1.68	1.44	1.15	1.36	1.32	1.68
Gd	3.53	6.03	5.44	3.78	4.97	4.51	6.41
Tb	0.63	1.08	0.97	0.80	0.89	0.82	1.14
Yb	2.44	4.75	4.15	2.71	3.28	3.01	4.17
Lu	0.39	0.75	0.61	0.33	0.51	0.45	0.67
Ti/Y	237.68	274.79	265.24	264.27	248.84	274.22	261.62
Zr/Nb	10.22	11.66	12.56	11.97	10.41	10.74	12.42
Zr/Y	3.10	3.00	3.07	3.15	2.79	3.02	3.26
Th/U	14.50	10.56		3.78	14.20	4.13	4.37
La/Th	9.31	10.48	8.85	6.76	13.48	11.23	12.43
Zr/Hf	31.80	28.91	33.49	55.14	31.98	31.82	36.67
Nb/Ta	31.99	26.16	24.80	36.95	29.82	32.88	25.53
(La/Yb)N	1.38	1.31	1.16	1.06	1.82	1.44	1.30
Eu/Eu*	0.90	0.95	0.90	1.23	0.93	1.00	0.88

Table C-4. Trace Elements of basalts from Mount Ada Basalt

Element	Mount Ada Basalt							
	McPhee Reward Section							
	MAmr1	MAmr2	MAmr3	MAmr4	MAmr5	MAmr6	MAmr7	MAmr8
Rb	3.08	2.05	1.03	7.19	2.05	1.03	1.03	6.16
Ba	45.00	27.00	55.00	141.00	18.00	22.00	76.00	50.00
Sr	221.67	139.66	134.71	98.48	79.02	169.72	225.89	217.44
Th	1.20	0.96	1.25	0.83	0.55	0.39	1.39	1.34
U	0.36	0.15	0.41	0.15	0.14	0.23	0.47	0.35
Sc	20.46	25.41	18.29	23.72	27.56	33.69	21.51	19.86
V	294.00	351.00	354.00	303.00	257.00	194.00	329.00	319.00
Cr	37.18	43.03	40.57	21.98	60.19	230.07	42.83	30.81
Co	43.34	36.05	34.41	37.28	42.01	40.67	39.03	41.39
Ni	51.35	56.49	57.52	49.30	76.00	83.19	53.41	38.00
Y	38.23	32.92	38.56	41.30	23.86	20.72	39.94	41.48
Zr	157.82	128.06	162.89	144.27	77.90	64.17	167.73	181.20
Nb	12.19	11.20	13.93	13.57	6.27	5.42	16.27	17.16
Hf	4.26	3.15	3.80	3.39	1.95	1.50	4.45	4.14
Ta	0.22	0.45	0.71	0.55	0.48	0.59	1.10	0.98
La	11.74	9.60	10.23	6.00	4.58	9.99	12.11	11.02
Ce	28.35	22.90	25.78	15.92	11.40	8.63	28.76	25.68
Nd	18.80	14.89	15.92	10.58	7.09	5.44	19.31	20.44
Sm	5.59	4.18	5.02	4.08	2.54	1.88	5.66	5.52
Eu	1.79	1.32	1.65	1.28	0.84	0.65	1.84	1.64
Gd	6.29	4.79	5.87	4.79	3.14	2.37	6.47	6.42
Tb	1.08	0.83	1.03	0.84	0.56	0.43	1.12	1.12
Yb	3.38	2.77	3.08	3.44	2.03	1.63	3.65	3.31
Lu	0.52	0.40	0.44	0.53	0.30	0.24	0.52	0.50
Ti/Y	312.32	282.50	318.98	232.45	256.50	228.76	307.96	319.67
Zr/Nb	12.95	11.43	11.69	10.63	12.42	11.84	10.31	10.56
Zr/Y	4.13	3.89	4.22	3.49	3.26	3.10	4.20	4.37
Th/U	3.34	6.20	3.05	5.40	3.86	1.73	2.93	3.82
La/Th	9.77	10.05	8.16	7.21	8.26	25.61	8.73	8.25
Zr/Hf	37.03	40.61	42.86	42.57	39.92	42.79	37.72	43.78
Nb/Ta	54.19	24.90	19.60	24.70	13.10	9.26	14.80	17.59
(La/Yb)N	2.11	2.10	2.01	1.06	1.37	3.71	2.01	2.02
Eu/Eu*	0.93	0.90	0.94	0.89	0.91	0.94	0.93	0.85

Table C-5. Trace Elements of basalts from the North Stra basalts

Element	North Star Basalt								
	Talga Coongan Section								
	NSmb1	NSmb2	NSmb4	NSmb3	NSmb5	NSmb6	NSmb7	NSmb8	NSmb9
Rb	70.87	45.29	17.67	13.35	18.18	22.49	22.49	2.05	5.14
Ba	185.00	153.00	175.00	168.00	49.00	27.00	59.00	89.00	18.00
Sr	163.00	176.03	125.35	148.16	98.57	84.84	123.48	130.85	94.68
Th	0.95	0.89	0.25	0.70	0.85	0.92	0.92	0.68	0.87
U	0.22	0.30	0.02	0.16	0.27	0.23	0.23	0.13	0.03
Sc	47.86	40.67	46.32	36.56	48.38	47.35	47.35	34.61	39.85
V	244.00	246.00	354.00	272.00	364.00	324.00	337.00	420.00	278.00
Cr	329.69	296.83	162.69	162.07	82.27	90.49	90.49	27.42	302.99
Co	52.79	43.75	59.67	44.37	54.33	50.84	50.84	58.75	54.33
Ni	149.95	114.01	115.03	221.85	53.41	57.52	57.52	69.84	138.66
Y	20.00	21.67	25.34	21.75	29.81	43.98	27.43	33.52	20.41
Zr	77.00	75.06	64.78	64.11	89.98	130.23	87.62	110.58	76.73
Nb	8.00	6.85	7.06	5.96	7.61	11.93	7.32	8.67	6.58
Hf	2.38	2.07	1.93	2.67	2.94	2.89	2.89	3.36	2.19
Ta	0.24	0.20	0.17	0.31	0.27	0.25	0.25	0.27	0.26
La	5.75	4.98	3.48	7.68	7.49	7.32	7.32	6.04	5.96
Ce	13.87	12.32	8.22	15.92	18.49	17.97	17.97	15.00	13.87
Nd	7.29	6.47	6.47	9.65	11.30	9.86	9.86	9.35	7.91
Sm	2.43	2.17	2.43	4.61	3.59	3.29	3.29	3.74	2.18
Eu	0.86	0.69	0.92	0.98	1.17	1.13	1.13	1.41	0.66
Gd	3.01	2.85	3.27	4.38	4.48	4.11	4.11	4.92	2.72
Tb	0.54	0.53	0.61	0.69	0.81	0.74	0.74	0.91	0.49
Yb	2.50	2.14	2.74	3.01	3.31	2.95	2.95	2.93	2.07
Lu	0.40	0.31	0.43	0.57	0.50	0.49	0.49	0.43	0.34
Ti/Y	177.00	163.36	246.25	204.14	221.40	148.70	240.61	247.02	170.50
Zr/Nb	9.63	10.96	9.18	10.76	11.82	10.92	11.97	12.75	11.66
Zr/Y	3.85	3.46	2.56	2.95	3.02	2.96	3.19	3.30	3.76
Th/U	4.32	3.00	12.00	4.25	3.19	4.09	4.09	5.08	28.33
La/Th	6.05	5.57	14.13	11.00	8.78	7.92	7.92	8.91	6.82
Zr/Hf	32.35	36.18	33.55	24.01	30.63	45.12	30.36	32.92	35.07
Nb/Ta	33.33	33.43	40.36	19.15	28.61	48.30	29.63	31.91	24.83
(La/Yb)N	1.39	1.41	0.77	1.55	1.37	1.51	1.51	1.25	1.74
Eu/Eu*	0.98	0.85	1.01	0.67	0.90	0.95	0.95	1.01	0.83

Table C-6. Trace Elements of basalts from North Star Basalt

Element	North Star Basalt						
	McPhee Reward Section						
	NSmr1	NSmr2	NSmr3	NSmr4	NSmr5	NSmr6	NSmr7
Rb	22.60	16.95	11.30	6.16		4.11	7.19
Ba	182.00	234.00	104.00	242.00	158.00	48.00	51.00
Sr	124.05	120.06	195.02	114.85	107.74	126.79	148.14
Th	1.52	1.54	1.45	0.70	0.85	0.67	0.63
U	0.56	26.70	0.39	0.15	0.20	0.20	0.24
Sc	26.18	25.39	27.37	33.89	34.30	32.56	32.04
V	407.00	324.00	320.00	363.00	357.00	338.00	282.00
Cr	27.83	17.05	121.09	67.89	39.65	58.13	72.72
Co	45.81	42.42	39.23	38.10	36.56	36.87	39.85
Ni	69.84	11.30	55.46	50.33	51.35	73.95	46.22
Y	55.70	38.18	35.80	27.44	30.24	29.48	23.29
Zr	208.80	138.81	142.87	93.06	104.55	94.19	72.93
Nb	15.03	12.50	12.18	10.94	8.85	10.05	8.90
Hf	3.80	4.03	3.74	1.95	2.58	2.22	1.92
Ta	0.45	0.61	0.49	0.29	0.30	0.29	0.44
La	13.14	8.86	9.41	5.15	6.35	5.47	4.67
Ce	24.03	27.01	24.34	12.02	15.30	13.15	11.09
Nd	16.13	13.45	13.25	6.98	10.58	6.98	6.98
Sm	6.32	4.20	4.54	2.58	2.97	2.51	2.35
Eu	1.33	1.60	1.39	0.85	0.93	0.96	0.74
Gd	5.95	5.68	5.17	3.16	3.64	3.28	2.84
Tb	0.93	1.07	0.89	0.56	0.65	0.60	0.50
Yb	3.87	3.28	3.30	2.32	2.56	2.25	1.98
Lu	0.66	0.45	0.53	0.33	0.40	0.34	0.31
Ti/Y	248.83	245.15	261.45	253.64	246.03	215.74	247.32
Zr/Nb	13.89	11.10	11.73	8.51	11.81	9.37	8.19
Zr/Y	3.75	3.64	3.99	3.39	3.46	3.20	3.13
Th/U	2.69	0.06	3.71	4.53	4.37	3.42	2.65
La/Th	8.64	5.75	6.50	7.37	7.45	8.20	7.46
Zr/Hf	54.94	34.48	38.22	47.69	40.56	42.46	37.97
Nb/Ta	33.72	20.52	24.71	37.77	29.41	34.58	20.20
(La/Yb)N	2.06	1.64	1.73	1.34	1.50	1.48	1.43
Eu/Eu*	0.67	1.00	0.88	0.91	0.87	1.03	0.88

Table C-7. Trace Elements of the North Star basalts

Element	North Star Basalt			
	Withnell Creek Section			
	NSwc1	NSwc2	NSwc3	NSwc4
Rb	3.08	5.14	7.19	2.05
Ba	71.00	34.00	40.00	12.00
Sr	208.14	118.33	185.05	206.05
Th	1.17	0.87	1.05	0.77
U	0.24	0.31	0.32	0.13
Sc	22.27	33.28	18.80	27.21
V	207.00	428.00	245.00	240.00
Cr	147.39	179.94	72.10	235.20
Co	37.18	36.05	45.71	36.87
Ni	80.11	93.46	59.57	69.84
Y	40.86	36.92	23.69	21.33
Zr	172.06	115.80	94.04	70.81
Nb	14.25	12.93	12.17	7.16
Hf	3.61	3.10	2.32	1.80
Ta	0.40	0.29	0.26	1.22
La	9.48	6.41	7.49	5.19
Ce	21.67	15.92	20.13	12.32
Nd	12.32	9.55	11.50	7.81
Sm	4.57	3.57	3.37	2.25
Eu	1.41	1.22	1.15	0.76
Gd	5.17	4.48	3.68	2.71
Tb	0.89	0.81	0.62	0.48
Yb	3.02	3.11	2.16	1.63
Lu	0.44	0.47	0.32	0.29
Ti/Y	185.02	287.65	303.93	247.54
Zr/Nb	12.07	8.96	7.73	9.89
Zr/Y	4.21	3.14	3.97	3.32
Th/U	4.96	2.83	3.29	5.77
La/Th	8.10	7.34	7.15	6.73
Zr/Hf	47.73	37.33	40.51	39.40
Nb/Ta	35.94	45.28	45.93	5.85
(La/Yb)N	1.90	1.25	2.10	1.92
Eu/Eu*	0.89	0.94	1.00	0.95

References

Barley, M. E. et. al., 1984. Archaean calc-alkaline volcanism in the Pilbara Block, West Australia. Precambrian Research, v. 24, p. 285-319.

Bickle, M. J., et. al., 1983. A 3500 Ma plutonic and volcanic calc-alkaline Province in the Archaean East Pilbara Block. Contrib. Mineral. Petrol., v. 84, p. 25-35.

Bickle, M. J., 1989. Mantle evolution. In: Early Precambrian Basic Magmatism (edited by R. P. Hall and D. J. Hughes), Chapman and Hall, New York, p. 111-135.

Boryta, Mark D., 1988. Geochemistry and origin of igneous rocks from the Archean Belt Bridge Complex, Limpopo Belt, South Africa. (Master thesis, unpublished, 1990).

Cattell, A. C. and Taylor, R. N., 1989. Archean basic magmas. In: Early Precambrian Basic Magmatism (edited by R. P. Hall and D. J. Hughes), Chapman and Hall, New York, p. 11-39.

Condie, Kent C., 1975. A mantle plume model for the origin of Archean greenstone belts based on trace element distribution. Nature, v. 258, p. 413-414.

Condie, Kent C., 1981. Archean greenstone belts. Elsevier Scientific Publishing Company, 434 pp.

Condie Kent C., 1985. Secular variation in the composition of basalts. an index to mantle evolution. Journal of Petrology, v. 26, p. 545-563.

Condie, Kent C., 1986. Origin and early growth rate of continents. Precambrian Research, v. 32, p. 261-278.

Condie, Kent C., 1987. Geochemistry and origin of late Archean volcanic rocks from the Rhenosterhoek Formation, Dominion Group, South Africa. Precambrian Research, v. 37, p. 217-229.

Condie, Kent C., 1989. Plate tectonics and crustal evolution. (3rd edition) Pergamon Press, Oxford, 476 pp.

Condie, Kent C., 1989. Geochemical characteristics of Precambrian basaltic greenstones. In: Early Precambrian Basic Magmatism (edited by R. P. Hall and D. J. Hughes), Chapman and Hall, New York, p. 40-55.

Condie Kent C. and Hunter, D. R., 1976. Trace element geochemistry of Archean granitic rocks from the Barberton region, South Africa. Earth Planet. Sci. Lett., v. 29, p. 389-400.

Crow, Clay and Condie, Kent C., 1988. Geochemistry and origin of late Archean volcanics from the Ventersdorp Supergroup, South Africa. Precambrian Research. v. 42, p. 19-37.

DePaolo, Donald J., 1981. Trace element and isotopic effects of combined wallrock assimilation and fractional crystallization. Earth and Planetary Science Letters, v. 53, p. 189-202.

Glikson, A. Y., 1979. Siderophile and lithophile trace element evolution of the Archaean mantle. BMR J. Aust. Geol. Geophys., v. 4, p. 253-279.

Glikson, A. Y. and Hickman, A. H., 1981. Geochemical stratigraphy and petrogenesis of Archean basic-ultrabasic volcanic units, eastern Pilbara Block, Western Australia. Spec. Publs Geol. Soc. Aust., v. 7, p. 287-300.

Glikson, A. Y. and Hickman, A. H., 1981. Geochemistry of Archean volcanic successions, eastern Pilbara Block, western Australia. Aust. Bur. Min. Resour. Record 1981/36.

Glikson, A. Y., et. al., 1986. REE and HFS (Ti, Zr, Nb, P, Y) element evolution of Archean mafic-ultramafic volcanic suites, Pilbara Block, western Austrralia. Aust. BMR Rec. 6.

Goodwin, A. M., 1977. Archean basin-craton complexes and the growth of Precambrian shields. Can. J. Earth. Sci., v. 14, p. 2737-2759.

Goodwin, Alan M., 1981. Archean plate and greenstone belts, In: Precambrian Plate Tectonics (edited by A. Kroner), Elsevier Scientific Publishing Company, New York, p. 105-129.

Gruau, G., et. al., 1987. Age of the Archean Talga-Talga Subgroup, Pilbara Block, Western Australia, and early evolution of the mantle: new Sm-Nd isotope evidence. Earth and Planetary Science Letter, v. 85, p. 105-116.

Hall, R. P. and Hughes, D. J., 1990, Basic magmatism and crustal evolution. In: Early Precambrian Basic Magmatism (edited by R. P. Hall and D. J. Hughes), Chapman and Hall, New York, p.1-7.

Hallett, R. Bruce, 1990, Geology and Geochemistry of early Proterozoic Granitoids from the Northern Western Wet Mountains-Southern Front Range, South-Central Colorado. (Master thesis, unpublished, 1990)

Haskin, L. A., 1984. Petrogenetic modelling: use of rare earth elements. In: Rare earth element geochemistry (edited by P. Henderson), Elsevier Science Publishers B. V.

Hess, Paul C., 1989, Origins of Igneous Rocks. Harvard University Press, Cambridge, Massachusetts, 336 pp.

Hickman, A. H., 1981. Crustal evolution of the Pilbara Block. In: Archean Geology (edited by J. E. Glover and D. I. Groves) Int. Arch. Symp., Second, Perth, Geol. Soc. Aust. Spec. Pub. 7, p. 57-69.

Hickman, A. H., 1983. Geology of Pilbara block and its Environs. Geological Survey of Western Australia Bulletin 127, Perth, 127 pp.

Hofmann, Albrecht W., 1988. Chemical differentiation of the Earth: the relationship between mantle, continental crust, and oceanic crust. Earth and Planetary Science Letters, v. 90, p. 297-314.

Horwitz, R. C., 1990. Palaeogeographic and tectonic evolution of the Pilbara Craton, Northwestern Australia, Precambrian Research, v. 48, p. 327-340

Jahn, Bor-Ming, Glikson, A. Y., Peucat, J. J. and Hickman, A. H., 1981. REE geochemistry and isotopic data of Archean silica volcanics and granitoids from the Pilbara Block, Western Australia: implications for the early crustal evolution. Geochimica et Cosmochimica Acta, v. 45, p. 1633-1652.

Jahn, B. M., 1989. Early Precambrian basic rocks of China. In: Early Precambrian Basic Magmatism (edited by R. P. Hall and D. J. Hughes), Chapman and Hall, New York, p. 294-316.

Kroner, A., 1981. Precambrian plate tectonics, In Precambrian Plate Tectonics (edited by A. Kroner), Elsevier Scientific Publishing Company, New York, p. 57-83.

Marsh, Julian S., 1987. Basalt geochemistry and tectonic discrimination within continental flood basalt provinces. Journal of Volcanology and Geothermal Research, v. 32, p. 35-49.

Pharaoh, T. C. et al, 1987. Geochemical and mineralisations of Precambrian. volcanic suites.

Pidgeon, R. T., 1978. 3.450 M.y.-old volcanics in the Archaean layered greenstone succession of the Pilbara Block, Western Austalia, Earth Planet. Sci. Lett., v. 37, p. 421-428.

Pidgeon, R. T., 1984. Geochronological constraints on early volcanic evolution of the Pilbara Block, Western Australia, Australian Journal of Earth Science, v. 31, p. 237-242.

Powell, Roger, 1984. Inversion of the assimilation and fractional crystallization (AFC) equations; characterization of contaminates from isotope and trace element relationships in volcanic suites. J. Geol. Soc. London, v. 141, p. 447-452.

Purvis, A. C., 1989. Early Precambrian basic rocks of Australia. In: Early Precambrian Basic Magmatism (edited by R. P. Hall and D. J. Hughes), Chapman and Hall, New York, p. 317-338.

Sun, S. S., 1984. Geochemical characteristics of Archean ultramafic and mafic volcanic rocks: implications for mantle composition and evolution. In: Archean geochemistry (edited by A. Kroner, et. al.), Springer-verlag Berlin Heidelerg, p. 25-46.

Weaver, Barry L., 1991. Trace element evidence for the origin of ocean-island basalts. Geology, v. 19, p. 123-126.

Wilson, M., 1989. Igneous Petrogenesis. Unwin Hyman Ltd, Boston, 466 pp.

Windley, B. F., 1977. The evolving continents. J. Wiley & Sons, New York, N. Y., 385 pp.